NUCLEAR ENGINEERING

MASSACHUSETTS INSTITUTE
OF TECHNOLOGY

ASPECTS OF ENVIRONMENTAL AND SAFETY ANALYSIS OF FUSION REACTORS

by

M. S. Kazimi, Editor
D. A. Dube, R. W. Green, L. M. Lidsky,
N. C. Rasmussen, R. W. Sawdye and J. A. Sefci

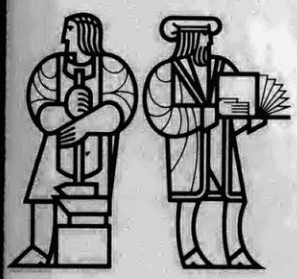

DEPARTMENT OF NUCLEAR ENGINEERING
MASSACHUSETTS INSTITUTE OF TECHNOLOGY
Cambridge, Massachusetts 02139

October 1977

ASPECTS OF ENVIRONMENTAL AND SAFETY ANALYSIS OF FUSION REACTORS

by

M. S. Kazimi, Editor
D. A. Dube, R. W. Green, L. M. Lidsky,
N. C. Rasmussen, R. W. Sawdye and J. A. Sefcik

Progress Report for the Period
October 1, 1976 to September 30, 1977
Contract EY-76-S-02-2431
U.S. Energy Research and Development Administration

ABSTRACT

This report summarizes the progress made between October 1976 and September 1977 in studies of some environmental and safety considerations in fusion reactor plants. A methodology to assess the admissible occurrence rate of major accidental releases is outlined. The pathways for tritium releases are defined. Preliminary assessment of the important factors in evaluation of the reactor containment building response to Li-Air fire is presented.

TABLE OF CONTENTS

LIST OF FIGURES

LIST OF TABLES

I. INTRODUCTION AND SUMMARY

1.1 Introduction

The effort to define the potential for electric power production from nuclear fusion has significantly intensified within the last few years. The choice among the energy resource options is influenced by, among other factors, the environmental impact of the technology associated with each option. Thus, an early determination of the potential advantages and hazards of each of the long-term energy options, such as nuclear fusion, is an integral part of the effort to define the desirability of each option in a risk-benefit context.

Beyond this obvious goal of comparison among alternative future energy sources, early attention to the environmental and safety considerations will tend to minimize the environmental hazards by appropriately influencing the fusion reactor designs as well as research and development plans. Thus, it is not surprising to find several recent publications on environmental and safety considerations in fusion power plant designs.[1-5]

Associated with any power system containing radioactivity there exists a potential hazard or risk resulting from possible accidental releases. A study of the risks associated with commercial fission power reactors in the United States was detailed in the Reactor Safety Study Report (WASH-1400)[6].

From a radiological risk perspective, fusion reactor plants appear to have inherently two potential advantages over the fission reactors:

1) The radioactivity associated with the fuel cycle itself is less hazardous than that of the fission reactor fuel cycle. The radioactivity induced in the structures depends greatly on the materials employed. Hence, there is a large degree of latitude in minimizing the total radioactivity in the fusion reactors of the future.

2) The radioactivity of the structures so far considered in fusion reactor design is of a half-life that is considerably shorter than that of the fission reactors, which mitigates the problems of waste disposal.

The broad objectives of the present study, which was initiated in October of 1976, are:

1) To develop a methodology for assessment of radiological hazards from fusion reactor power plants.

2) To develop design criteria to ensure adequately low levels of radiological hazards of fusion power plants.

It is obvious that such broad objectives have to be pursued within the bounds of available reactor plant design data. While several conceptual designs for fusion power plants exist, more emphasis is currently placed on the Tokamak

concepts. Thus, the UWMAK-III design has been selected as a reference reactor plant for this initial study.[7] The UWMAK-III design has been described in sufficient detail to allow a reasonable level of quantitative assessment of the radioactivity inventory and distribution, and, hence, radioactivity hazard analysis. However, in many respects, there is sufficient similarity in safety and environmental concern among the various fusion reactor designs to render the conclusions from the present study relevant to other concepts. It should be noted that the radioactivity inventories used in the present study were among the highest possible in Tokamak reactors since no credit was taken for isotopic tailoring to minimize radioactivity.[8]

Radiological hazards may be classified as associated with routine releases from the reactor plant or with accidental releases. The former case results in a "definite" environmental impact while the later results in a "potential" impact. The probability of the accidental impact is commonly defined in "safety analyses" of a reactor plant. Assessment of the realistic radiological hazards of both routine and accidental releases involves combining the probability and the consequence of the releases. In Figure 1.1, the steps undertaken in such an assessment are defined. Such an assessment was employed in the "Reactor Safety Study"[6] pertaining to accidental releases from commercial nuclear fission power plants.

Figure 1.1

FUSION REACTOR CONCEPT

A Proposed Methodology of S&EI Assessment

Task	Safety	Environmental Impact
(1) Assess Radioactivity Inventory 1. Tritium 2. Structural 3. Corrosion products		
(2) Define Conditions of Radioactivity Release to Containment	Perform Mechanistic Evaluation of Faulty Conditions e.g.: 1. Loss of Blanket Coolant 2. Loss of Diverter Coolant 3. Loss of Magnet Coolant 4. Containment events a. lithium spill b. helium pipe rupture	Define Rate of Release Under Normal Operating Conditions 1. Tritium Diffusion 2. Radioactivity Streaming 3. First Wall Replacement 4. Blanket Replacement
(3) Establish Probability of Release of x ci/hr in Each Event		Probability = 1.0
(4) Define Radioactivity Dispersion in Atmosphere		
(5) Define Consequences of Release of x mrem/hr		

Two major sources of radioactivity hazards are easily identified: (1) the tritium inventory and (2) the activation products in the structures. Tritium release to the atmosphere is the major radioactivity source during normal operation. However, under severe accident conditions where the structural activation products may be released to the atmosphere, the contribution of tritium to the total biological hazard potential may not be dominant.

For UWMAK-III design, the potential radioactivity release associated with vaporization of the TZM first wall is illustrated in Figure 1.2. It is clear that the total radioactivity of the first wall, which is roughly 25% of the induced radioactivity in the structures, is twice as large as radioactivity of the tritium inventory. More significantly, tritium, a beta particle emitter, can be permitted at a higher concentration in air than the structural nuclides. As shown in Table 1.1, the inventories of several isotopes will require larger volumes of air to become diluted to the maximum permissible concentration (MPC) than does tritium. Compared with the energy requirement to vaporize the structural material, only two sources of energy within the reactor plant appear to be signigicant, as illustrated in Figure 1.3:

a) Lithium-Air or Lithium-Concrete reactions

b) The energy stored in the toroidal magnetic field.

Thus, considerable attention should be given to the mechanisms by which the available energy can be deposited in the first wall, which has the highest specific (per unit volume) structural radioactivity.

Figure 1.2 First Wall Activity Inventory

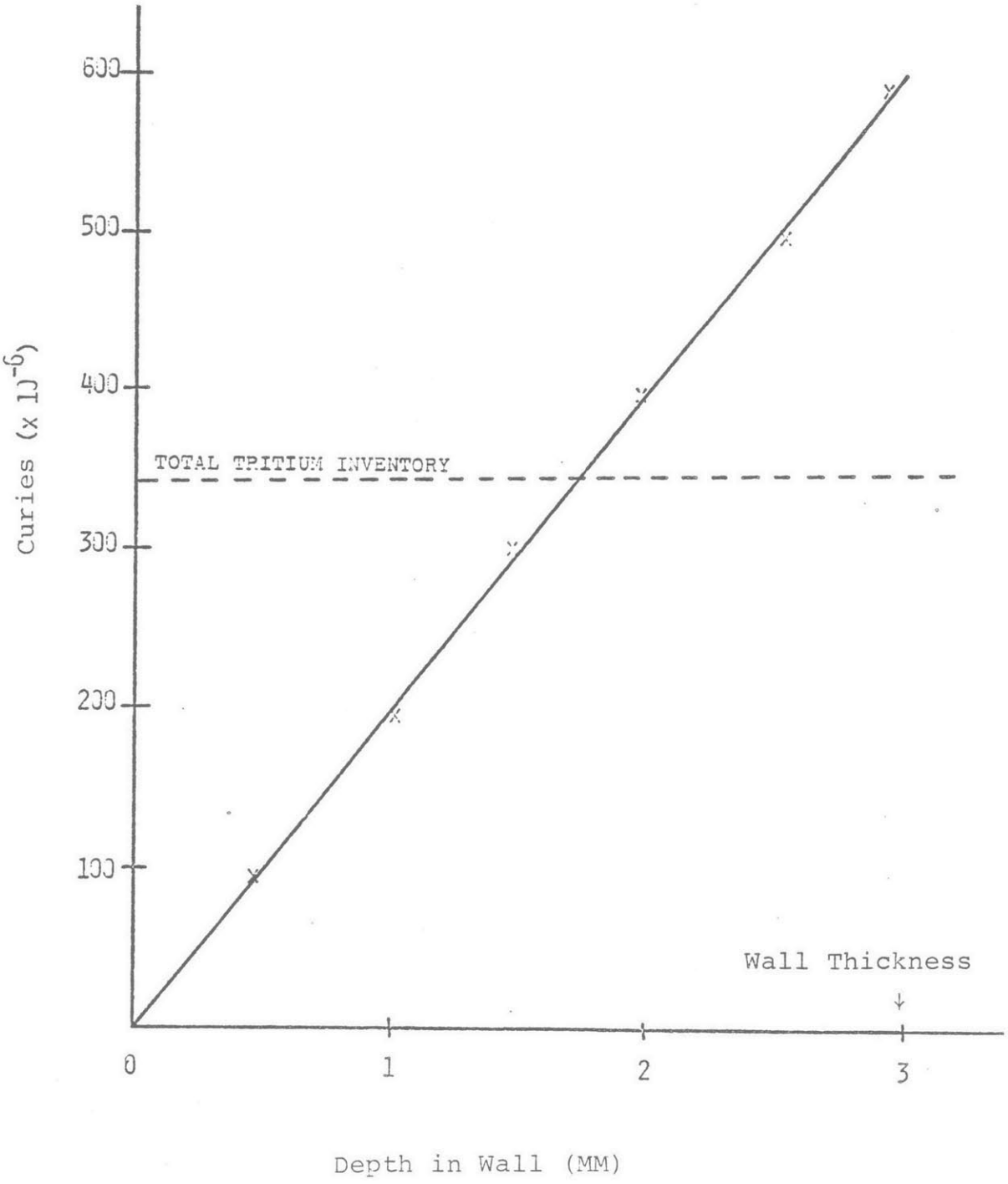

TABLE 1.1

Radiological Hazard Potential for Radioisotopes of UWMAK-III (TZM First Wall)

PRINCIPAL FIRST WALL ISOTOPE	TOTAL KM^3 of AIR TO DILUTE TO MPC	TOTAL CURIES
Nb 92^m	8.7×10^7	8.7×10^6
Zr 89	7.0×10^7	7.9×10^6
Nb 95^m	6.2×10^7	6.2×10^6
Mo 99	4.0×10^7	2.8×10^8
Nb 96	3.9×10^7	3.9×10^6
Nb 91^m	2.2×10^7	2.2×10^6
T	1.72×10^6	3.43×10^8
Tc 101	1.5×10^6	1.5×10^5
Mo 101	1.5×10^6	1.5×10^5
Nb 95	3.3×10^6	9.9×10^6
Zr 95	2.1×10^6	2.1×10^5
Mo 93	5.7×10^5	5.7×10^4
Tc 99^m	5.7×10^5	27.7×10^7
Mo 91	2.4×10^6	2.4×10^5
Y 88	5.7×10^5	5.7×10^4

TOTAL = 596.7×10^6 Ci

(For Total First Wall Inventory)

Figure 1.3
Energy Requirement for
Vaporization of First Wall

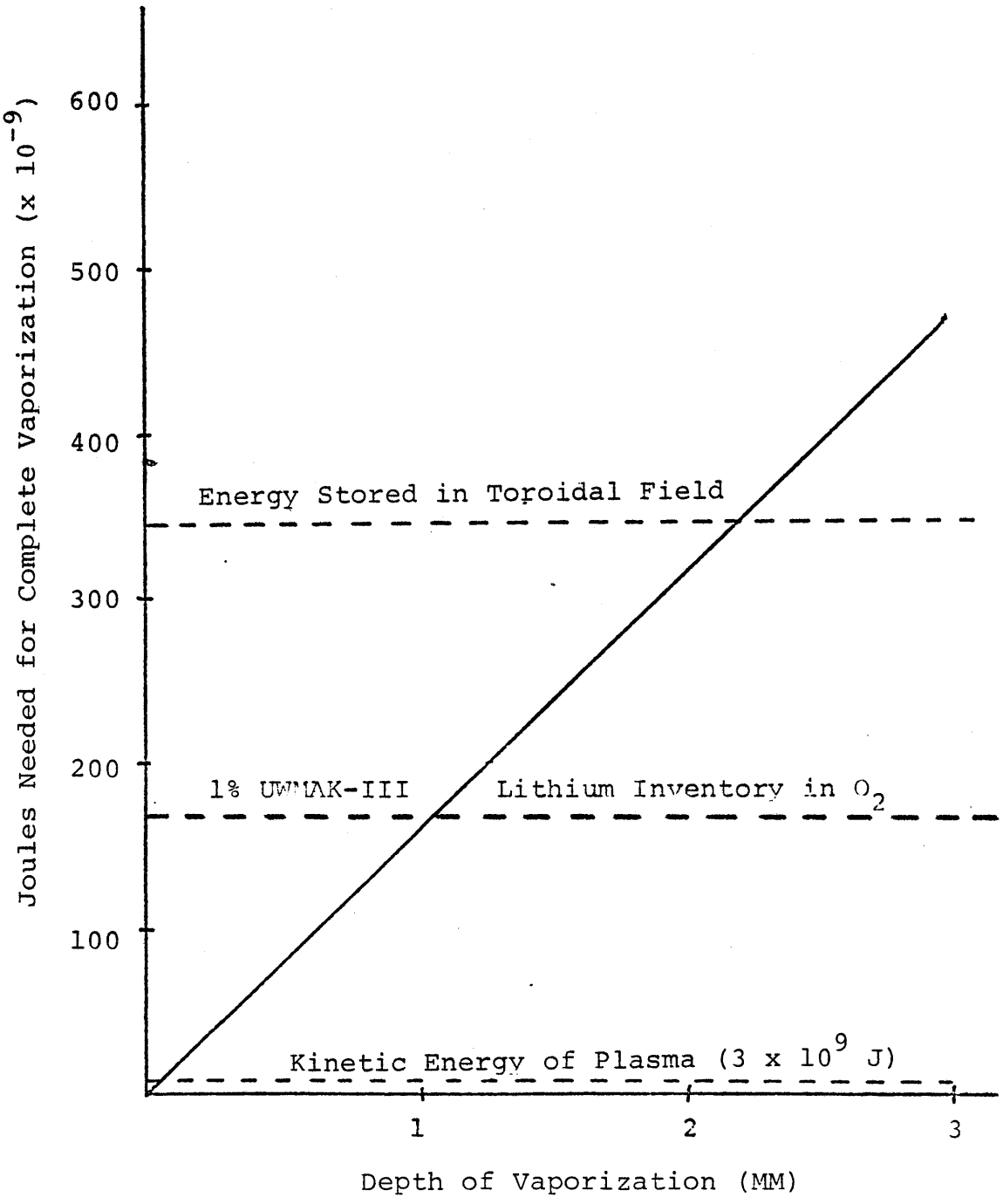

In Chapter II, several considerations in assessment of the hazards from the induced radioactivity and tritium are presented. A proposed methodology to assess the admissible occurrence rate of major releases is outlined. The pathways for tritium releases are defined.

In Chapter III, preliminary assessment of the important factors in evaluation of reactor containment building response to Li-air fire is presented. Also, the potential for generating sufficiently high temperatures during the fire to vaporize the structural material is evaluated from basic thermodynamic considerations.

Many aspects of the work reported here are under ongoing investigation, and it is hoped that some of the uncertainties may be reduced in the near future.

1.2 Summary

The following is a summary of the major results and conclusions of this preliminary study.

1) A methodology has been proposed to determine admissible radioactivity release probabilities, from comparisons of consequences of radioactivity releases to established acceptable levels or risk. One example of this technique is the use of the results of the Reactor Safety Study, representing an admissible risk for current commercial nuclear power plants. The release probability constraints thus determined may be used to set major component reliability requirements for a Tokamak reactor design.

2) To illustrate the proposed methodology, preliminary calculations have been performed for releases of stainless steel activation products. The admissible release probability is dependent on the accident release magnitudes. Therefore, a range of possible values for this parameter must be determined for each structural material. The consequences of activation product releases are also sensitive to the site population characteristics.

3) For a release to occur, both disruption of structural material and its transport from the reactor are required. A study of the melting rates of stainless steel and TZM for sudden energy dumps

shows that the steel, with a lower BHP value, melts slower for a heat flux if no significant material ablation takes place. If material ablation is significant, the steel is then found to have a higher melting rate than the molybdenum alloy.

4) Potential pathways for different release modes of tritium have been defined.

5) Elemental tritium conversion rates to the oxide form is such that the order of the reaction, the rate of the reaction, and the dominant conversion mechanism are not clearly established. An attempt to analyze actual tritium releases with the presently accepted conversion rates have been unsuccessful.

6) During lithium fires, a substantial amount of the tritium released may be converted to condensible lithium compounds. The principal products appear to be LiH, LiOH, H_2O, and H_2. The amount of these products formed is highly specific to the lithium-air tritium-air molar ratios.

7) Thermodynamic considerations indicate that in case of a Li-O_2-N_2 fire, the maximum flame temperature will be 2500°K or less, depending on the molar ratios of the interacting materials. For oxygen-depleted atmosphere, the maximum temperature will be 1315°K or less. The Li-O_2 reaction is dominant when the volumetric percentage of O_2 in the O_2-N_2 mixture is greater than about 1%.

8) The energy released in lithium-oxygen fires may lead to a significant overpressure in containments of proposed plant designs. However, the degree of overpressurization will depend on various parameters, notably on the oxygen concentration, heat transfer rates from the interaction zone to the gases and containment wall and floor. Several design options to mitigate the consequences of a lithium spill are being analyzed and will be reported on in the near future.

Chapter I References

1. D. Steiner and A. P. Frass, "Preliminary Observation on the Radiological Implications of Fusion Power," Nuclear Safety, 13 (5), September-October, 1972.

2. F. N. Flakus, "Fusion Power and the Environment," International Atomic Energy Agency, Vienna, Austria, October 1974.

3. D. Okrent, et. al., "On the Safety of Tokamak-Type Central Station Fusion Power Reactors," Nucl. Eng. Design 39, 215, 1976.

4. R. G. Clark, "Safety Review of Conceptual Fusion Power Plants," BNWL-2024, November 1976.

5. J. Powel, Editor, "Aspects of Safety and Reliability for Fusion Magnet Systems," BNL-50542, January 1976.

6. Reactor Safety Study, WASH-1400, United States Nuclear Regulatory Commission, October 1975.

7. The University of Wisconsin Fusion Feasibility Study Group, "UWMAK-III, A Non-circular Tokamak Power Reactor Design," UWFDM-150, July, 1976.

8. R. W. Conn, K. Okula and W. Johnson; "Minimizing Long-Term Radioactivity in Fusion Reactors by Isotopic Tailoring," Trans. Am. Nucl. Soc., 26, 27 (1977).

II. RADIOACTIVITY HAZARDS AND ADMISSIBLE RISKS

2.1 Introduction

Most of the radioactivity in Tokamak reactors with a deuterium-tritium fuel cycle is in two forms: the activated structural materials exposed to radiation from the plasma and the tritium used as a fuel for the fusion reaction and bred in the reactor blanket. Serious accidents resulting in the disruption of the reactor first wall or blanket structural materials are required to release any induced radioactivity. However, because of its mobility, tritium poses a potential hazard due to normal operational releases as well as releases resulting from accidents. The total amount of activity in a fusion reactor system may be on the order of 10^9 Ci.,[2] which is comparable to the total inventory at a commercial light water fission reactor plant.

The risk assessment report for commercial nuclear power plants (WASH-1400)[1] was based on analyses of the probability of accidents that may lead to radioactive releases to the atmosphere. These releases were then used in a consequence model, the Calculations of Reactor Accident Consequences (CRAC) computer code,[1] to evaluate the probability of exceeding consequences of a given magnitude as a result of radioactive releases. A similar technique can be utilized to investigate the potential hazard of the radioactivity in Tokamak fusion reactor plants. The sources of radioactivity

must be identified and the activity releasing accidents must be described. Some type of consequence model can then be employed to translate the release accidents into risk curves or consequence magnitude ranges.

The concept of an acceptable or admissible risk for electricity generation utilitzing nuclear power may be controversial, but can be useful in determining system reliability requirements. If the fusion reactor accident consequences are compared to a risk curve representing an admissible risk to the public (the risk may be defined in terms of probability of adverse health effects) an admissible failure rate or frequency of occurrence for release accidents can be derived. Thus, if an admissible or tolerable level of risk is assumed or established for nuclear power plants, then the allowable rate of release or probability for certain accidents can be determined and may be used to set reliability requirements for major system components of a fusion power plant.

The goal of this work is to establish a methodology to determine probable consequences of radioactivity releases from fusion reactors under accident as well as routine operational conditions and to utilize the consequence spectrum to assess the reliability constraints for major Tokamak system components.

2.2 Induced Radioactivity

During the operation of a fusion reactor, there will inevitably develop an inventory of induced radioactivity, or activation products, in the first wall and blanket structures. The amount and assortment of radioisotopes will depend on the nature of the particle fluxes, the type of structural materials and, to some extent, the duration of exposure to these particles. The designers of fusion reactor systems should attempt to minimize the potential hazards presented by this induced activity by developing reliable designs with safety features and by proper selection of structural materials. Using the conceptual designs which are available for Tokamak type reactors, the radioactivity inventories can be identified and possible accidents can be examined to determine the amounts of radioactivity that may be released to the atmosphere. The characteristics of the releases must be described before a consequence model can be used to calculate the risks to the public associated with these reactors. Much work still needs to be done in this area of accident analysis before useful and realistic consequence results can be developed, however, some preliminary results and an example of the use of the methodology are presented in this report.

By examining the potential hazards of activation product releases and comparing them with an acceptable level of radioactivity-induced risks, for example with the hazards

presented by commercial fission power plants, a system reliability requirement can be established in the form of a maximum tolerable activation product release rate. This requirement would attempt to prevent induced radioactivity in fusion plants from posing a greater risk to the public than conventional nuclear systems. Also, a comparison of the reliability requirements determined for activation product and tritium releases should reflect the relative hazards that the two forms of radioactivity represent in the risk assessment of fusion reactor systems.

2.2.1 Radioisotope Inventory

The first concern in assessing the potential radioactivity hazard is to determine the inventory and distribution of activity in the reactor system. Two reasonably well defined systems, UWMAK-I[3] and UWMAK-III,[4] will be used to exemplify the Tokamak-type fusion power reactor system. Studies have been made to determine the activation products which will be induced during the operation of these reactors. The two systems employ different blanket structural materials (316SS in UWMAK-I; TZM in UWMAK-III). Neither material was assumed to be tailored to minimize radioactivity. If such tailoring were to be used,[16] the total radioactivity would be substantially below that reported in References 3 and 4.

A calculational scheme has been developed at the University of Wisconsin to determine the blanket activation product inventories.[5] The model computes the activity per kilowatt for each radioisotope, which can then be divided by their maximum permissible concentration in air (MPC) to obtain a quantity known as the biological hazard potential (BHP). The MPC values are determined by the best available data on the biological effects of each radioisotope. When this biological data is lacking, a conservative, or low MPC value is used, resulting in a high BHP value for the particular isotope.

Using the BHP values from Reference (5), a list of significant isotopes was compiled for each structural material, excluding all isotopes with half lives less than 25.0 minutes and all those contributing less than approximately 1% of the total BHP of the remaining group. The half life criterion was used in the Reactor Safety Study (WASH-1400)[1] to simplify the consequence calculations by greatly reducing the number of radioisotopes that had to be considered. This is based on the assumption that these isotopes would contribute little hazard in an accident situation due to the delay between shutdown and the time it would take for radioactivity to reach the nearby population. The change in the total radioactivity between shutdown and 30 minutes is relatively small for the inventories studied here. The significant

isotopes are listed in Table 2.1. The activities, BHP values and the isotopes themselves are all subject to change as more information on biological effects of various radioisotopes is developed and the computational model is refined.

The activation products are concentrated in the blanket regions of the Tokamak reactor with a large fraction of the hazard potential in the first wall. Detailed descriptions of isotope distributions in the blanket regions are not available at present, however, they will only be necessary or useful when detailed accidental release mechanisms and sequences are defined.

2.2.2. Radioisotope Releases

Most of the attention given to induced radioactivity in fusion reactors has focused on the problems of waste disposal and reactor maintenance, and relatively little has been done to investigate its release into the atmosphere. The release of activation products requires the disruption of the first wall or blanket, escape of radioactivity from the reactor into the primary containment, and finally, a breach of containment structures. The first wall and blanket structures are part of a vacuum vessel which is surrounded by large magnet coils, piping and structural members. This assembly is encased in shielding and is completely enclosed by a primary containment.

TABLE 2.1

Activity and Biological Hazard Potential Values for the Dominant Radioisotopes at Shutdown after Two Years Operation

Radioisotopes	Structural Materials			
	316SS		TZM	
	activity (Ci/kWth)	BHP (km^3 air/kWth)	activity (Ci/kWth)	BHP (km^3 air/kWth)
Mn-54	75.6	75.6		
Mn-56	388.	19.4		
Fe-55	258.	8.6		
Co-57	26.0	26.0		
Co-58	131.	65.5		
Co-60	6.21	20.7		
Ni-57	4.5	4.5		
Zr-89			8.97	89.7
Zr-95			2.2	2.2
Nb-95			6.9	2.3
Nb-96			4.59	45.9
Mo-99	28.7	4.1	1204.	172.
Tc-99m			1450.	2.9

With an inert atmosphere and steel liners on exposed concrete surfaces, to prevent or mitigate the exothermic liquid metal reactions with air and concrete, the possible energy releases for a fusion reactor system appear to be smaller than for a fission system.

The possible energy sources for the disruption of the structures are the magnet system (including the liquid helium coolant), the plasma, the liquid metal coolants, and the after heat or decay heat in the first wall and blanket after shutdown. The plasma, with a total energy on the order of 10^9 J, could melt or vaporize part of the first wall if a quench was sufficiently localized.[4] However, this event itself is not likely to result in a breach of the reactor structures. The much larger stored energies associated with the toroidal magnetic field, which is on the order of 10^{11} J,[4] could result in disruption of part of the structures (see Figure 1.3) if there is a mechanism by which a sufficiently localized energy dump can occur. The helium coolant of the magnet system could potentially cause structural damage due to thermal interactions and overpressurization following its vaporization. Large amounts of heat energy could be generated by liquid metal interactions with air and concrete resulting in potential structural damage and volatilization of activation products. However, as discussed in Chapter III, lithium-air peak flame temperature is approximately 2500°K, which

would melt blanket materials like stainless steel, but not TZM. Also, it has been suggested that highly reactive chemical species such as oxygen, hydrogen and nitrogen could be released during liquid metal fires and may lead to the rapid ablation of the first wall materials.[2]

Much of the future work concerning the induced radioactivity will be directed towards determining how energy may be deposited in activated structures, the extent of possible material disruption and the amount and form of radioactivity which may be released from the reactor and the containment structure. This information is crucial for any attempt at assessing the possible hazards of induced radioactivity in a Tokamak fusion reactor.

2.2.3. Consequence Calculations and System Reliability Requirements

Preliminary studies have been performed to construct event trees for accident sequences,[2] but due to the conceptual nature of the reference designs, determination of release probabilities is practically impossible. However, using a

maximum permissible risk criterion, calculations of various release consequences can establish a maximum tolerable failure rate, which may in turn be used to set reliability requirements for major reactor system components. This approach avoids the necessity for detailed design definitions, which are not presently available and are not likely to be developed in the near future.

The calculations of release consequences requires the determination of the radioisotopes involved, the fraction of the inventory released to the atmosphere, the conditions which describe the radioactive plume, and specification of the weather conditions and population distrubution around the reactor site. In the present study, the computer code developed for the Reactor Safety Study (WASH-1400), the CRAC code, is being modified to handle releases of the activation products. The output of the consequence code, which is in the form of consequence probability distribution functions, can be used to determine the required limitations on failure rates. A description of the CRAC code and the methodology for determining the reliability requirements, along with a preliminary example of this technique, will be presented in the rest of this section of the report.

2.2.3.a Consequence Model[1]

The "Calculations of Reactor Accident Consequences" (CRAC) code was developed, as part of the Reactor Safety Study, to perform the computations to determine consequence

magnitudes and their probabilities for potential releases of radioactive materials following commercial nuclear fission power plant accidents. A schematic outline of the model is shown in Figure 2.1. The starting point for the calculation is the magnitude of radioactivity released to the atmosphere. For the commercial nuclear plants, the spectrum of releases were discretized into nine Pressurized Water Reactor and five Boiling Water Reactor categories, each with an associated probability of occurrence and release magnitude. (As applied in the present study, a certain fraction of the radioactivity inventory was assumed to be released, without assigning any probability for the release.) A meteorological model computes the dispersion and deposition of radioactive materials as a function of time after the accident and distance from the reactor. This model incorporates factors accounting for the decay of the radioactivity and includes the effects of thermal stability, wind speed and precipitation in a Gaussian dispersion model. The temporal variations of these weather parameters are obtained by using samples from a year's weather data from reactor sites. Variations of the mixing layer are included. The effects of the plume lifting off the ground due to the release of sensible heat is also included, and the plume is not allowed to penetrate the mixing layer.

Once the concentration of the radioactivity in the air and on the ground is determined, the model calculates the possible doses from various modes of exposure. These include external irradiation from the cloud and radioisotopes on the ground,

Figure 2.1

Schematic Outline of Consequence Model

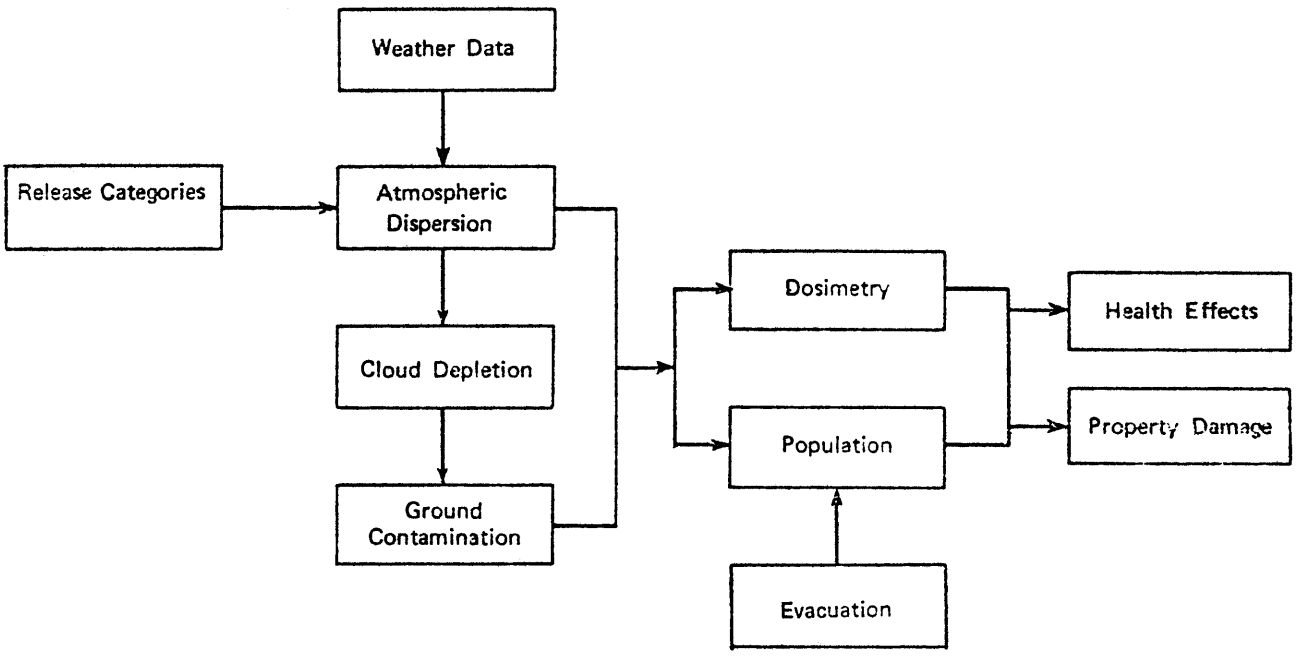

(from the Reactor Safety Study)

and internal irradiation from inhaled radioisotopes and ingestion of contaminated crops, water and milk. The distribution of people about the reactor site is used along with an evacuation model to obtain a set of doses for the affected population. These doses are transformed to actual health effects, such as early (within a year) fatalities, early illnesses, cancer deaths and genetic effects. The health effects are used as the measure of the accident consequences.

The final results, which include property damage in addition to health effects, are formed by combining the consequence probability distribution functions for the spectrum of release conditions at the various reactor sites using the spectrum of weather conditions. Thus, the assessment of a large number of individual reactor accidents is then expressed as a set of complementary cumulative distribution functions for each of the potential consequences.

2.2.3.b Example to Illustrate Methodology

A preliminary determination of the consequences of stainless steel activation product releases has been performed. Since specific values for the required parameters, which describe the possible releases, have yet to be defined for accidents in a Tokamak system, values were chosen which were similar to those used for fission reactor accidents in WASH-1400.[1] The values were varied to determine the sensitivity of the consequences to each parameter. Table 2.2 summarizes the cases that were investigated, where the reference case

TABLE 2.2

Release Conditions for Reference Case and Sensitivity Study

Parameter	Reference Case	Range of Variation: Sensitivity Study
release magnitude (percent of total inventory)	1.0	0.1 - 3.0
time between shutdown and release (hrs.)	0.5	0.25 - 1.0
warning time to evacuate (hrs.)	0.5	0.25 - 1.0
energy release rate (cal./sec.)	10^7	10^4 - 10^7
release height (m.)	25	1 - 25
duration of release (hrs.)	3.0	0.5 - 10.0

denotes the one used in the preliminary example calculations of system reliability requirements.

It was found that the consequence magnitudes were strongly dependent on certain conditions and parameter values. The reactor site population distribution and the release magnitude were the most influential parameters. The time delay between shutdown and release, the warning time to evacuate, the energy release, the duration of release, and the release height all had secondary effects on the consequence magnitudes. Table 2.3 summarizes the influence of these parameters.

To determine the actual reliability requirements, or admissible failure rates, the fusion reactor accident consequences must be compared to similar risk assessments for systems posing acceptable public hazard levels. Using the results of the Reactor Safety Study[1] to establish an acceptable hazard level for nuclear power generation, a probability distribution function for a particular fission reactor accident consequence can be compared with a normalized probability distribution function, or "risk profile," for the fusion reactor accident, to graphically produce a maximum admissible failure rate. This maximum tolerable frequency of occurrence prevents the public risks associated with a particular fusion reactor accident, or set of accidents, from exceeding the risks calculated for fission reactors. The same technique could be used to compare risk profiles

TABLE 2.3

Sensitivity of Consequence Magnitudes to Various Release Conditions

Parameter Increased	Change in Consequence Magnitudes
population density	increase
release magnitude	increase
time between shutdown and release	decrease
warning time to evacuate	decrease
energy of release	increase
release height	increase for illnesses; decrease for fatalities
duration of release	consequence increase for release durations of up to several hours (exact time depends on release magnitude), then decrease for longer durations

for fusion reactor accident consequences with other similar risk assessments that have been deemed to represent an acceptable level of risk.

As an example, Figure 2.2 contains the early fatality probability distribution curve for a fission plant on a highly populated site with particularly unfavorable weather conditions. Plotted on the same graph is the probability distribution profile for the same health effect consequence resulting from the release of about 1% of the Tokamak reactor inventory of stainless steel activation products. The fusion reactor is on the same site and the release occurs with the same weather conditions used for the fission reactor, and the release conditions are those of the reference case. The fusion curve is normalized in the consequence model because a frequency of occurrence equal to one per reactor-year is assigned to the release. The comparison process consists of placing the normalized curve on the probability-consequence graph as far up on the probability scale as is possible while remaining totally beneath the fission curve. The ordinate intercept, which in this case is 10^{-4} per reactor-year, determines the maximum allowable probability for the releases. It must be emphasized that these curves have been developed and used to demonstrate a methodology and should not be considered as having any significance in a risk assessment.

The same fusion reactor consequence probability profile may be compared to the early fatality complementary cumulative cistribution function for all fission

Figure 2.2

An Example of the Method to Determine Maximum Admissible Failure Rates Using Fission Risk Functions and Fusion Risk Profiles

Early Fatalities: Using the Highly Populated Site Fission Curve

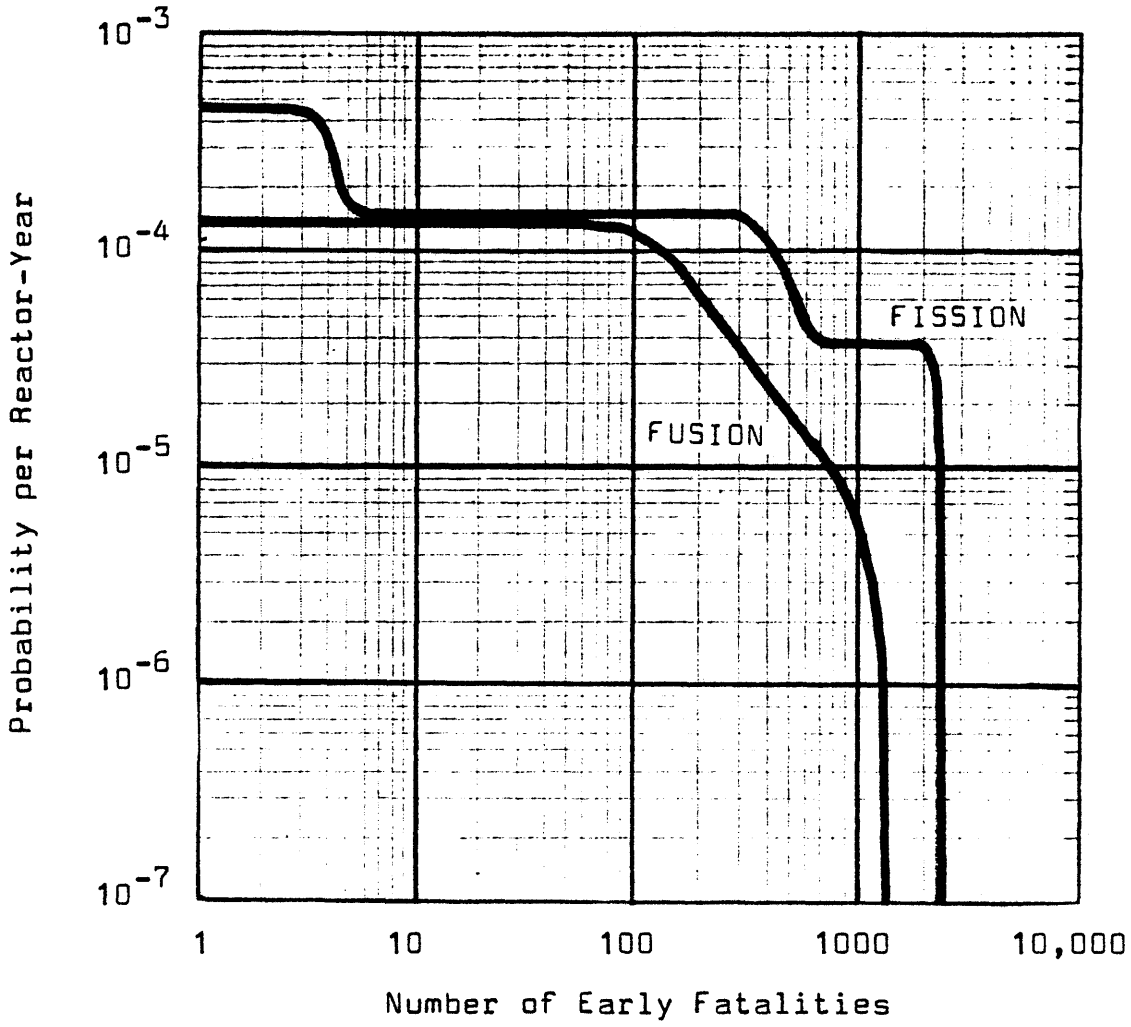

Note: Both computations employ the equivalent of an entire year of severe weather conditions, therefore, the results do not represent actual risk assessments.

reactors at the various sites and with the spectrum of weather conditions employed in the Reactor Safety Study. An allowable failure rate of 10^{-7} per reactor-year is then obtained revealing the inherent conservatism in using only the highly populated site for the fusion reactor. Further studies will include the development of composite curves for fusion reactors with various sites and weather conditions, providing a more valid comparison with the composite fission curves. Similar results are obtained from Figure 2.3 in which early illness probability distribution curves are compared. The preliminary reliability results are summarized in Table 2.4.

A particularly interesting relation between the admissible release rate and the release magnitude is shown in Figure 2.4. The two curves are derived from a series of normalized early fatality and early illness probability distribution profiles for various magnitudes of activated steel releases from a Tokamak reactor on a highly populated site, which were compared with the two corresponding probability distribution functions for fission reactor accidents on the same site with the same weather. The curves in Figure 2.4 reveal that the reliability requirements for the fusion system are very sensitive to the possible release magnitudes, and that releases of more than approximately 2% of the steel activation product inventory should be limited to the very low rates of less than 10^{-6} per reactor-year.

Figure 2.3

An Example of the Method to Determine Maximum Admissible Failure Rates Using Fission Risk Functions and Fusion Risk Profiles

Early Illnesses: Using the Highly Populated Site Fission Curve

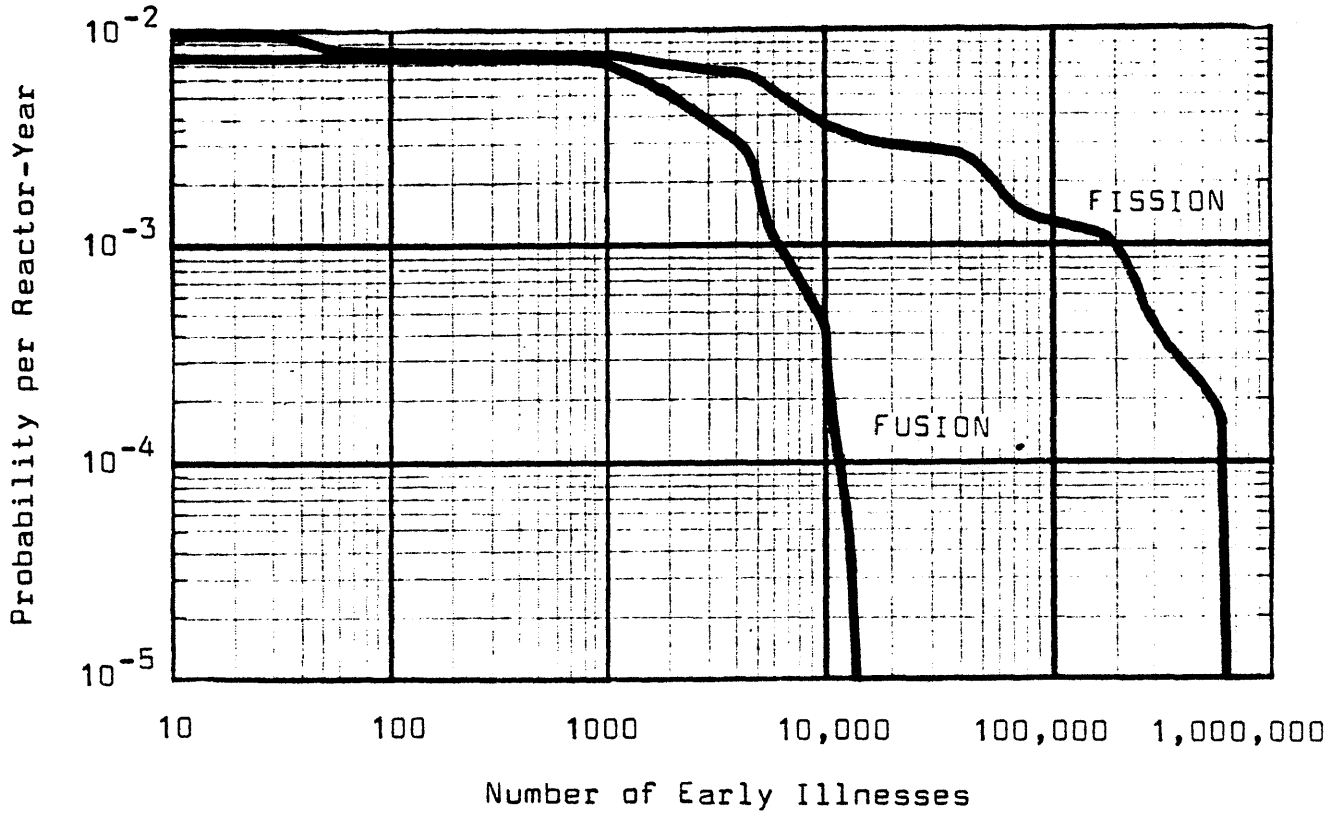

Note: Both computations employ the equivalent of an entire year of severe weather conditions, therefore, the results do not represent actual risk assessments.

TABLE 2.4

Exemplary Reliability Requirements from Comparisons of Fission Risk Curves and Fusion Risk Profiles

Fusion Profiles (1% inventory release)	Fission Curves (from WASH-1400)	Admissible Failure Rate (per reactor-year)
early fatalities	early fatalities: high pop. site	1×10^{-4}
early illnesses	early illnesses: high pop. site	7×10^{-3}

Figure 2.4

Sensitivity of the Exemplary Reliability Requirements to the Stainless Steel Activation Product Release Magnitudes

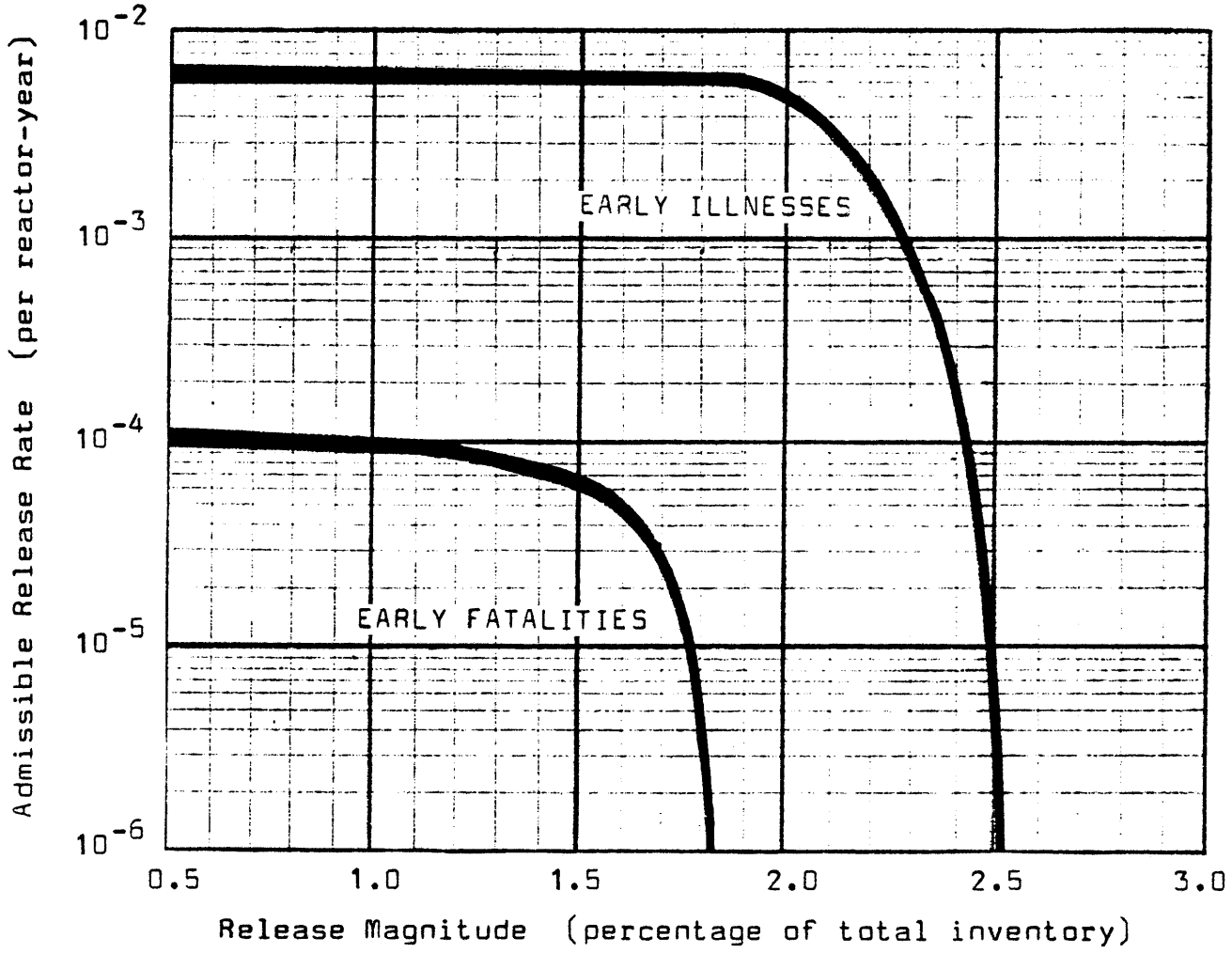

Note: The numerical values are not as significant as the properties or characteristics of the functions.

A similar methodology can be used to investigate other possible structural materials. Initial considerations of a TZM first wall have been undertaken.[6] Analysis of the response of first wall materials to an energy dump reveal that the relative melting rates for TZM and stainless steel depend on the rate of the energy dump. For an energy dump during which material ablation does not occur, TZM melts faster than the steel. If material ablation is involved, the steel will have the higher melting rate. Since the molybdenum alloy has a larger BHP value associated with its induced activity, it appears that TZM may pose a greater hazard than the stainless steel when considering release accidents. Further study will investigate the effects on the consequences and reliability requirements of this material choice.

Future efforts concerning the potential hazards of induced radioactivity will center on the determination of important parameters describing possible release accidents in Tokamak systems. Knowing these parameters with greater certainty, more realistic consequence calculations may be performed and the subsequent reliability requirements may serve as a valid basis for system designs. Most importantly, however, a methodology with which a radiological hazard may be translated into system reliability requirements will be demonstrated.

2.3 Tritium Radioactivity Releases

One of the most abundant radioisotopes which will be present in fusion reactors operating with the deuterium - tritium fuel cycle is tritium, an isotope of hydrogen that decays via beta emission with a half life of 12.36 years.

Tritium inventories in proposed fusion reactor designs range from 5 to 36 kilograms (about 5×10^7 to 36×10^7 curies). In the latter case, this amount represents about three times the present (1977) natural, steady-state inventory of the atmosphere. Boiling water reactors release from 1 to 100 Curies/reactor/year whereas pressurized water reactors release about 600 Curies/reactor/year. In 1963 the total tritium inventory in the atmosphere went as high as 2000 MCi because of atmospheric weapons testing.[7]

A limiting factor in fusion reactor environmental impact and safety research is the lack of detailed design data. The UWMAK-III conceptual Tokamak fusion reactor has been examined for tritium hazards since the design report for this reactor has the most developed tritium handling system described for fusion reactors.[4] The analysis of the tritium hazards in the UWMAK-III reactor design will in a large part be applicable to other conceptual fusion reactor designs using a D-T fuel cycle.

There are four types of coolant used in the UWMAK-III design. The inner hot shield is cooled by helium gas which is circulated in a closed cycle to a helium turbine which produces 585Mw(e).

Energetic tritons and alpha particles diffusing from the plasma are diverted via magnetic fields and impinge on the divertor section of the vacuum chamber. The heat deposited in the divertors is transferred via a liquid sodium loop through a steam generator to a conventional Rankine cycle steam turbine system which produces 285 Mw(e).

The plasma operates on a deuterium-tritium cycle and for this reason it is desirable to breed tritium in the reactor. This is accomplished by the use of liquid lithium as a blanket material in the outer portion of the torus. The 14.1 Mev neutrons produced by the fusion reaction interact with the lithium via:

$$^{6}Li + n = {}^{4}He + {}^{3}H.$$

The liquid lithium then goes to an intermediate sodium heat exchanger and this sodium then flows through a sodium-helium heat exchanger. The hot helium is then used to drive two turbines which are identical to the turbine used in the inner blanket power cycle.

The fusion reaction in the Tokamak is pulsed with a plasma burn time of thirty minutes. The duty factor of the power cycle is 95%. During the down time of the cycle it is necessary to provide a thermal storage medium so that the production of electricity in not interrupted. The intermediate sodium serves in this capacity. The total power system uses dry cooling towers for waste heat rejection. The power cycle flow diagram is shown in Figure 2.5.

Figure 2.5 Flow Diagram for UWMAK-III
(from Reference 4)

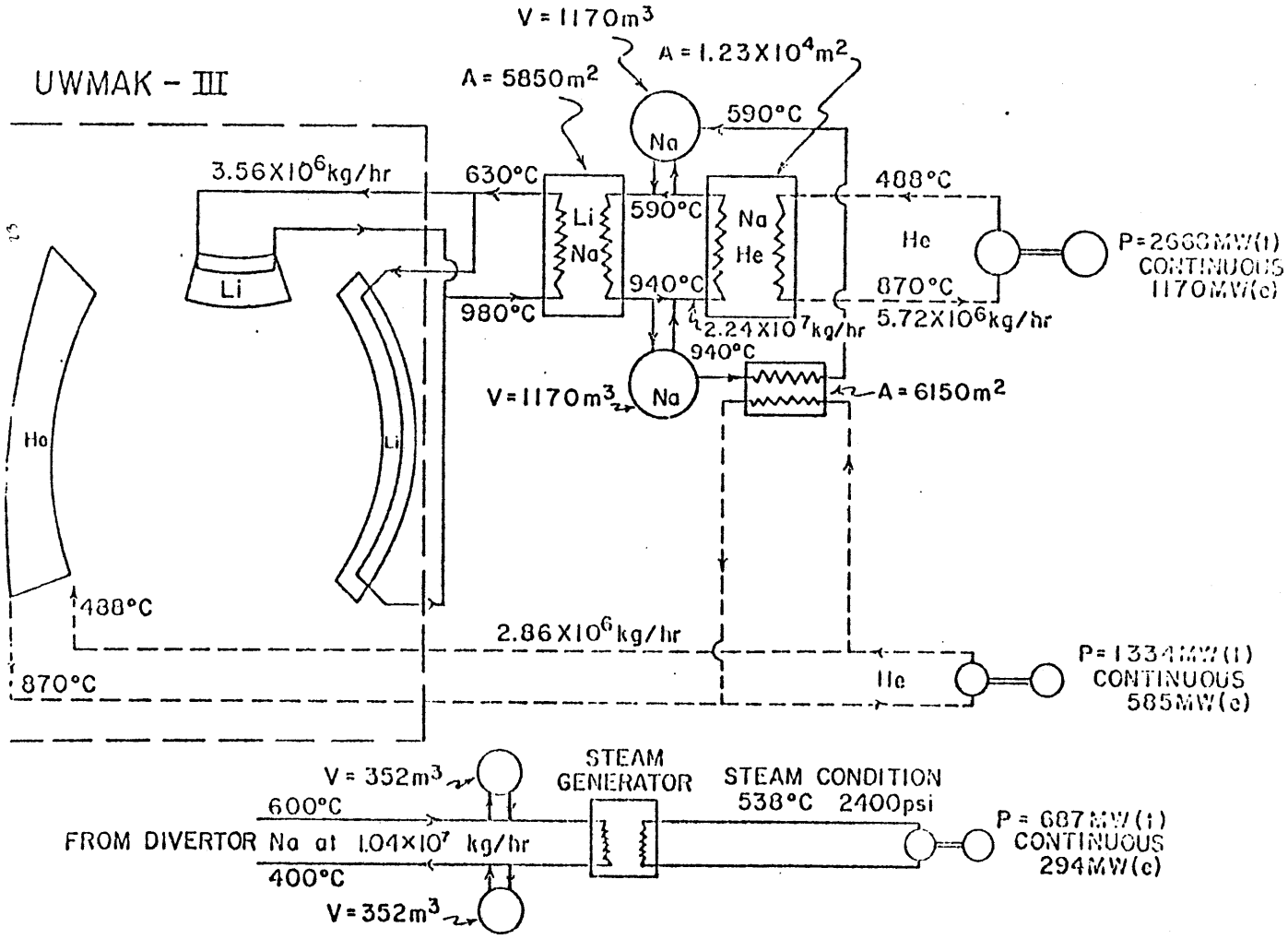

2.3.1 The Tritium Fueling System

The tritium extraction system in UWMAK-III has been designed to maintain a tritium partial pressure in the containment of 7.6×10^{-10} Torr. This is achieved by back-designing the coolant system and fuel extraction devices to insure loss rates to the building environment of less than 1 Curie per day. The tritium handling facilities of the UWMAK-III system are outlined in Figure 2.6.

The steady-state tritium concentration in the lithium is about 2.08 ppm. The circulation rates and inlet and outlet temperatures of the heat transfer fluids are shown in Figure 2.5. The lithium passes over a niobium-palladium-yttrium "window" designed like a heat exchanger and the tritium diffuses through the window. The tritium then emerges on the downstream side where it catalytically reacts with oxygen in a flowing helium stream. The T_2O is then adsorbed on molecular sieves and the helium and oxygen are recycled. The sieves are regenerated by heating and the T_2 is sent to the tritium storage area. As is the case with most of the fuel separation columns in the UWMAK-III system, this section is operated in tandem modes--while one set of adsorbers is collecting tritium, the other set is regenerating.

The production of tritium in the liquid lithium is accompanied by the production of an equal amount of helium. Impurities cleanup and helium venting would require diversion of about 1% of the lithium flow whereas the tritium extraction system would require diversion of about 5% of the total lithium flow.

Figure 2.6 Tritium in UWMAK-III System

(from Reference 4)

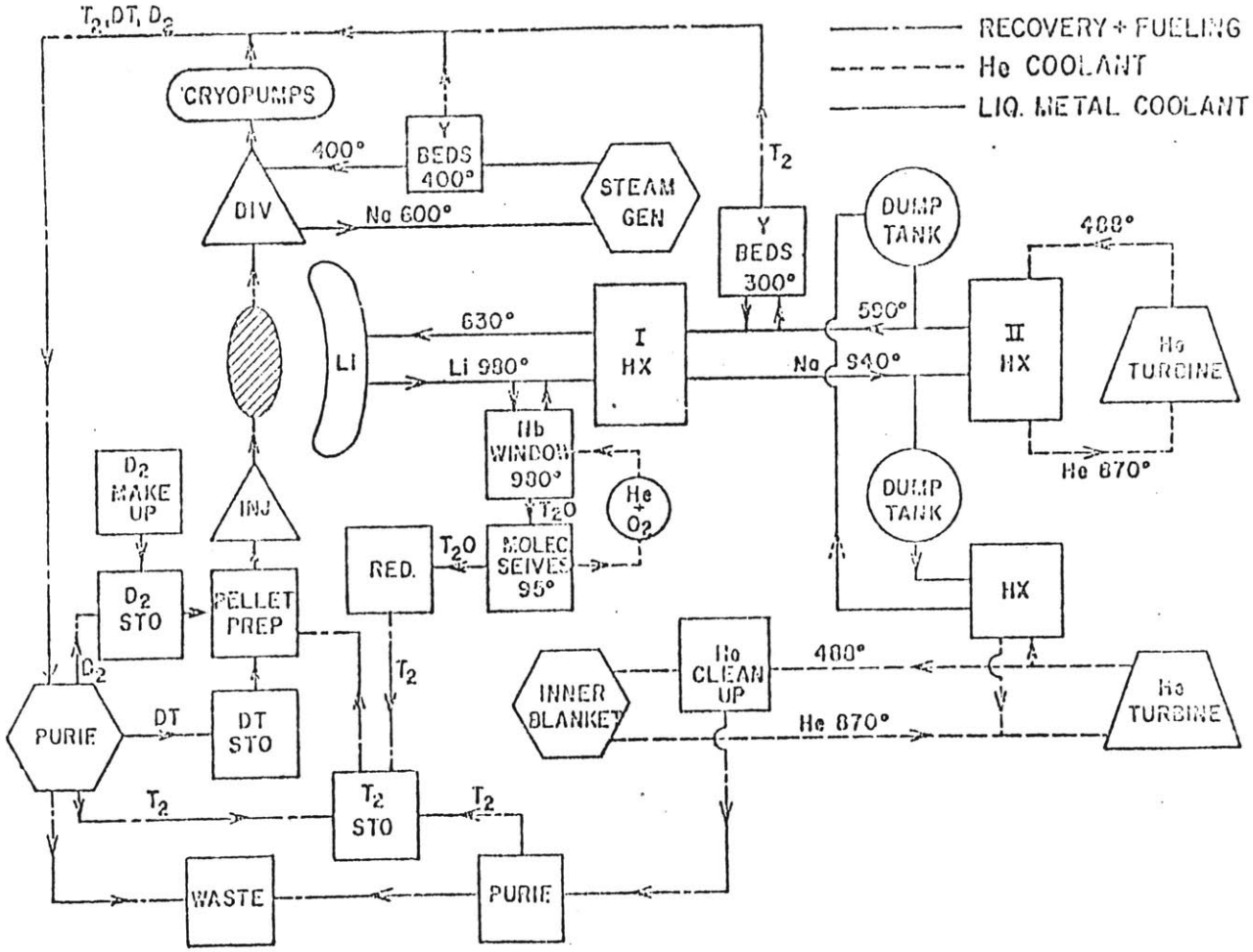

Tritium diffuses into the sodium IHX and into the sodium in the divertor power system. This tritium must be extracted. In both cases, the cold leg sodium will react with a yttrium getter bed system operating in tandem modes.

Tritium can form in the inner shield via neutron interaction with the boron in the boron carbide. This tritium can diffuse into the inner blanket helium coolant. Since this helium goes directly to the turbine hall it must be continually processed for the removal of tritium.

The tritium extracted from the lithium blanket flow is transferred to the T_2 storage facility. The T_2 is stored in a gaseous form, under pressure, in an austentitic stainless steel tank. The tritium extracted from the yttrium beds and the helium cleanup system must first be purified before use as a fuel.

Solid fuel pellets are injected into the torus during the burn cycle. 1.63 kg of T_2 and 1.085 kg of D_2 are injected during the burn. Only 0.620 kg of T_2 and 0.413 kg of D_2 are consumed. The unburned fuel is collected in cryopumps and adsorbed on molecular sieves. One set of cryopumps is in operation while the other set is being regenerated. The process stream is purified and the various hydrogen isotopes are separated and sent to storage.

The total tritium inventory in UWMAK-III is reported to be 35.8 kg. A complete description of the tritium handling system can be found in the reference design report.[4]

2.3.2 Containment Systems and Equipment Locations

The plant schematic for the reference design is shown in Figure 2.7. The four buildings that are of primary concern in this analysis are the reactor containment building, the heat exchanger building, the auxiliary building, and the turbine hall. Only the latter does not have a specified emergency detritiation system.

The emergency containment detritiation system is designed to process the building atmosphere for tritium removal in the event of a release. The buildings are designed to operate with inert atmospheres but this may be neither economical nor practical. In any case, a normal atmosphere must be used for maintenance operations.

Additional safety can be provided by the use of secondary containment systems used to isolate components with high tritium inventories. Techniques similar to those developed at Mound Laboratories can be used to control tritium releases from such components.[9]

The tritium bearing systems of major concern in the reactor containment area:

Helium piping
Sodium piping
Lithium piping
Vacuum chamber
Cryopumps
Pellet Injection system

The sodium and helium piping are exposed to the reactor room. The lithium piping is double walled to decrease the tritium permeation rates and permit the passage of a helium sweep gas through the annulus.

Figure 2.7
Plant Schematic - UWMAK-III
(from Reference 4)

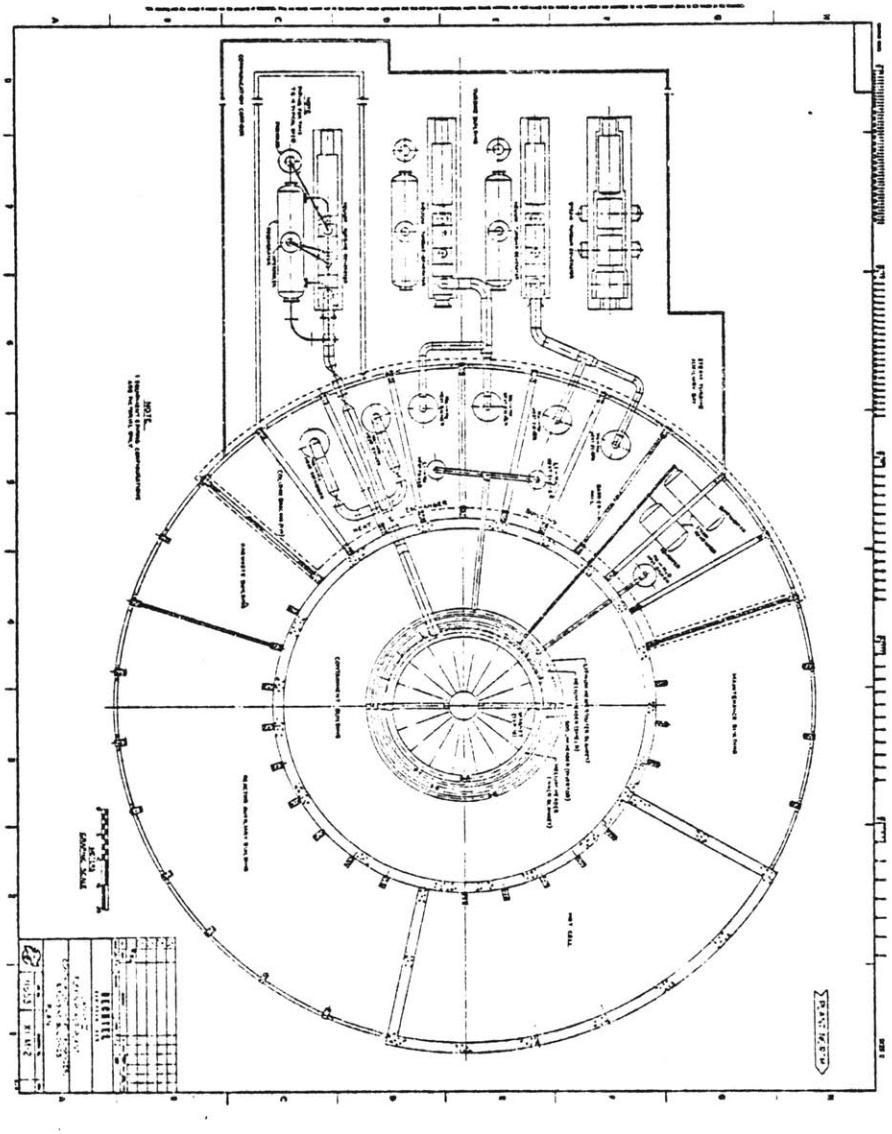

The torus is composed of 18 removable sections which are replaced every 2 years. Since some leakage is expected through the seals, the design calls for a chamber to surround the torus, field coils, and cryopumps. This chamber will be held at 75 Torr to reduce pumping losses. This chamber may need a detritiation system. The pellet preparation system and the pellet injector are also prime candidates for glovebox detritiation systems because of their unusually high tritium inventories.

The tritium bearing systems of major concern in the heat exchanger building are:

- Helium piping
- Main lithium piping
- Diverted lithium piping
- Divertor yttrium beds
- IHX yttrium beds
- Sodium impurities cleanup lines
- Regenerators and heat exchangers

Sufficient design data is not available to determine whether secondary containments are feasible in the heat exchanger building. Whereas the yttrium beds are located near the main sodium lines, the regenerated tritium must be pumped to the auxiliary building for purification. About 1% of the sodium from the Divertor and IHX can be channeled to the auxiliary building for cleanup. Likewise, 5% of the lithium stream can be diverted to the auxiliary building for tritium extraction and cleanup. The only tritium not contained in the liquid metal coolants in the heat exchanger building is in the yttrium bed process lines. The coolant tritium inventories would be released only in the event of a sodium or lithium spill. Releases from these

types of spills are under investigation.

All tritium fuel recovery, purification, and isotope separation should be performed in the auxiliary building. The major systems of concern are:

Li-Na-He cleanup systems
Tritium recovery from lithium
Tritium purification system
Isotope separation and storage

Each of these systems can be contained in an isolated glovebox to minimize the hazards of tritium release. The possibility of liquid metal fires exists in two of the containments while the possibility of hydrogen explosion exists in the storage area. The atmospheres of the gloveboxes and the auxiliary building may be inert. It may be necessary to forego this feature since some "hands-on" manipulation of the fueling equipment may be desired. Nevertheless, the tritium recovery systems require oxygen in the molecular sieves to catalyze the tritium. This may increase the possibility of an explosion.

The possible tritium releases, and hence, hazard potential for the UWMAK-III system are listed in Table 2.5. Estimates of the releases from major systems components are designed to reflect a conservative viewpoint. The inventories used are peak inventories, ignoring the fact that in a given system the inventory may cycle from zero to peak as a function of time. The estimates for releases from piping are based on the inventory or the coolant from UWMAK-III design data. Errors in these estimates may stem from:

TABLE 2.5

Possible Tritium Release Inventories

Reactor Room Containment:	Curies
Helium Piping	ND*
Sodium Piping	6.00×10^3
Lithium Piping	5.60×10^5 Ci/Loop
Vacuum Chamber	1.01×10^7
Pellet Injector	1.63×10^7
Cryopumps	7.75×10^7
Heat Exchanger Building:	
Helium Cleanup	ND
Helium Piping	ND
Diverted Sodium Piping	2.00×10^3
Diverted Lithium Piping	5.00×10^5
IHX Yttrium Beds	1.60×10^3
Divertor Yttrium Beds	5.10×10^3
Main Lithium Piping	5.60×10^5 Ci/Loop
Auxiliary Building	
Cleanup Systems	1.00×10^5
Lithium Recovery System	2.50×10^7
Purification System	7.75×10^7
Storage and Isotope Separation	1.86×10^8

* Helium piping tritium inventories are crucially dependent on the type of tritium cleanup system used. This was not specified in UWMAK-III.

Uncertainty in the tritium permeation rates
Inefficiencies in tritium cleanup devices
Surface adsorption of tritium on pipes
Uncertainty in breeding ratios
Lack of design data for valves and pumps.

The tritium released from coolant piping will probably not represent the principle hazard. The importance of such pipe breaks relates to liquid metal fires which may be the initiating event for serious tritium accidents.

Preliminary hazard diagrams for each of the three major containment buildings are sketched in Appendix I.

2.3.3 The Chemical Forms of Tritium

The beta particle from tritium decay has a maximum energy of 18 Kev and an average energy of 5.7 Kev. The maximum range of the tritium beta in skin tissue is about 0.005 mm. This is not sufficient to penetrate the dead epidermal skin layer of the human body. External doses from tritium are negligible. When tritium in the form of T_2 or HT is inhaled in the lungs about 0.4% will be retained in the body. All the tritium inhaled in the oxide form (HTO or T_2O) will be retained. Under conditions of uniform immersion in a cloud of HTO, the amount of tritium transpired through the skin will equal the amount absorbed by the lung tissue in a normal man. It is therefore essential to specify the form of the tritium in the dispersed plume following a reactor accident.[8,10]

Four mechanisms exist for the conversion of HT to HTO; namely,

1) Isotopic exchange with hydrogen

2) Autoradiolytic oxidation

3) Catalytic reaction on active metal surfaces

4) Reaction with O_2 in the presence of a radiation field.

A summary of tritium conversion experiments is listed in Table 2.6. The rate constants, the orders of the reactions and the experimental conditions reported by the investigators are listed. Figure 2.8 is a plot of the conversion rate of tritium to the oxide form versus initial T_2 concentration for the various experiments reported. Substantial disagreement exists in the determinations of the rate constants, the order of the reaction, and in the determination of the rate controlling mechanism. In the latter case, Eakins and Hutchison have demonstrated that the conversion rates are substanially higher in humid air for a wide variety of conditions. This suggests that the isotopic exchange process is dominant. However, Belovodskii found that the conversion rates in air with 50% humidity and in an argon-tritium-oxygen system were nearly identical, leading him to conclude that the dominant process was radiolytic oxidation.[11]

Two cases of tritium accidental release from the Savannah River Plant are described in Table 2.7. On May 2, 1974, a 479,000 Ci release of T_2 from a 200 ft exhaust stack occurred.[12] A tritium forms sampler located at Springfield, S.C. (the

TABLE 2.6

Summary of Tritium Conversion Work

Investigator	Conditions	Rate Constant	Order
Dorfman (1955)	$2T_2 + O_2 \rightarrow 2T_2O$ Oxidation at high tritium concentrations	1.2×10^{-4}/min.	1
Casaletto (1962)	$2T_2 + O_2 \rightarrow 2TO$ Oxidation at $T_2(0)$ between 10^{-2} and 1 curie/liter	$1.03 \times 10^{-5} \frac{L}{Ci\text{-}min.}$	2
Yang Gevantman (1964)	$T_2 + H_2O \rightarrow HT + HTO$ Isotopic exchange in inert atmosphere	$2.5 \times 10^{-5} \frac{L}{Ci\text{-}min.}$	2
Eakins Hutchinson (1973)	Oxidation in dry air	$0.933 \times 10^{-5} \frac{L}{Ci\text{-}min.}$	2
	100% humidity in air	$4.83 \times 10^{-5} \frac{L}{Ci\text{-}min.}$	2
	Brass: Dry	$1 \times 10^{-5} \frac{L}{Ci\text{-}min.}$	2
	Humid	$1.43 \times 10^{-3} \frac{L}{Ci\text{-}min.}$	2
	Steel: Dry	$7 \times 10^{-5} \frac{L}{Ci\text{-}min.}$	2

TABLE 2.6 (cont.)

Investigator	Conditions	Rate Constant	Order
	Steel:		
	Humid	$1.01 \times 10^{-3} \frac{L}{Ci\text{-}min.}$	2
	Aluminum:		
	Dry	$6.5 \times 10^{-5} \frac{L}{Ci\text{-}min.}$	2
	Humid	$1.6 \times 10^{-4} \frac{L}{Ci\text{-}min.}$	2
	Platinum:		
	Dry	$4 \times 10^{-4} \frac{L}{Ci\text{-}min.}$	2
	Humid	$1.4 \times 10^{-2} \frac{L}{Ci\text{-}min.}$	2
Belovodskii (1975)	Oxidation isotope exchange $T_2(0)$ between	$\frac{d(HTO)}{dt} = 10^{-6} C_T^{5/3}$	
	10^{-3} and 10^{3} ci/L	$\frac{Ci}{Li\text{-}min.}$	5/3
		C_T in curies	

Figure 2.8 Experimental Observations of T_2 Conversion Rates

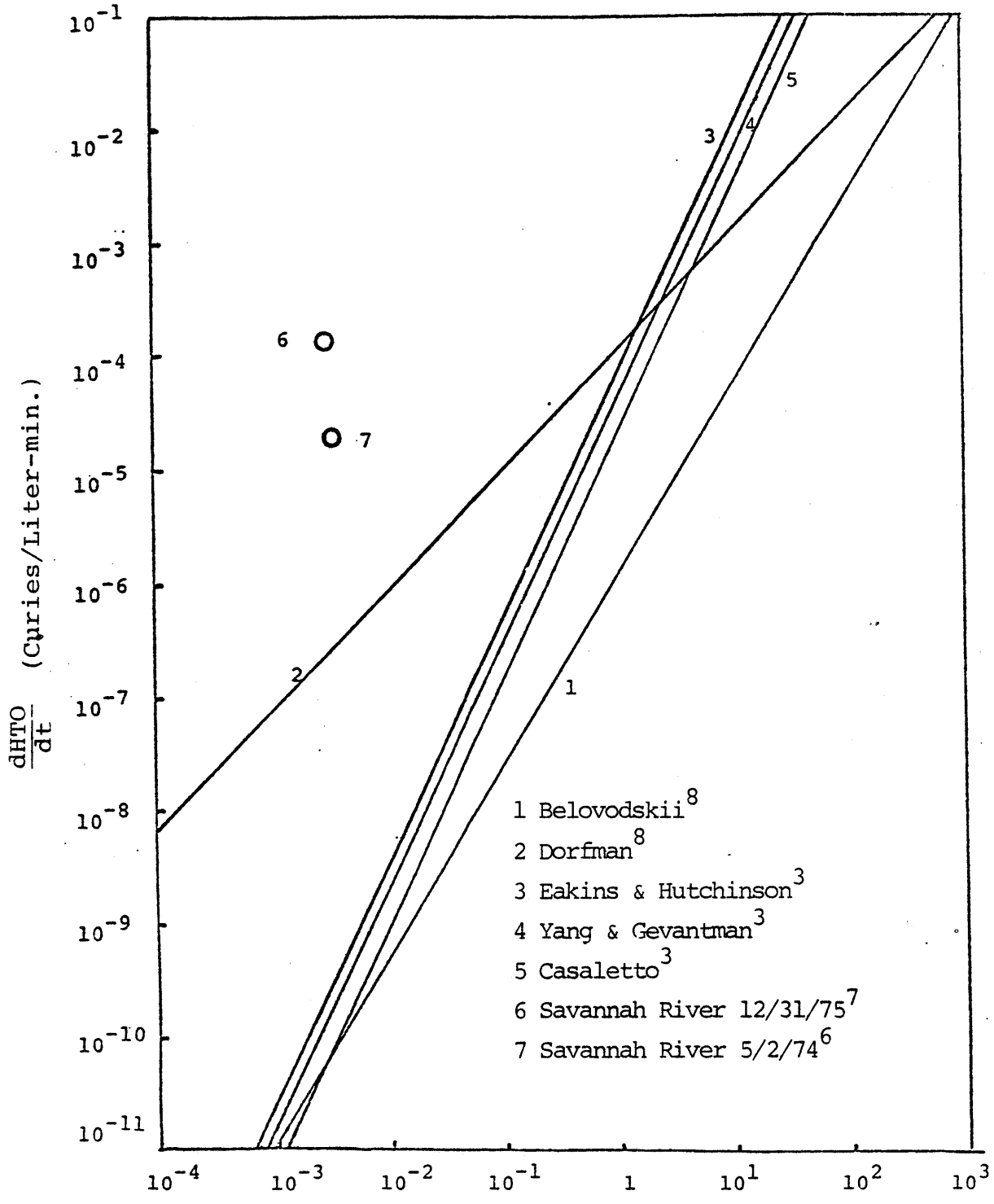

TABLE 2.7

Savannah River Release Incidents

	5/2/74	12/31/75
Amount of Release	479,000 Ci	182,000 Ci
Form at Release	T_2	T_2
Location of oxide (HTO) Detector	Springfield, S.C., 20 miles (5 Hr.) Downwind of Plume Centerline	in stack
% Detected as Oxide	0.213%	0.6%
Duration of Release	4 min. (99%)	1.5 Min (90%)
Exhaust Flow	135,000 ft^3/min	135,000 ft^3/min
Total Liters of Air in Mixture	13,804,034	5,637,500
Average T_2 Conc.	13 PPM (Vol)	12 PPM (Vol)
T(o) (Total Mixing)	.0347 Ci/L	.032 Ci/L
$[T_2]$ at Fencepost	ND	10^{-7} Ci/L
Curies (HTO) Formed	1020.27	1092
Curies (HTO) Formed Per Liter	7.39×10^{-5}	1.92×10^{-4}
Curies (HTO)/L-Min	1.85×10^{-5}	1.28×10^{-4}

plume centerline) showed a relative HTO-HT concentration of 0.2% after five hours from the time of release. Assuming that all the HTO formation occurred in the stack during the four minute residence period, the tritium conversion rate is much higher (orders of magnitude) than the reported conversion rates, as shown in Figure 2.10.

During the release of December 31, 1975, stack gas monitors detected that 0.6% of the 182,000 Ci released was in the oxide form.[13] Furthermore, the report states that the oxide was probably formed after the release incident. A similar analysis for this release is presented in Table 2.7. The results are plotted in Figure 2.8. Once again, prediction and actual operating experience differ by several orders of magnitude. The uncertainty in the SRP data casts some doubt on the validity of the comparisons. However, the degree of discrepency indicates that a need for experimental verification of the tritium conversion rate is required.

Some of the tritium in proposed fusion reactor designs will already be in the oxide form. The best example is tritium cycled through molecular sieves or dessicant beds. This tritium represents a greater hazard than tritium in the elemental form. In the event of a fire or an explosion, the conversion of the T_2 to the oxide form will be nearly complete. Data from nuclear explosive tests appears to support this contention.[10] Oxygen must be assumed to be present if the containment ruptures or if the accident occurs

during maintenance operations. Additionally, the requirement of an inert atmosphere is not rigid so that come containments may be operated with normal atmospheres.

For steady-state releases, the tritium must travel a release pathway which will in most circumstances result in tritium in the oxide form. For instance, tritium may diffuse from the divertor sodium into the steam generator and eventually end up in the condenser water. Tritium passage through water results in almost complete conversion to the oxide form. Low level steady-state tritium emissions can be characterized by long tritium migration times and releases via piping in the power cycles which will come in contact at some point with condenser water.

A large spectrum of possible tritium releases can be envisioned. They extend from low level steady-state tritium-oxide emissions through larger releases of T_2, HT or HTO in accident modes to possible large level HTO releases under "worst case" accident conditions.

The chemical behavior of tritium during lithium or sodium fires is an important concern. The chemical equilibrium code TRAN72 has been used to investigate the potential behavior of tritium during lithium fires.[14] A description of the code is given in Section 3.2.2. One of the main assumptions of the thermodynamic model is that equilibrium has been reached. All of the free energy liberated goes into the formation of products at the equilibrium temperature. The chemical behavior of the lithium-nitrogen-oxygen-hydrogen system has been examined

with emphasis on the chemical composition of the hydrogen products. Tritium was taken to be the only isotope of hydrogen in the system.

Tables 2.8 to 2.12 list the various hydrogen products formed, their relative percentage of all hydrogen products, and the equilibrium temperature of the reactants for a wide range of lithium to air and hydrogen to air molar ratios. The principal forms of the hydrogen released appear to be LiH, LiOH, H_2O, and H_2. Lithium hydride is a solid below 953 ^{o}K whereas LiOH solidifies below 723 ^{o}K. The decomposition temperatures of LiH and LiOH are 1245 ^{o}K [15] and 1197 ^{o}K respectively. Under certain initial conditions, the temperature of the reaction is below the melting points of these materials. In these cases, the tritium release may be decreased on account of the condensible nature of these gases.

A single loop of the UWMAK-III lithium heat removal system contains about 3.16×10^6 moles of lithium. The containment volume is capable of containing 1.12×10^7 moles of air at STP. Under the equilibrium assumptions, with complete mixing, the lithium to air molar ratio is about 0.282. Figure 2.9 shows the behavior of the principal hydrogen products at various hydrogen to air molar ratios for the lithium to air molar ratio of 0.212.

As an example, consider the release of the tritium inventory in one of the cryopumps (7.75×10^7 Ci). For a lithium fire involving the loss of the lithium in only one

TABLE 2.8

Percent of Hydrogen Released Which Forms the Designated Product Versus $(H_2)/(AIR)$ for $(Li)/(AIR) = 0.0021$

$\frac{(H)}{(AIR)}$	.00106	.00212	.01	.0212	.05	.212	.5	.9	2.12	21.19
PRODUCT										
H							.465	.096		
H_2						.005	15.785	52.963	80.085	93.225
H_2O		50	89.4	95	97.9	99.420	83.113	46.811	19.911	1.990
OH						.075	.436	.008		
NH_3									.004	4.781
$Li_2O_2H_2$										
LiH										
LiH(s)										
LiOH						.499	.201	.113		
LiOH(s)	100	50	10.6	5	2.1					.005
T(°K)	335	344	408	497	714	1656	2382	2025	1404	511

TABLE 2.9

Percent of Hydrogen Released Which Forms the Designated Product Versus $(H_2)/(AIR)$ for (Li)/(AIR) = 0.0212

$\frac{(H)}{(AIR)}$	.00106	.00212	.01	.0212	.05	.212	.5	.9	2.21	21.19
PRODUCT										
H							.468	.092		
H_2						.005	17.438	53.984	80.494	93.591
H_2O	.944	.475	4.16	50	90.423	94.904	79.715	44.789	19.157	1.900
OH						.102	.377	.008		
NH_3									.004	4.459
$Li_2O_2H_2$						.021			.014	
LiH								.001		
LiH(s)										
LiOH						4.973	2.000	1.127	.330	
LiOH(s)	99.056	99.525	95.84	50	9.577					.050
T(^{O}K)	542	554	642	727	889	1704	2373	2017	1414	515

TABLE 2.10

Percent of Hydrogen Released Which Forms the Designated Product Versus $(H_2)/(AIR)$ for (Li)/(AIR) = 0.212

	$\frac{(H)}{(AIR)}$	.00106	.00212	.01	.0212	.05	.212	.5	.9	2.12	21.19
PRODUCT											
H							.014	.350	.055	.003	
H_2							.148	34.324	63.980	84.961	96.569
H_2O		2.0	4.489	16.676	26.513	36.072	50.844	46.136	24.938	13.325	1.001
OH		0.5	.499	.531	.452	.377	.575	.069	.002		
NH_3										.002	1.930
$Li_2O_2H_2$				.106	.151	.216	.077	.008	.038	.028	
LiH								.025	.017	.001	
LiH(s)											
LiOH		97.5	97.012	82.687	72.885	63.335	48.343	19.087	10.970	1.678	
LiOH(s)											.500
T(^{o}K)		1846	1845	1843	1845	1870	2103	2243	1927	1607	565

TABLE 2.11

Percent of Hydrogen Released Which Forms the Designated Product Versus $(H_2)/(AIR)$ for (Li)/(AIR) = 1.06

$\frac{(H)}{(AIR)}$	.00106	.00212	.01	.0212	.05	.212	.5	.9	2.12	21.19
PRODUCT										
H		.339	.292	.347	.472	.500	.251	.131	.031	
H_2				.208	1.614	55.407	81.717	91.389	98.416	99.352
H_2O			.146	.485	1.401	3.125	1.809	1.006	.192	
OH		.339	.219	.173	.076	.004				
NH_3									.003	.148
$Li_2O_2H_2$					.024		.012	.008	.002	
LiH			.073	.139	.289	1.046	.776	.536	.246	
LiH(s)										
LiOH	100	99.322	99.271	98.648	96.147	39.893	15.435	6.929	1.110	
LiOH(s)										.500
T(^{O}K)	2484	2483	2470	2449	2383	2182	2092	2015	1843	746

TABLE 2.12

Percent of Hydrogen Released Which Forms the Designated Product Versus $(H_2)/(AIR)$ for (Li)/(AIR) = 2.12

$\frac{(H)}{(AIR)}$	.00106	.00212	.01	.0212	.05	.212	.5	.9	2.21	21.19
PRODUCT										
H				.057	.245	.006	.003	.002		
H_2	49.44	60.23	79.03	84.659	90.024	95.074	96.878	97.907	98.990	96.866
H_2O										
OH										
NH_3								.005	.003	.034
$Li_2O_2H_2$										
LiH	50.56	39.77	20.97	14.772	9.927	4.865	3.093	2.086	1.007	
LiH(s)										3.000
LiOH					.245					
LiOH(s)										
T(^{O}K)	1651	1651	1648	1645	1636	1586	1515	1490	1426	896

Figure 2.9 Hydrogen Product Chemical Form as a Function of $(H_2)/(AIR)$ Molar Ratio for (Li)/(AIR) = 0.212

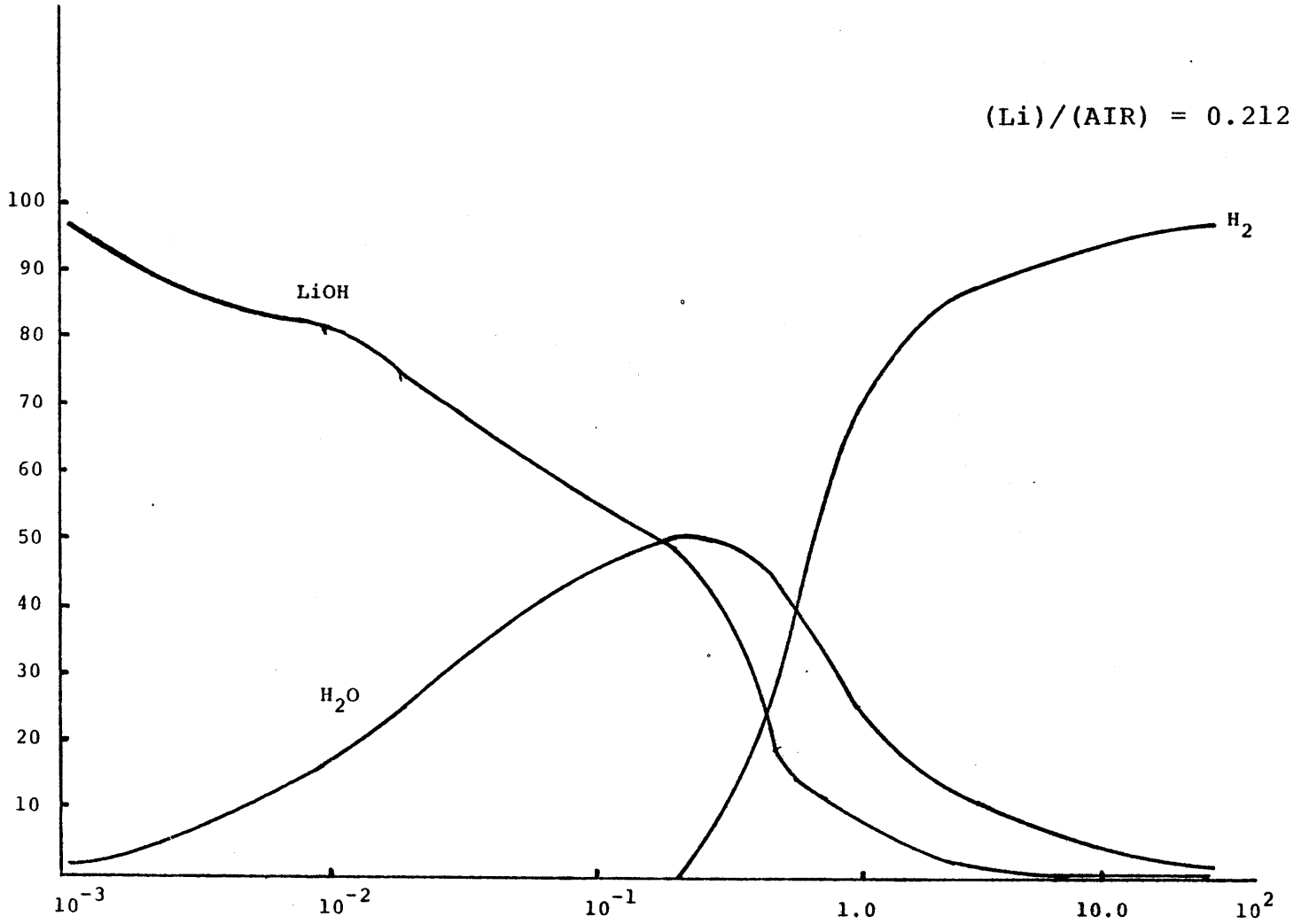

of the 18 coolant loops in the UWMAK-III system, a hydrogen to air molar ratio of 3.5×10^{-4} results. Figure 2.9 shows that the limiting behavior of the products at low hydrogen concentration favors the formation of condensible hydrogen hydroxide. At high concentrations (corresponding to tritium releases which are in confined spaces) a trade off begins between the formation of lithium hydroxide and water. Of course, if the fire occurs in a confined space the lithium to air molar ratio may be higher than 3.5×10^{-4}. At much higher hydrogen to air molar ratios, more hydrogen is available than can be consumed in the reaction.

Chapter II References

1. Reactor Safety Study; WASH-1400; United States Nuclear Regulatory Commission; October 1975

2. D. Okrent, et. al.; "On the Safety of Tokamak-type, Central Station Fusion Power Reactors;" Nuclear Engineering and Design, 39, 1976, pp. 215-238.

3. R. W. Conn, et. al.; A Wisconsin Tokamak Reactor Design, UWMAK-I; UWFDM-68; Nuclear Engineering Dept., University of Wisconsin; November 1973.

4. R. W. Conn, et. al.; UWMAK-III, A Noncircular Tokamak Power Reactor Design; UWFDM-150; Nuclear Engineering Dept., University of Wisconsin; July 1976.

5. W. F. Vogelsang; Radioactivity and Associated Problems in Thermonuclear Reactors; UWFDM-178; Nuclear Engineering Dept., University of Wisconsin; September 1976.

6. M. W. McQuade; "A Comparison of the Response of Fusion Reactor First Wall Materials to a High Energy Dump," S.B. Thesis Dept. of Nuclear Engineering, MIT, May 1977.

7. Eicholz, Geoffrey G., Environmental Aspects of Nuclear Power; Ann Arbor Science, Ann Arbor, Michigan, 1976.

8. Moghhissi, A. Alan, ed., Tritium; CONF-710809, Messenger Graphics, Las Vegas, Nevada, 1973.

9. Wittenberg, L. J., et. al., Evaluation Study of the Tritium Handling Requirements of a Tokamak Experimental Power Reactor, MLM-2259, Mound Laboratory, Miamisburg, Ohio, 1975.

10. Jacobs, D. G., Sources of Tritium, TID-24635, USAEC, Washington, D.C., 1968.

11. Belovodskii, L. F., et. al., Oxidation of Tritium in Air Under Action of Intrinsic Radiation, Atomnaya Energiya, Volume 38, No. 6, June 1975.

12. Marter, W. L., Environmental Effects of a Tritium Gas Release From the Savannah River Plant on May 2, 1974; DP-1369, 1974.

13. Jacobsen, W. R., Environmental Effects of a Tritium Gas Release From the Savannah River Plant on December 31, 1975, DP-1415, 1976.

14. Gordon and B. J. McBride, Computer Program for Calculation of Complex Chemical Equilibrium Compositions, Rocket Performance, Incident and Reflected Shocks, and Chapman-Jouquet Detonation, NASA SP-273, (1971).

15. JANAF Thermochemical Tables, (Midland, Mich., Dow Chemical Co., 1970).

16. R. W. Conn, K. Okula and W. Johnson; "Minimizing Long-Term Radioactivity in Fusion Reactors by Isotopic Tailoring," Trans. Am. Nucl. Soc., 26, 27 (1977).

III. LITHIUM FIRES

3.1 Introduction

At present, many tokamak fusion reactor designs use liquid lithium as coolant and breeding material because of its low melting point, high boiling point, low vapor pressure, low density, high heat capacity, high thermal conductivity, and low viscosity. Lithium requires less pumping power when flowing across magnetic field lines than most other liquid metals, and lithium is not activated to long-lived gamma emitting isotopes by neutron capture.[1]

However, liquid lithium reacts strongly in air, liberating about 3.7 times more energy on a weight basis than liquid sodium (which is itself being considered for use in the secondary loop). Lithium temperatures as high as 982°C will be reached in some designs where a refractory metal or alloy is employed as structural material.[2]

Should a large amount of liquid lithium become exposed to air within the reactor containment building, there is a potential for release of substantial amounts of energy, as can be seen in Table 3.1. Furthermore, lithium may interact with the concrete floors or structures, releasing even more energy. The designer of the reactor containment has to take such hypothetical accidents from lithium spills into consideration. Whereas a nitrogen atmosphere can be introduced into the containment to smother sodium fires, this would not

TABLE 3.1

Energy and Heat Sources and Sinks in UWMAK-I and III

SOURCES	UWMAK-I	UWMAK-III
Superconducting magnets	350×10^9 J	Approximately same
Kinetic energy of plasma	3×10^9 J	Approximately same
Thermal energy of liquid lithium*	32.5×10^9 J/% Li	15.8×10^9 J/% Li
Li-air reactions	$280\text{-}731 \times 10^9$ J/% Li	$65\text{-}170 \times 10^9$ J/% Li
Li-concrete reactions	1200×10^9 J/% Li	278×10^9 J/% Li
Thermal energy of gaseous helium*	$.34 \times 10^9$ J (from shield)	27×10^9 J (inner blanket)
SINKS		
Liquid helium*	84×10^9 J	same
Heat capacity of air*	61.1×10^6 J/^{o}C	95.7×10^6 J/^{o}C
Heat conduction through the concrete containment	$.8\text{-}1.0 \times 10^4 \frac{W}{^oC} (T-T_{amb})$	$1.2 \times 10^4 \frac{W}{^oC} (T-T_{amb})$

*Ambient is taken as zero-base in calculation of thermal energy

be possible with lithium because of the exothermic lithium-nitrogen reaction.[3] Hence, an inert atmosphere of other rare gases may have to be used to extinguish lithium fires.

The UWMAK-I design includes a double containment.[4] The inner primary containment is evacuated to a pressure of 1 Torr. It is designed to withstand an over-pressure of 10 psig caused by liquid helium coolant leakage and vaporization. It would have a 0.5 in. steel liner to prevent lithium-concrete reactions should a spill occur. The UWMAK-III design utilizes a single containment of roughly one and one-half the free volume of UWMAK-I (8.85×10^6 ft.^{3} compared to 5.65×10^6 ft.^{3}). The containment atmosphere is an inert gas and the structure is lined with 0.25 in. steel plate. The design overpressure is 15 psig.

Air could be introduced into an otherwise evacuated environment by a breach of the primary containment by a missle or by seismic activity. In these cases it would be impossible to prevent leakage of air into the containment and the main concern would lie in minimizing lithium leakage and peak flame temperatures. Also, under some circumstances, it may be preferable to operate with an atmospheric environment. If an inert containment atmosphere were properly maintained, and the steel liner was effective in separating the lithium from concrete, a lithium spill by itself would pose little danger to the containment integrity.

Because the lithium would be contained in a multiplicity of parallel systems (12 for UWMAK-I and 18 for UWMAK-III), rupture of a single lithium system could not release more than a small fraction of the total lithium inventory. However, in absolute terms, this could amount to a large spill nonetheless (312,000 lbs. in UWMAK-I and 48,400 lbs. in UWMAK-III). A spill of this size might cause large thermal stresses in the steel liner possibly causing it to buckle and allowing lithium to contact the concrete structure beneath. Lithium reacts readily with concrete giving off hydrogen, oxygen, carbon dioxide, and water vapor. Release of these gases might further displace the liner, allowing still more leakage.

If a lithium spill occurs, the lithium's tritium inventory would be released into the containment atmosphere creating a radiation hazard. The lithium also contains activated blanket wall erosion and corrosion products. If a fire occurs it is possible that some products be volatilized and released into the containment atmosphere. The fire might also supply the energy needed to disrupt the first wall and other activated reactor structures. Determination of peak flame temperatures would show whether melting or vaporization of the structures is possible. The radiological hazard combined with the very large potential energy release necessitates that we gain a detailed understanding of lithium fires.

In this section, the results of two scoping studies are summarized. First, the adiabatic flame temperature due to

Li reaction with oxygen and/or nitrogen has been estimated. Such a temperature will not be achieved under realistic conditions due to the expected heat losses from the reaction zone. This study utilized a generalized NASA code for flame temperature analysis.[5]

Secondly, a parametric study of the lithium-air fire in a containment building was conducted. The study utilized a converted version of the SPOOL-FIRE code which was developed at Argonne National Laboratory to analyze LMFBR sodium-fire accidents.[6]

3.2 Lithium-Air Reactions

3.2.1 Thermodynamic Considerations

The major concern with using liquid lithium as a fusion reactor coolant is its exothermic reaction in air as well as with the concrete containment should a lithium spill occur. Unlike sodium, liquid lithium also reacts exothermically with nitrogen gas at room and elevated temperatures. The reactions of most interest in air at room temperature are:[1]

	ΔH^{o}_{298} kcal/mole	ΔG^{o}_{298} kcal/mole
$2\ Li(c) + \frac{1}{2}O_2 \rightarrow Li_2O(c)$	-142.75	-133.95
$2\ Li(c) + O_2 \rightarrow Li_2O_2(c)$	-151.9	-133.1
$Li(c) + \frac{1}{2}H_2 + \frac{1}{2}O_2 \rightarrow LiOH(c)$	-116.58	-105.68
$3\ Li(c) + \frac{1}{2}N_2(g) \rightarrow Li_3N(c)$	- 47.5	- 37.3

where ΔH^{o} is the change in enthalpy between the products and reactants (also known as the heat of formation), and ΔG^{o} is the change in Gibbs free energy. Negative values of ΔH^{o} indicate exothermic reactions. The zero superscript refers to enthalpy changes with respect to the standard state (1 atmosphere of pressure).

The heat of formation ΔH^{o} is a function of reaction temperature as well. Most thermodynamic data give values of ΔH^{o} at room temperature ($298.15^{o}K$ to be precise). However, one would expect the heat of formation at a given temperature ΔH^{o}_{T} to more accurately reflect the energy release for reactions which occur at temperatures other than $298.15^{o}K$. Table 3.2 gives the heats of formation and the change in Gibbs free energy of $Li_2O(c)$ and $Li_3N(c)$ for various temperatures.[7]

In any chemical situation the forward reaction may be specified by

$$A + B \rightarrow C$$

while the reverse reaction may be specified by

$$C \rightarrow A + B.$$

At chemical equilibrium, one obtains the standard form

$$A + B \rightleftharpoons C.$$

TABLE 3.2

Heats of formation and changes in Gibbs free energy for $Li_3N(c)$ and $Li_2O(c)$

TEMP (^oK)	ΔH_T^o (kcal/mole)		ΔG_T^o (kcal/mole)	
	$Li_3N(c)$	$Li_2O(c)$	$Li_3N(c)$	$Li_2O(c)$
298	-47.2	-143.1	-36.8	-134.3
400	-47.4	-143.3	-33.3	-131.3
500	-49.8	-144.9	-29.5	-128.2
600	-49.9	-145.0	-25.4	-124.8
700	-49.7	-145.0	-21.3	-121.5
800	-49.2	-144.9	-17.3	-118.1
900	-48.7	-144.7	-13.3	-114.8
1000	-48.0	-144.5	- 9.5	-111.5
1100	-47.2	-144.1	- 5.7	-108.2

JANAF Thermochemical Tables

(Dow Chemical Co., Midland, Mich., 1970)

Large negative values of ΔG_T^o indicate, in general, that the forward reaction goes nearly to completion, while large positive values of ΔG_T^o indicate that the reverse reaction is preferred thermodynamically.

One can represent a chemical transformation for ideal gases, for example, by the equation

$$aA + bB \rightleftharpoons cC + dD, \tag{3.1}$$

where the lower-case letters represent the number of moles and the upper-case letters represent the reactants and products. One can then represent ΔG_T^o mathematically by

$$\Delta G_T^o = -RT \ln K \tag{3.2}$$

where

$$K = \frac{[C]^c \ [D]^d}{[A]^a \ [B]^b} \tag{3.3}$$

and is called the thermodynamic equilibrium constant. R is the universal gas constant (1.987 cal./gm-mole ^oK) and T is the absolute temperature. The values in the brackets refer to the corresponding mole concentrations of the products, while the lower-case letters are exponents in the above expression for K. Hence, large negative values of ΔG_T^o indicate relatively high concentrations of the products C and D, and the forward reaction more nearly goes to completion at chemical equilibrium.

Gibbs free energy can more accurately be represented by

$$G^{o} = H^{o} - TS^{o} \tag{3.4}$$

while the change in Gibbs free energy is represented by

$$\Delta G^{o}_{T} = \Delta H^{o} - T\Delta S^{o} \tag{3.5}$$

for infinitesimal changes under isothermal conditions. ΔS^{o} represents the change in entropy for the reaction in the standard state. A more complete discussion of chemical thermodynamics for reactions involving liquids, solids, and changes in state is treated by Klotz[8] for example.

3.2.2 Lithium-Air Flame Temperature and Energy Release

Of primary concern in lithium fires is the peak flame temperature which can be achieved. To a large extent, this will determine whether many radioactive species become airborne by vaporization or aerosol formation in fusion reactor accidents. The standard procedure is to assume a number of constraints on the lithium-air reaction to establish peak flame temperatures - in essence, 1) reactant stoichiometry, 2) chemical equilibrium between the product species, and 3) overall adiabatic conditions. In reality, one can expect significantly lower temperatures to be achieved because of

radiative heat transfer and constraints on the reaction rates. These further constraints will be considered later. However, the present analysis does provide an absolute upper bound for the flame temperature, albeit a very conservative one.

The procedure used in determining chemical equilibrium is an established one and treated especially well by Zeggeren and Storrey.[9] In brief, the idea is to minimize Gibbs free energy for all the reactants and products considered. It is assumed that all of the energy released is used in heating the product species to the equilibrium temperature.

According to Gibbs phase rule, the entire chemical system can be specified by two independent variables. For the calculation of adiabatic flame temperatures, pressure and enthalpy are assumed independent. Moreover, the pressure is fixed at one atmosphere for ease of calculation, leaving only the enthalpy to be specified. The enthalpy for each species is in turn a function of temperature.

Gordon and McBride[5] have developed a special computer program, CEC 71, for calculating thermodynamic values in rocket engines. This code, developed for NASA, and available at MIT under the name TRAN72, includes other options used in studying jet propulsion, but are not considered here. Thermodynamic and physical data for some 62 reactants and 421 reaction species in liquid, solid, and gaseous states are included. The input requires specifying the reactant concentrations (by weight or moles) and the initial enthalpies (or temperatures) of these reactants. The resulting output

provides information on the product concentrations, equilibrium temperature, density, effective molecular weight, and so forth. Of greatest interest is of course the equilibrium temperature, but the product concentrations further provide information on which reactions are or are not predominant.

Using this computer code, a number of cases were run under similar conditions but with slight changes in reactant concentrations to note the contribution of the various reactants to the total energy release.

In case 1, it is assumed that a leakage of 16% of the total lithium inventory of UWMAK-III (about three coolant loops) has resulted and reacted with the volume of air within the containment. The reaction is assumed to occur with air at room temperature, 1 atmosphere of pressure, and 50% relative humidity. Case 2 was similar to case 1 but dry air was used instead. Case 3 considered only lithium, oxygen, and nitrogen as reactants. In case 4, only nitrogen and lithium were used as reactants. Table 3.3 summarizes the assumptions and the results of all four cases.

It is significant to note that the equilibrium temperature reached is quite insensitive to those reactants considered other than nitrogen and oxygen. Further analysis shows that in the presence of even the smallest concentrations of oxygen, the percentage of nitrogen which underwent reaction is very small. Several reasons can be given to account for this observation.

TABLE 3.3

Thermodynamic results from sample calculations for determining adiabatic flame temperature.

		Case 1	Case 2	Case 3	Case 4
INPUT					
Reactants Considered and Mole Fractions	Li(l)	.45800	Similar	.468	.27
	N_2	.41000	but	.419	.73
	O_2	.11000	no H_2O	.113	-
	H_2O	.01862		-	-
	Ar	.00495		-	-
	CO_2	.00026		-	-
	H_2	.00005		-	-
OUTPUT					
Equilibrium ^oK Temperature		2498	2498	2500	1094
Energy Released (kcal/gm Li reacting)		10.4	10.4	10.4	2.3
Products resulting and mole fractions (greater than 1×10^{-5})	Ar	.00722	.00722	-	-
	Co	.00010	.00010	-	-
	Co_2	.00028	.00028	-	-
	Li	.08670	.08670	.08767	.00151
	LiO	.00767	.00767	.00778	-
	LiOH	.00014	.00014	-	-
	$Li_2(g)$	.00006	.00006	.00006	.00002
	$Li_2O(l)$	.11990	.11990	.12012	-
	Li_2O	.16524	.16524	.16703	-
	Li_2O_2	.00156	.00156	.00158	-
	NO	.00446	.00446	.00452	-
	N_2	.59579	.59579	.60024	.88433
	O	.00131	.00131	.00133	-
	O_2	.00957	.00957	.00968	-
	$Li_3N(s)$	-	-	-	.11414

For one, the lithium-oxygen reaction is significantly more exothermic than the lithium-nitrogen reaction. Hence, one would assume that in establishing equilibrium, reaction with oxygen would be preferred over nitrogen. In addition, the change in Gibbs free energy for the reaction is greater for oxygen than nitrogen, indicating that the forward reaction with oxygen is carried to greater completion than with nitrogen. Although the heat of formation of Li_3N is fairly constant over a wide range of temperatures, the value of ΔG_T^o increases significantly with temperature. At 298 ^oK, the value of ΔG_T^o is -36.8 kcal/mole, while it increases to -17.3 kcal/mole at 800 ^oK and still higher to +3.8 kcal/mole at 1500 ^oK.[1] This would indicate that the forward reaction of lithium-nitrogen at elevated temperatures is very slow. Note also that the melting point of Li_3N is 1123 ^oK so that Table 3.2 cannot be used above this temperature.

Close examination of lithium-oxygen reaction, on the other hand, shows that for $Li_2O(c)$, ΔG^o = -134.3 kcal/mole at 298 ^oK, -118.1 kcal/mole at 800 ^oK, and -95.4 kcal/mole at 1500 ^oK. Hence, the forward lithium-oxygen reaction is still very important at elevated temperatures. Indeed, these observations imply that liquid lithium-nitrogen reaction would be important only at relatively low combustion temperatures of 400-500 ^oK, and unimportant in the regime of temperatures above 1000 ^oK. However, the fact that lithium-nitrogen reactions are exothermic at all temperatures still means that nitrogen would be insufficient for the extinguishment of lithium fires.

Several other cases were investigated to determine the effects of the relative mole fraction of Li-to-air and Li-to-nitrogen on the final equilibrium temperature. Figures 3.1 and 3.2 illustrate this as well as the effect of the lithium release temperature on the final temperature. Calculations were made for lithium release temperatures of 1173 ^{o}K, 1000 ^{o}K, 800 ^{o}K, and 600 ^{o}K, but only the curves for 1173 ^{o}K and 600 ^{o}K are plotted. The peak flame temperature obtained for lithium fires in air is 2502 ^{o}K, while the peak flame temperature for Li in N_2 is 1315 ^{o}K. The value of 2502 ^{o}K compares quite closely with the value of 2400 ^{o}K obtained by Okrent et. al.[10] It was also found that for environments of low oxygen concentration (4 and 8%), the peak flame temperatures were reduced significantly to 1580 ^{o}K and 1800 ^{o}K respectively at Li release temperatures of 1173 ^{o}K. Moreover, it was found that except for environments with extremely low oxygen concentrations (< 1% volume), lithium-nitrogen reactions were unimportant at chemical equilibrium.

This would lead to the following conclusions:

1) The lithium-oxygen reactions predominate in atmospheric environments, while the lithium-nitrogen reactions are relatively unimportant except at very low concentrations of oxygen.

2) In an N_2 environment, lithium reacts exothermically with the nitrogen gas, although the forward reaction is constrained by thermodynamic considerations, resulting in peak flame temperatures which are significantly lower than those found in an air environment.

Fig. 3.1 Equilibrium Temperature vs. Lithium to Air Mole Ratio for Various Li Release Temperatures

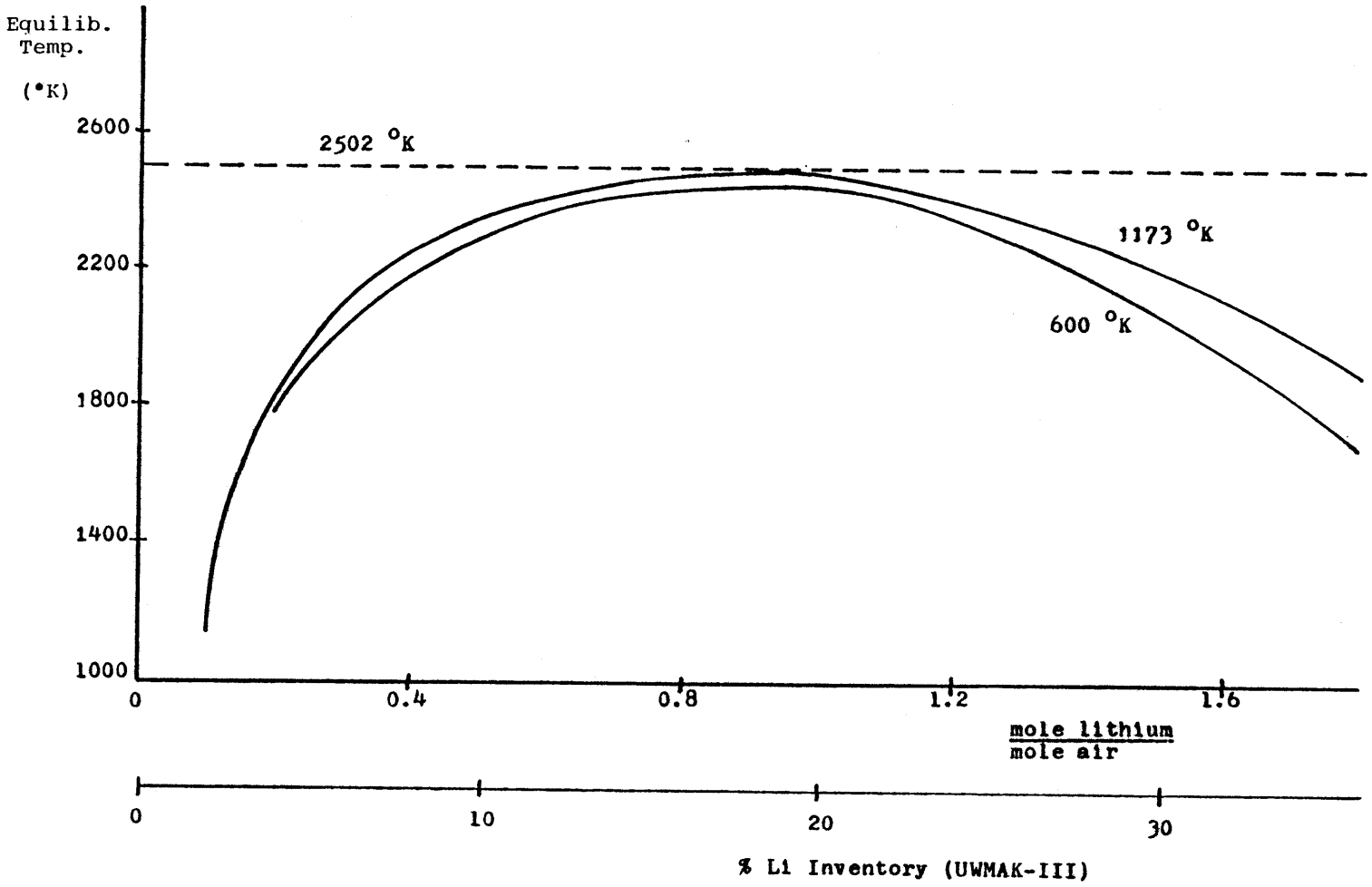

Fig. 3.2 Equilibrium Temperature vs. Lithium to Nitrogen Mole Ratio for Various Li Release Temperatures

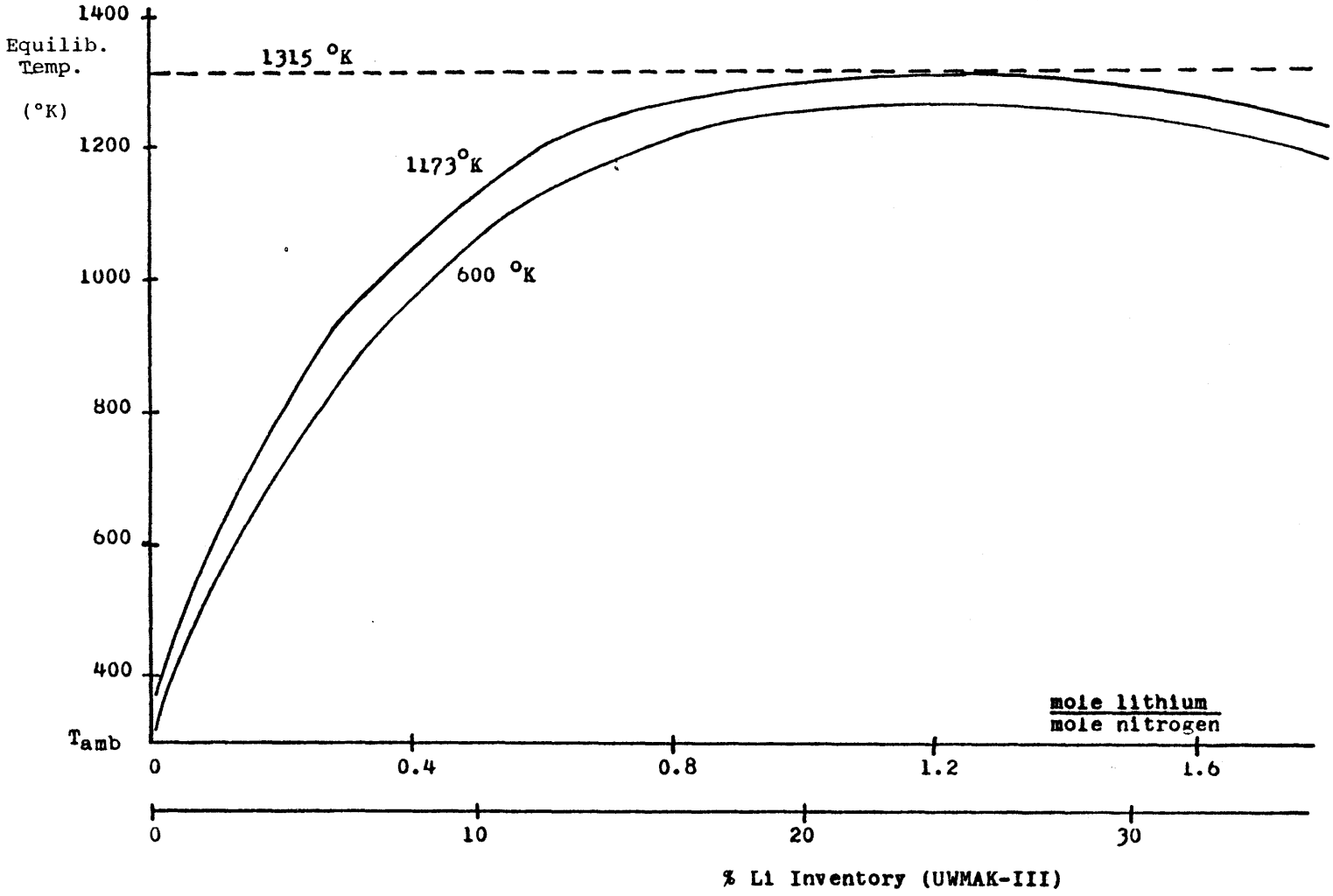

The first conclusion suggests that it would be possible to model lithium-oxygen reactions in an atmospheric environment in much the same way as was done in several studies with sodium fires in LMFBR's.[6,11,12,13] This would make it possible to predict the temperature-pressure history of containment resulting from lithium fires. At lower oxygen concentrations, the model would have to be modified to account for lithium reactions with nitrogen.

Of considerable interest is the possible vaporization of reactor materials in the event of a lithium fire. Table 3.4 gives the melting points and some vaporization points for those metals considered likely to be used as first wall or as structural material. It can be seen that even at temperatures of 2502 ^{o}K (which is the highest peak flame temperature calculated from this investigation), none of the materials would vaporize, although several would melt. Further study would have to be made to determine if aerosol formation is significant at these temperatures when assessing the overall mobilization of radioactive species. This is especially important because of the generation of free oxygen atoms. Free oxygen is highly reactive and may oxidize several potential structural materials.

TABLE 3.4

Melting and boiling points of some metals being considered as first wall or structural materials

	M.P. (^{o}K)	B.P. (^{o}K)
Titanium	2000	3550
Molybdenum	2883	-
Zirconium	2125	3900
Aluminum	932	2600
Stainless Steel	>1700	>3000
Niobium	2760	5000
Vanadium	1890	3800

3.3 The Adaptation of SPOOL-FIRE Code to Lithium Fires

3.3.1 Sodium-Fire Computer Models

Because of the similarity between most alkali metal fires, computer codes developed for analyzing liquid sodium fires in LMFBR's can be modified to study liquid lithium fires. In particular the SPRAY,[14,15,16] SOFIRE II,[12] CACECO,[13,17] and SPOOL-FIRE[6,18] codes have been considered. With the exception of SPOOL-FIRE, the analytical modelling behind these codes has been reviewed by Sarma et. al.[19,20]

A liquid metal fire caused by a piping rupture would probably consist of two parts, a spray fire as the coolant is rapidly expelled out of the broken piping, and a pool fire after the coolant has collected on the containment floor. SPRAY utilizes a dynamic combustion zone model about a moving spray droplet to provide the time-temperature-pressure history of a spray fire. CACECO models a combined spray-pool fire within a four-cell containment. Heat and mass may be transferred between all cells and between each cell and the ambient exterior. Options include sodium-concrete reactions, water release from heated concrete, ventilation in and out of the containment, emergency space cooling and the effects of equipment heat sinks within the containment. SOFIRE II is a two cell pool fire code which models the containment heat transfer using the finite difference technique. SPOOL-FIRE is an adaptation of SOFIRE II model converted to the IBM CSMP method of formulation combined with a simple spray fire model first proposed by Humphreys.[21]

The version of the code which was received from Argonne National Laboratory is described in detail in the next section. Table 3.5 summarizes the options available in each code. The SPOOL-FIRE code was chosen in this initial study because of its use of the IBM-CSMP[22] methodology which makes it relatively easy to modify. Proposed modifications will also be indicated in the next section.

3.3.2 Description of the Spool-Fire Model and Modification Needs

SPOOL-FIRE is a computer code developed at Argonne Laboratory to describe the temperature and pressure history within a containment building resulting from a sodium fire. The code accounts for heat loss from the building, and containment atmosphere leakage caused by over-pressurization. The code's use of the IBM-CSMP methodology allows the model used to be readily changed by the user.[6]

3.3.2.a Spray Fire Model:

The spray fire is modeled by assuming that a fixed amount of lithium reacts instantaneously, adiabatically, and stoichiometrically with the oxygen in the containment atmosphere. The equilibrium temperature of the components 1, 2 ..., i, ...n of the resultant mixture is then given by:

$$\int_{T_o}^{T_p} M_L\, C_L\, dT_L + M_L\, Q_c = \sum_{i=1}^{n} \int_{T_{o,i}}^{T_f} M_i\, C_i\, dT_i \qquad (3.6)$$

TABLE 3.5

Summary of Desired Features for Lithium Combustion Model and Applicable Sodium Fire Computer Codes

Desired Feature	SPRAY	SOFIRE-II	CACECO	SPOOL-FIRE
1) Lithium-nitrogen reactions	–	–	–	–
2) Spray fires	✓	–	✓	✓
3) Pool fires	–	✓	✓	✓
4) 0 to 21 % w/o oxygen	✓	✓	✓	✓
5) Gas ventilation into containment	–	–	✓	–
6) Gas ventilation out of containment	✓	–	✓	–
7) Multi-cell containment	–	2 cells	4 cells	1 cell
8) Temp.-press. history	✓	✓	✓	✓
9) Humidity effects	–	–	–	–
10) Emergency space cooling	–	–	✓	–
11) Gas leakage from overpressure	–	–	–	✓
12) Pool drain tank	–	✓	–	–
13) Equipment heat sinks	–	–	✓	–
14) Extinguishment of fire by chemical addition	–	–	–	–
15) Dissociation of reaction products	–	–	–	–
16) Two mechanisms of mass transfer	–	–	–	–
17) Inclusion of combustion zone	–	–	–	–
18) Aerosol effect on thermal radiation	–	–	–	–
19) Easy modification of equations	–	–	–	✓

where M = mass

C = specific heat = f(T)

T = temperature

T_o = initial atmosphere temperature

T_p = lithium spill temperature

T_f = final mixture temperature

Q_c = heat of combustion

Substitution of the formulae for C as a function of temperature of O_2, N_2, and Li_2O, and carrying out the integrations leads to a fourth order polynomial of which the positive real root constitutes the desired solution. The intricate subroutine (ROPE) supplied by ANL to find all the roots of eq.(3.6) was replaced at MIT with a simpler iterative technique, which finds only the desired root. The results from both methods were checked and found to be in agreement.

The amount of lithium which reacts as spray must be provided by the user. To calculate this analytically would be very difficult because it would be a function of droplet size, speed, initial temperature, and the time between ejection and impact on containment walls or lithium pool. These parameters are dependent on the specific accident, and are determined by the size orientation, and location of the break and the driving pressure differential. Krolikowski[23] has studied explosive spray fires with very small droplets

($\sim$ 572 μ diameter) under very large driving pressures. Shire[24] has studied spray fires resulting from sodium being expelled from a nozzle and impinging on a flat plate. This configuration results in much larger droplets (0.21 in. diameter) but much lower droplet velocities. Both experiments show only a small fraction (5%) of a sodium spray will react before the spray imparts a solid boundary. It may be possible, however, to postulate conditions under which a larger fraction of the spray is consumed. Although the combustion rate and exposed surface area of sodium droplets are very large, each droplet's time in flight is very short. In such cases, the assumption of instantaneous combustion seems reasonable.

There may be several conditions that will affect the consequences of a liquid metal fire, but are not accounted for in the SPOOL-FIRE model. First, it is likely that the piping in which a break occurs will take a significant amount of time to empty. Kastenberg et. al. suggest that it may take on the order of one hour for a blanket segment to drain during a LOCA, if the magnetic field remains active during drainage.[25] Some energy may be transferred out of the containment and the containment temperature and pressure may decrease. Secondly, at present only one combustion product may be used in the SPOOL-FIRE code. Possible nitrogen reactions are not included and no attempt is made to find the chemical equilibrium of the reaction products. The

assumption that the product is 100% Li_2O_2 leads to the largest heat of combustion. Li_3N has a much lower heat of combustion, and would release less heat on a per weight basis than Li_2O or Li_2O_2. As discussed in the preceeding section, under very low oxygen concentration conditions, the reaction with nitrogen should be accounted for. Thirdly, the presence of moisture in the atmosphere should be accounted for. Water acts as a catalyst for the oxygen and nitrogen reactions as well as reacting with lithium itself.[26] Under very dry conditions near lithium's melting point the reaction might be slowed by the lack of moisture.

Future modifications of this code in the spray-fire area should include:

a) a rate of spray release model;

b) a spray fire combustion model that would provide the fraction of spray consumed in combustion;

c) a combustion model which included both oxygen and nitrogen reactions in the proper propagation for chemical equilibrium;

d) an accounting for the air humidity.

3.3.2.b Pool Fire Combustion Model:

The pool fire model assumes that the rate of lithium combustion is determined by the rate of oxygen transport to the pool surface. Assuming the usual mass transport-heat convection analogy, the mass transfer coefficient for a horizontal flat plate with the hot surface facing upward

may be expressed as[12]

$$h_f = .14\ D\ [g\ Sc\ \frac{B}{\upsilon 2}\ (T_s - T_g)]^{1/3}\ ,\ \text{ft./hr.} \tag{3.7}$$

where Sc = Schmidt number = υ/D

D = diffusion coefficient

B = coefficient of gas expansion

υ = kinematic viscosity

T_s = surface temperature

T_g = gas temperature

The combustion rates can then be determined from

$$\frac{1}{A_p}\ \frac{dm}{dt} = h_f\ COX\ \rho_g\ RCMB/3600. = CMBR,\ \text{lb. Li/sec-ft.}^2 \tag{3.8}$$

where COX = mass fraction of oxygen in cell gas

RCMB = stoichiometric combustion ratio, lb. Li/lb. O_2

CMBR = combustion rate

A_p = pool surface area

ρ_g = gas density

The total heat release rate by combustion is then

$$Q = CMBR\ A_p\ Q_c\ ,\ \text{BTU/sec.} \tag{3.9}$$

The heat of combustion is deposited in the lithium pool and the containment atmosphere in accordance with the value of the constant FCMB such that

$$Q_{pool} = FCMB\ Q \tag{3.10}$$

$$Q_{gas} = (1 - FCMB)\ Q \tag{3.11}$$

The value of FCMB must be supplied by the user. (The SOFIRE II model implicitly assumes it to be 1.)

The spill is assumed to occur instantaneously at time 0. The initial pool temperature is supplied by the user. The initial atmospheric temperature and pressure are the results of the spray fire computation.

This model has a number of deficiencies which should be modified. At present, only one reaction product may be considered, Li_2O, Li_2O_2, or a fixed ratio of the two. In reality Li_3N and LiOH may also be formed. The relative ratio of products formed will vary with the temperature at which the reaction takes place according to second law considerations. Also it is possible that the products formed may later react again or disassociate as their temperature changes. For instance, Li_2O_2 has a decomposition temperature of 468 ^{o}K. In a fire, if lithium behaves similiarly to sodium, it is likely that initially Li_2O will be formed. As it cools it may pick up another oxygen atom, releasing still more energy.

Li_3N forms very readily at lithium's melting point of 454 ^{o}K, but its free energy change, ΔG_T^o, varies very strongly with temperature. ΔG_T^o becomes positive around 1300 ^{o}K indicating that the reverse reaction $2Li_3N \rightarrow 6Li + N_2$ becomes

important. An accurate model of Li_3N formation is important for two reasons: 1) it is necessary for calculating the amount and rate of energy release. In low oxygen atmospheres, Li_3N would be the main or only product. And 2) because Li_3N is a very corrosive material, attacking common materials including steel.[26] Its corrosive action might cause the containment's steel sheathing to fail allowing lithium to contact concrete.

In pool fires of hydrocarbons, combustion takes place in a combustion zone separated from and slightly above the pool surface.[27,28,29] Fuel is carried to the zone by vaporization, and oxygen by convection and diffusion. The heat of combustion is transferred to the pool surface by radiation and conduction, and to the atmosphere by convection and radiation. Huber et. al.[30] further suggest the existence of such a zone for liquid sodium fires. If this is the case, then it is likely that the combustion zone theory would also describe lithium fires. The inclusion of such a model would eliminate the need for the constant FCMB, the fraction of heat transferred to the pool. In reality, FCMB is not constant but depends on the emissivities of the pool surface, combustion zone, and containment gas, and on the convective heat transfer coefficient. These are all likely to change with time as the fire progresses.

The present model makes no allowance for the release of aerosols into the containment atmosphere, the deposition of reaction products in the pool, or the rain-out of aerosols

from the cell in which the fire takes place. The accumulation of reaction product would change the heat capacity, thermal conductivity, and emissivity of both the pool and containment gas. The present model retains a constant mass and constant pool thermal properties (those of lithium) throughout the fire. The reaction products should cause those to change with time. Lithium has been observed to burn with a dense white smoke[26] but the present model does not include the effects of smoke and aerosol emission during the pool fire. The reaction product of the spray fire is assumed to be deposited in the containment gas and then assumed to remain there during the pool fire. No allowance is made for rain-out. Variable specific heats for N_2, O_2, and Li_2O or Li_2O_2 are used. Allowances are made for containment leakage and for oxygen depletion by the fire.

Future modifications in the pool-fire area should include:

a) inclusion of Li_3N and LiOH formation;

b) variation of reaction equilibrium with temperature according to second law considerations;

c) the use of the combustion zone theory to calculate the combustion rate and the release of energy into the containment gas and pool. The individual heat and mass transfer mechanisms involved need to be better understood;

d) variation of thermal properties of the pool and containment gas caused by the deposition of reaction products;

e) the use of a Li pool drain tank as an option. Such a tank might be used to lessen the amount of energy released into the containment;

f) inclusion of the use of chemical fire extinguishers as an option. The effect of these chemicals will be strongly dependent on pool temperature which controls disassociation energies and rates. Some chemicals used might be graphite, NaCl, and LiF.[3]

3.3.2.c Containment Thermal Model:

The basic containment model is shown in Fig. 3.3. The model considers four major parts: the containment atmosphere, wall structure, floor structure, and the lithium pool. These are divided into a number of separate elements. Each element is lumped into a single node. The nodes are interconnected by thermal admittances equal to the reciprocal of the thermal resistance between the elements.

The containment atmosphere is assumed to be a single, well mixed mass. It therefore contains only a single node. SPOOL-FIRE divides the pool into 4 layers each with a single node. To prevent numerical instability and excessively long run times caused by using very small elements, as encountered in our analysis, we have altered the code so that only a single pool node is used. For the base case used, the pool depth was only 0.51 inches. Considering the large thermal conductivity of lithium, it seems from physical considerations as well that a single node is enough. The

Fig. 3.3 Basic Containment Model

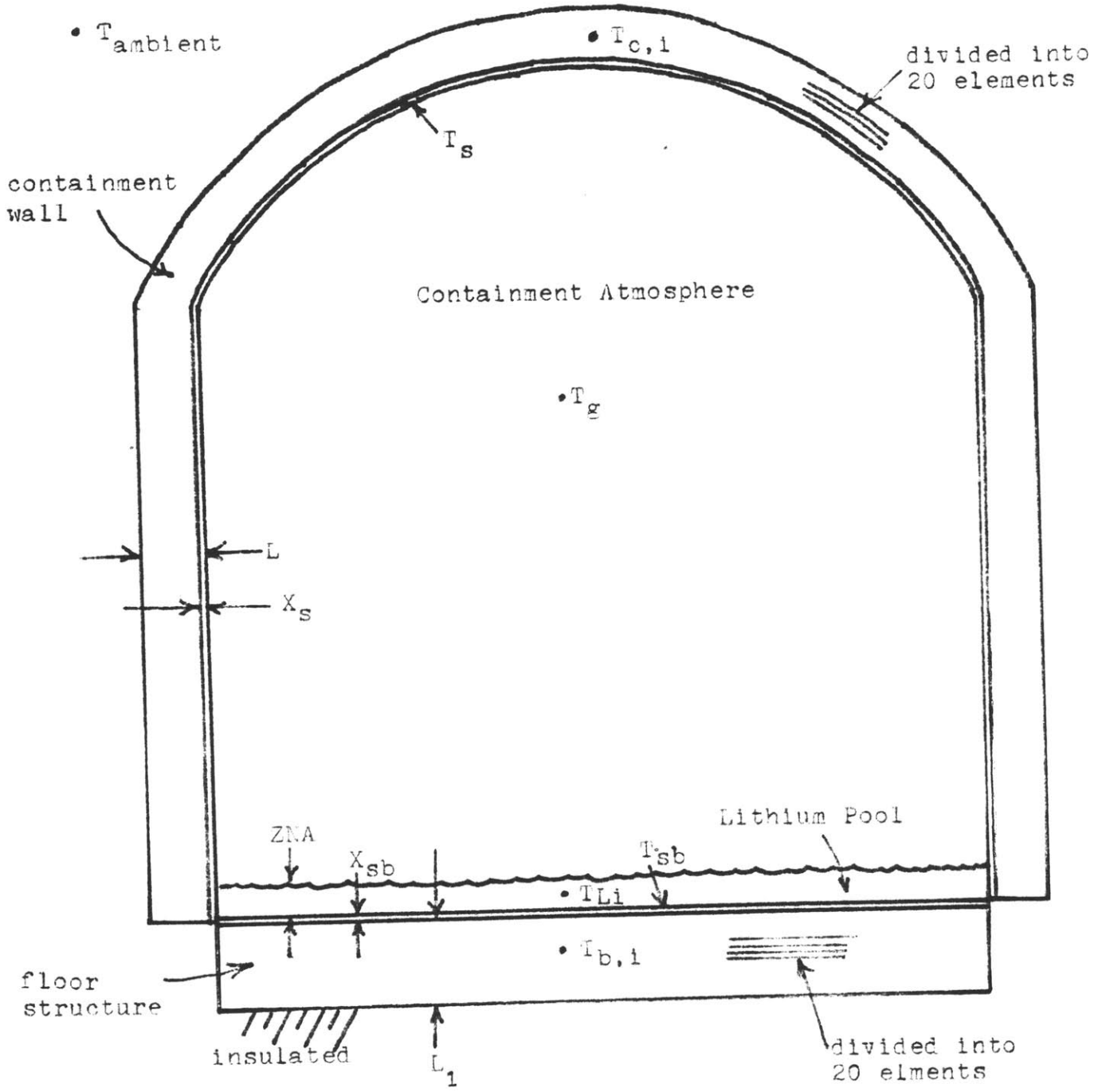

containment walls and floor have similiar structures, using concrete sheathed with a plate steel liner. Heat transfer through the structures is assumed to be one dimensional. The liner is assumed to be separated from the concrete surface by a small gas gap. Heat is transferred between the two by conduction and radiation. The wall transfers heat out to the ambient surroundings through a convective surface film. The external surface coefficient is taken to be 8.33×10^{-5} BTU/sec.-ft.^{2}-^{o}F, a conservative figure for natural convection. The SPOOL-FIRE model allows the floor to reject heat to either the containment atmosphere or the ambient surroundings. We have modified this by assuming that the bottom of the floor is insulated. This is in keeping with the very small heat transfer that will take place into the earth below the containment. For both the floor and the wall, the steel liner was treated as a single element and the concrete was divided into 20 elements. Rebar and tensioning tendon[5] embedded in the concrete were not included. The thermal property values used in the code are shown in Table 3.6. These are hard coded into SPOOL-FIRE and are not easily changed.

The convection heat transfer coefficient from the pool to the gas was calculated from the equation recommended by McAdams.[31]

$$h_c = 0.14 \frac{K}{L} (Gr \cdot Pr)^{1/3} \qquad (3.12)$$

TABLE 3.6

Thermophysical Data used in
SPOOL-FIRE Heat Transport Calculations

Material	Density (lbm/ft^3)	Specific Heat ($Btu/lbm-^oF$)	Thermal Conductivity ($Btu/hr-ft-^oF$)
Carbon Steel (liner)	490	0.2	30
Concrete	144	0.156	1
Lithium	27.4	1.0	36.3
Air (liner-concrete gap)	--	--	0.015

where

K = gas thermal conductivity

L = square pool side length

Gr = Grashof number based on the temperature difference between the pool surface and the cell gas

Pr = Prandtl number evaluated for air at the average film temperature.

Because of the high temperatures generated by the fire, radiative heat transfer becomes very important. The SPOOL-FIRE model includes radiation between the pool surface and the containment atmosphere and walls and between the steel liner and the concrete surface. The net radiation exchange between any two surfaces is described by

$$Q_{1-2} = \text{EMNA } A_s \sigma(T_1^4 - T_2^4) \tag{3.13}$$

where

σ = Stephen-Boltzman constant

A_s = surface area of either surface 1 or 2

EMNA = the radiation interchange factor between 1 and 2 based on surface area A_s

EMNA is a function of the emissivities of the two surfaces and the view factor between the two. These functions are derived below.

A schematic of the equilibrium radiative heat exchange between the pool surface, the cell gas, and the cell walls

is shown in Fig. 3.4. By circuit reduction, the heat transfer from the pool to the walls is

$$Q_{p-w} = \frac{A_p \sigma (T_p^4 - T_w^4)}{\frac{1-E_p}{E_p} + \frac{A_p}{A_w}\frac{1-E_w}{E_w} + \frac{1}{(1-E_g) + E_g/(1+A_p/A_w)}} \tag{3.14}$$

where F_{12} is the geometric view factor between surfaces 1 and 2. For this case, $F_{pg} = F_{wg} = F_{pw} = 1$.

If $A_p << A_w$, then

$$Q_{p-w} = \frac{A_p \sigma (T_p^4 - T_w^4)}{1/E_p} \tag{3.15}$$

By comparison with eq. (3.13)

$$\text{EMNAC} = E_p = \text{radiative interchange factor between the pool and the walls.} \tag{3.16}$$

Similiarly the radiative exchange between the pool and the cell gas is

$$Q_{p-g} = \frac{A_p \sigma (T_p^4 - T_g^4)}{\frac{1-E_p}{E_p} + \frac{1}{E_g}} \tag{3.17}$$

By comparison with eq. (3.13)

$$\text{EMNAG} = \frac{E_p E_g}{E_g - E_g E_p + E_p} = \text{radiative interchange factor between the pool and the cell gas.} \tag{3.18}$$

Fig. 3.4 Equivalent Circuit for Radiation Heat Exchange between Lithium Pool Surface, Cell Gas, and Containment Walls

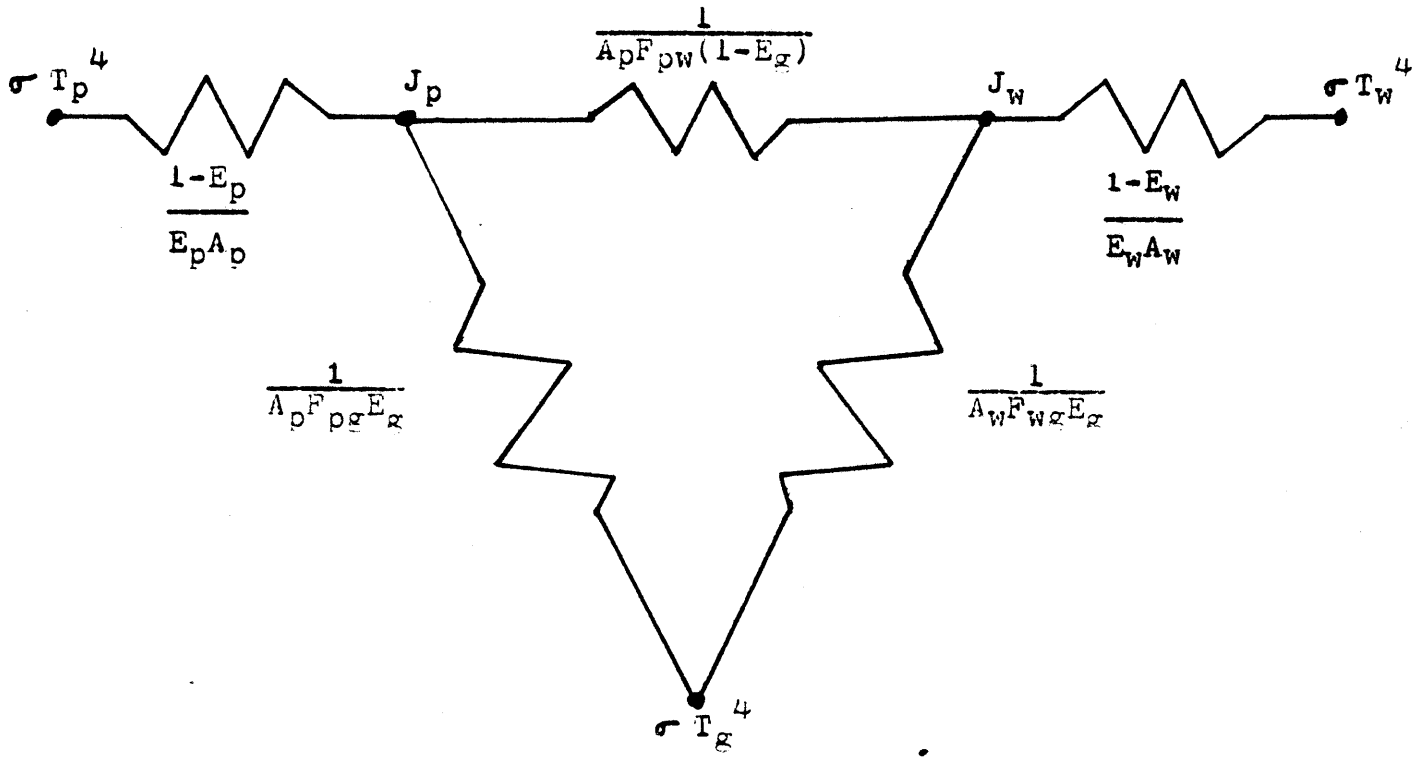

T = temperature (absolute)
J = radiosity
A = surface area
E = emissivity
F = view factor
σ = Stephen-Boltzman constant

subscripts
- p = pool
- w = containment steel liner
- g = cell gas
- c = concrete surface

From eq. (3.18), it is clear that EMNAG = 0 for $E_g = 0$ and EMNAG = E_p for $E_g = 1$. Thus, EMNAG is always less than or equal to EMNAC.

The interchange factor between the liner and the concrete surface may be found from the equation for radiation between two parallel infinite flat surfaces.

$$Q_{w-c} = \frac{A_w \ (T_w^4 - T_c^4)}{\frac{1}{E_w} + \frac{1}{E_c} - 1} \tag{3.19}$$

By comparison to eq. (3.13)

$$\text{EMNAW} = \text{EMNAB} = \frac{E_w E_c}{E_w + E_c - E_w E_c} \tag{3.20}$$

where EMNAW = radiative interchange factor between the wall liner and the concrete wall surface

EMNAB = radiative interchange factor between the floor liner and the concrete floor surface

EMNAG, EMNAC, EMNAW, and EMNAB are treated as constants and must be supplied by the user.

Some modifications to the thermal model should be made to improve the accuracy of the representation of the physical system, and to enhance the capability of the code. These can be summarized as follows:

a) inclusion of forced ventilation of the containment as an option. This would allow the flooding of the containment with inert gas to extinguish the fire being studied;

b) inclusion of equipment heat sinks within the containment;

c) inclusion of emergency space cooling as an option;

d) change EMNAG and EMNAC from constants to functions of E_p and E_g which change as the pool fire progresses.

3.3.2.d Containment Pressure:

The pressure within the containment is calculated using the ideal gas law. A correction is made for the depletion of oxygen by the fire and for containment leakage. Modifications for the depletion of nitrogen and for inert gas flooding should be made.

3.3.2.e Containment Leakage

The equation used to describe the leakage rate through an intact containment vessel structure is

$$\text{LEAK} = K\,(\text{OVERP})^{a}\text{ , fraction of gas mass/sec.} \qquad (3.21)$$

where

OVERP = containment over-pressure in psig.

While each containment will have its own unique leakage characteristics, SPOOL-FIRE assumes that turbulent flow through the leaks occurs so that a = 0.5 and K = 2.588 x 10^{-9}/sec-psi$^{0.5}$. These could be easily changed if needed. The total leakage out of the containment is found by integrating the leakage rate. This gives the total fraction of the gas mass released. This fraction may be applied to the total

radioactive inventory within the containment to find the total released dose.

An important modification which should be made is to include an option which would account for leakage through a break (hole) in the containment.

3.3.2.f Methodology of Solution (CSMP):

SPOOL-FIRE makes use of the IBM CSMP translator.[22] CSMP (Continuous Systems Modeling Program) allows the user to model a physical problem using a set of ordinary differential equations with corresponding initial conditions. For instance, the temperature of a thermal element may be found from the solution to

$$mc \frac{dT}{dt} = q_1 + q_2 + q_3 + \ldots, \; T = T_o \text{ at } t = t_o \tag{3.22}$$

where mc is the element's heat capacity and q_1, q_2, q_3, ... are heat flows into the element. This could also be expressed as

$$T = \int_{t_o}^{t} \frac{1}{mc} (q_1 + q_2 + q_3 + \ldots) \, dt + T_o \tag{3.23}$$

In CSMP this is expressed as

$$T = \text{INTGRL}(T_o, dT/dt) \tag{3.24}$$

Once the governing equations for the model have been written, it is a relatively simple matter to write a CSMP

program from them. The CSMP translator then translates that program into Fortran, adds the necessary subroutines, and then compiles and runs the resultant Fortran program. Because an up-to-date version of the CSMP was not available, and to cut down on computing costs, SPOOL-FIRE was edited so that it would run in Fortran. A set of subroutines was then added to do the integrations. Most of the CSMP methodology was retained however. Two methods of integration were provided, Simpson's Rule and Fourth Order Runge-Kutta methods. The former was used for most calculations because it was faster, and the latter was used as a check.

3.4 Application of SPOOL-FIRE to Lithium Fires in UWMAK-III

3.4.1 Description of UWMAK-III Containment

The UWMAK-III containment building is shown in Fig. 3.5. The structure is reinforced concrete lined with 0.25 in. thick steel plate. To prevent lithium fires, the containment will have an inert atmosphere. The structure is designed to withstand a 15 psig over-pressure (caused by a liquid helium pipe rupture). The structure would house the reactor, its piping and immediate peripheries, e.g. neutral beam injectors etc. Heat exchangers, energy storage devices, refrigeration equipment, hot cells, waste storage, and other auxilaries would be housed in separate structures located around the circumference of the containment building. This is significantly different from the UWMAK-I containment which utilizes a double containment. The reactor is located in the primary containment

Fig. 3.5 Cross Section of UWMAK-III Primary Containment Building

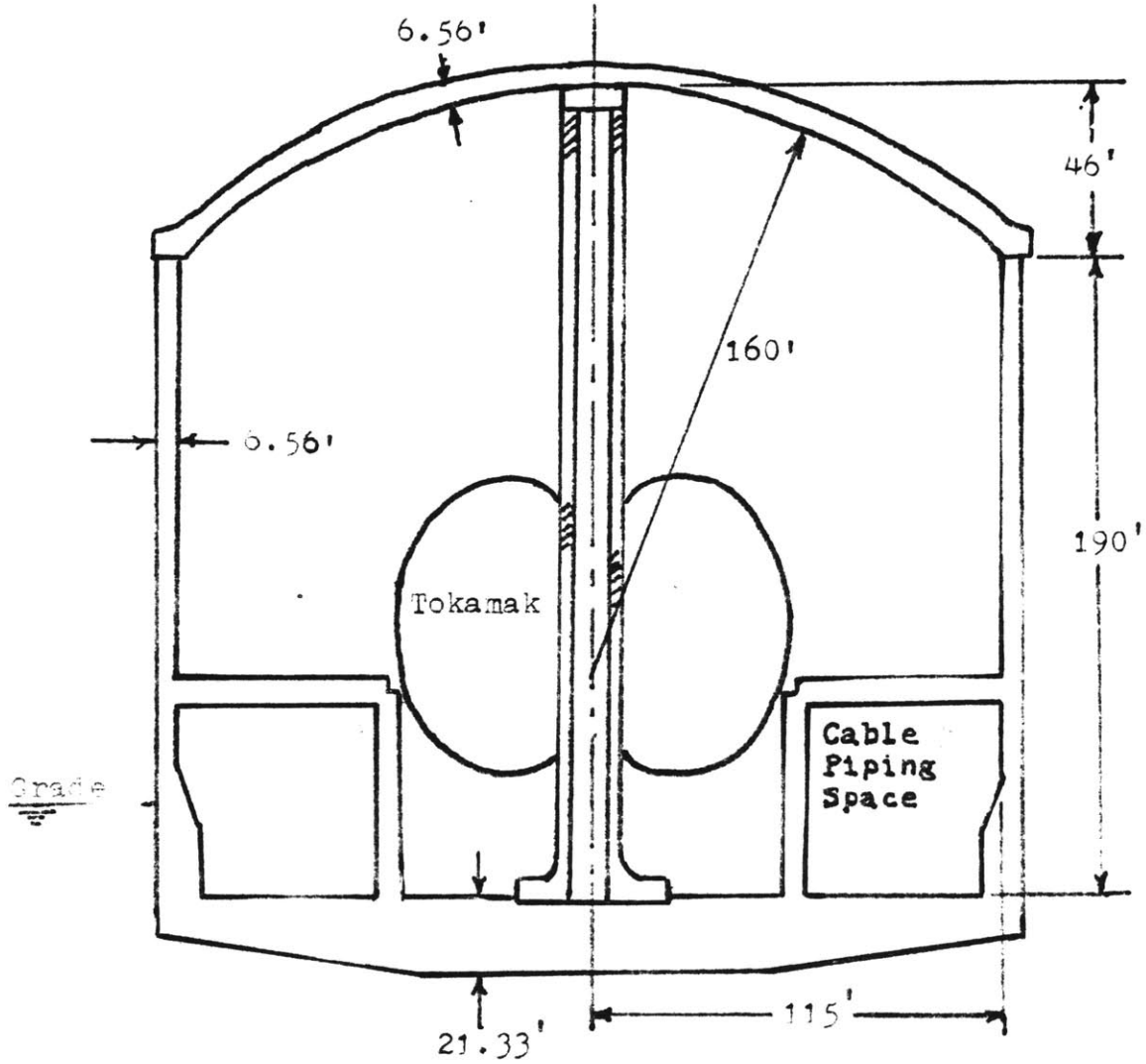

Total Floor Area	41548 ft^2
Total Volume	8855700 ft^3
Wall Area	183532 ft^2
Total Lithium Mass	870975 lbm.
1/18 Total Lithium	48388 lbm.
Ambient Temperature	538 °R
Initial Pressure	14.7 psia

Lined with .25 in. steel plate with a 0.02[illegible] in. gas gap between the plate and the concrete surface.

vessel and the auxilaries are located in the surrounding secondary containment building.

For the sensitivity study reported below, the building dimensions shown in Fig. 3.5 were used. The effect of varying the building dimensions was not studied.

3.4.2 Discussion of Important Base Case Parameters

A sensitivity study of the consequences of lithium spills was performed using the slightly modified SPOOL-FIRE. The results are reported in the next section. An attempt was made to realistically estimate the necessary input parameters. This was designated the base case. The parameters were then varied individually to study the effects of the resultant fire. The selection of values for these parameters will be discussed in order of their importance. A summary is presented in Table 3.7.

The initial containment gas composition was assumed to be a normal atmosphere of 23.1% oxygen and 76.9% nitrogen by weight. This was done in order to get some idea of the maximum consequences of a lithium fire and because SPOOL-FIRE at present can only handle lithium-oxygen reactions. With an inert operating atmosphere, only lithium-concrete reactions could take place. If the containment were breached, the containment over-pressure would no longer be important since the containment would already be vented to the outside. Cases were run with 2%, 5%, and 10% oxygen weight percent in the oxygen-nitrogen mixture.

TABLE 3.7

Input Values for the Base Case

Spill size	SPILL = 48388 lbm. Li
Fraction of spill mass consumed as spray	SPRAY = 1%
Lithium pool surface area	ASNA = 10387 ft^2
Oxygen content of cell gas	WO2 = 23.1% by weight
Reaction product	100% Li_2O
Heat of combustion	CMBR = 18510 Btu/lbm Li
Fraction of heat of combustion deposited in pool	FCMB = .90
Initial lithium spill temperature	TNAI = 2256 ^oR
Radiative exchange factors	EMNAC = .20
	EMNAG = .20
	EMNAB = 0.0
	EMNAW = 0.0
Method of Integration used	Simpson's Rule, IMETH = 3

UWMAK-III uses roughly 1/4 the amount of lithium that UWMAK-I uses. This results from different blanket designs. In UWMAK-III lithium is used only in the outer half of the torus blanket. The inner half (guarding the donut hole) does not use lithium and is helium cooled. Helium is also used to cool the inner wall and the magnet shield. In UWMAK-I the entire blanket uses liquid lithium. Both designs use a small amount of lithium to cool the plasma divertors. UWMAK-III uses 18 toroidal field coils. The blanket therefore consists of 18 modular sections. We assumed that a header pipe broke in such a manner as to drain one blanket section i.e. 1/18 (5.56%) of the total lithium inventory is spilled. Because of lithium hold-up in piping and the heat exchangers, one blanket section would contain less than 1/18 of the total lithium inventory so that 1/18 is probably a conservative number. The lithium blanket sections are supplied and drained by two ring-shaped headers, one above and one below the reactor. These are connected to two lithium-sodium heat exchangers in an adjacent building. It may be possible that a pipe break could occur which would drain two or more blanket sections. A break might also occur in the heat exchanger building. The latter possibility was not investigated. Spill size was varied to study its effect. Cases using 1.39%, 2.75% and 11.1% of the total lithium inventory were run.

The lithium pool area (ASNA) was chosen to be 25% of the total floor area. Cable rooms surrounding the reactor form a hot well of that size. It seems likely that the lithium

spraying from a break would pool there. One case was run using the total floor area.

The radiative interchange factors for the base case were chosen by assuming the emissivity of the cell gas, E_{gas}, to be 1.0, the emissivity of the pool surface, E_{Li}, to be 0.20, and conservatively assuming that no radiation takes place between the steel liner and the concrete surface. We have been unable to find emissivity data for liquid lithium, so we assumed that it has a low emissivity like that of other liquid metals. Cases were run using E_{Li} of 0.4 and 0.1, and E_{gas} of 0.28 and 0.17. One case was run using an emissivity for steel of 0.85, and an emissivity for concrete of 0.90. One run was also made using all large emissivities.

Because of the large thermal conductivity of lithium, the fraction of the heat of combustion released in the pool (FCMB) was taken to be 0.90. Cases were also run using FCMB equal to 0.75 and 0.50. If a combustion zone model were included in the code this input parameter would not be needed.

The blanket exit temperature of lithium in UWMAK-III is 2256 ^{o}R. This was taken to be the spill temperature. Cases were also run using spill temperatures of 1620 ^{o}R and 1260 ^{o}R.

Studies of sodium spray fires show that only a very small fraction of the spray is consumed. Shire[24] reports pressure rises caused by a sodium jet impacting a deflector. In 5 of the 6 cases reported, pressure readings indicate that no more than 3% of the sodium reacted. In the sixth case, 15% may have

reacted. The experiment was done in low oxygen atmospheres, and the average drop size was 0.21 inches in diameter. Krolikowski[23] reports a calculation, for 572 micron sized drops under large driving pressures, which shows less than a 2% decrease in diameter. This would constitute less than 6% decrease in mass. In a severe break only a small portion would be sprayed. We assume 20%. If 5% of the spray is consumed then only 1% of the total spill mass is consumed in the spray fire. This was used as the base case. Cases were also run using 0%, 0.5%, 2%, 3%, and 5%.

Several runs were made to study other effects. At high temperatures the principle product is Li_2O and the base case used 100% Li_2O as the reaction product. However, one case was run using Li_2O_2 which has a larger energy release. SPOOL-FIRE assumes that the spill occurs instantaneously at time 0. Kastenberg[25] indicates that it may take 1 hour for lithium to drain out of the blanket. The code was modified so that the spill rate became a time function. One run was made assuming that the spill rate decays exponentially. 1/18 of the total lithium inventory was assumed to spill over a period of 3600 seconds which constituted 3 time constants.

In determining the rate of oxygen diffusion to the burning zone of the pool, SPOOL-FIRE used the analogy between heat and mass transfer to obtain eq. (3.7). The heat transfer coefficient, h_c, and the analogous gas transport coefficient,

h_g, were derived from the expression given by McAdams for free convection from isothermal horizontal plates.[32] The expression is explicitly written as

$$Nu = 0.14\ (Gr \cdot Pr)^{1/3} \tag{3.25}$$

and necessarily applies to horizontal plates with the heated surface facing upwards, and for flows in the turbulent regime, i.e.

$$Gr \cdot Pr > 10^8 \tag{3.26}$$

However, very little has been published for natural convection inside containments in the turbulent region. Several experimental investigations have been made for natural convection heat transfer for fluids confined by two horizontal plates and heated from below.[33,34,35] Specifically, Jakob in his analysis of the data of Mull and Reiker on air gives the relationship

$$Nu = 0.068\ (Gr)^{1/3} \tag{3.27}$$

which, for Prandtl numbers of 0.71 for air, differs from eq. (3.25) by a factor of two. Similarly, Globe and Dropkin obtained the expression

$$Nu = 0.060\ (Gr)^{1/3} \tag{3.28}$$

for air. Malkus, basing his relationship on the data of water and acetone at room temperature, proposed the expression

$$Nu = 0.085\ (Ra)^{0.325} \tag{3.29}$$

where

$$Ra = Pr \cdot Gr \tag{3.30}$$

These investigations suggest that the heat and mass transfer coefficients used by SPOOL-FIRE may be high by a factor of two. Hence, one computer run was made using the coefficient 0.07 in eq. (3.7) rather than 0.14, making the necessary corrections in SPOOL-FIRE where applicable.

3.4.3. Results of Sensitivity Study

The important results of the sensitivity study are compiled in Table 3.8. Because of the large thermal conductivity of both lithium and steel, the floor liner very rapidly reaches a temperature approximating that of the lithium pool. Hence, no separate column is provided in Table 3.8 for floor liner. In the two cases run using a large EMNAB and EMNAW (cases 24 and 25), the maximum concrete temperature occurred in the walls. The temperature histories of the lithium pool, containment, wall, and floor for the Base Case are shown in Figure 3.6. The parameters studied are reported below in order of decreasing importance.

3.4.3.a Increasing the Weight of Oxygen Available:

At low oxygen concentrations in the containment (2 w/o, 5 w/o), the fire is not self-sustaining. The lithium pool

TABLE 3.8

Compilation of Sensitivity Study

Run No.	Max. Li Temp. (°F)	Max. Gas Temp. (°F)	Max. Gas Press. (psig)	Max Wall Liner Temp. (°F)	Max. Concrete Temp. (°F)	Max. CMBRH (lb/hr-fr^2)	End of Li Fire (sec)
1 Base Case	3081	1849	43.5	1329	432	7.36	2900
2 ASNA=100% of total floor area	2963	2354	56.2	1637	404	6.44	804
3 Spill temp. = 1620 °R	3057	1817	42.7	1298	420	7.17	2923
4 Spill Temp. = 1260 °R	3044	1794	42.1	1277	413	7.06	3016
5 FCMB=.75	2851	1845	43.4	1292	431	6.80	3103
6 FCMB=.50	2389	1762	41.4	1197	430	5.64	3709
7 0% burned as spray	3083	1850	43.6	1330	432	7.38	2805
8 .5% burned as spray	3082	1851	43.6	1330	432	7.37	2801
9 2% burned as spray	3080	1850	43.5	1329	432	7.34	2801
10 3% burned as spray	3078	1846	43.5	1330	432	7.33	2802
11 5% burned as spray	3076	1852	43.6	1331	433	7.28	2706
12 $\%O_2$=2%	1796	249	4.6	167	123	.42	27001
13 $\%O_2$=5%	1796	406	8.6	282	191	1.08	—

Table 3.8 con't.

Run no.	Max. Li Temp. (°F)	Max. Gas Temp. (°F)	Max. Gas Press. (psig)	Max Wall Liner Temp. (°F)	Max. Concrete Temp. (°F)	Max. CMBRN (lb/hr-ft^2)	End of Li fire (sec)
14 $\%O_2$=10%	2028	797	18.3	564	327	2.21	25018
15 EMNAC=.1 EMNAG=.1	3888	1982	46.9	1382	425	8.67	2400
16 EMNAC=.2 EMNAG=.1	3391	1805	42.2	1377	431	7.87	2600
17 EMNAC=.4 EMNAG=.2	2666	1652	38.6	1289	436	6.62	3218
18 EMNAC=.4 EMNAG=.4	2410	1649	38.5	1222	435	6.15	3602
20 100% Li_2O_2	2275	999	21.7	709	389	2.76	13008
21 1.39% of total spilled	3171	817	19.51	472	167	8.03	700
22 2.78% of total spilled	3139	1334	32.4	854	258	7.77	1300
23 11.1% of total spilled	2982	1875	43.1	1399	698	6.74	18000
24 EMNAB=.78 EMNAW=.78	2194	920	20.1	542	1819	5.73	3506
25 EMNAC=.4 EMNAG=.4, EMNAB=.78, EMNAW=.78, FCMB=.50	1796	983	23.0	574	997	5.27	5700
26 exp. decaying spill rate	3068	1825	43.2	1302	419	7.94	2600
27 mass transfer eq. coef.=.07	2312	1167	26.7	864	409	2.96	7118

Fig. 3.6 Temperature History for a Lithium Fire in the UWMAK-III Containment

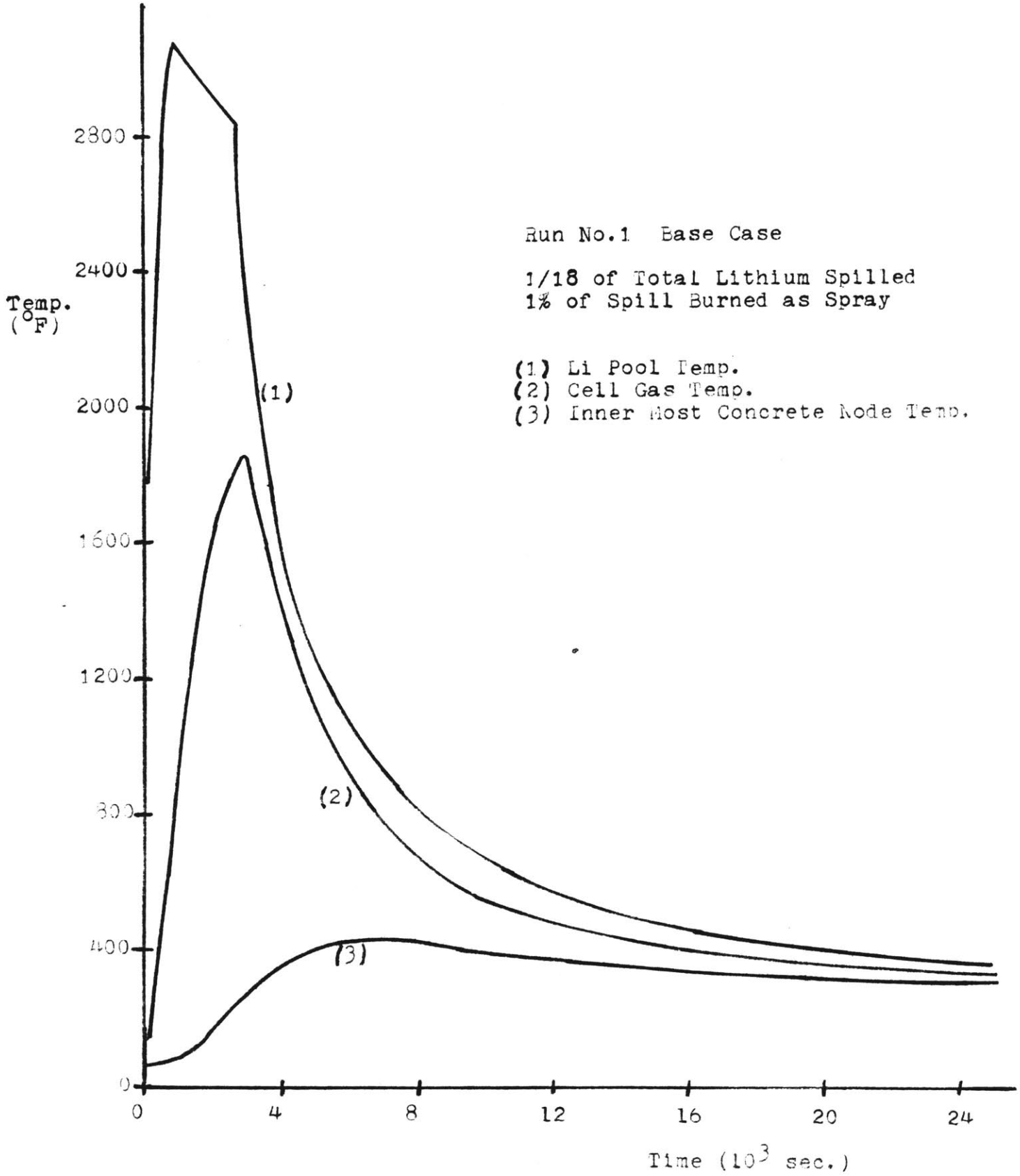

temperature drops off rapidly from its spill temperature. The reaction rate is so slow that the pool reaches the lithium melting temperature before all of the oxygen available is consumed. In a 10 w/o oxygen atmosphere, the fire seems to be self-sustaining. The maximum lithium temperature exceeds the spill temperature and drops to the melting point. However, the later stages of the fire show signs of oxygen depletion and a very slow reaction rate. At low oxygen concentrations, the nitrogen reaction would be important but no allowance is made for this in the current version of SPOOL-FIRE. The lithium pool temperature listing is shown in Figure 3.7 for various O_2 concentrations.

3.4.3.b Increasing the Amount of Lithium Spilled:

For smaller spills, the lithium oxidizes very quickly causing the containment to reach a maximum pressure that increases with spill size. The Base Case nearly results in producing the maximum containment pressure for all the cases investigated. As expected, doubling the spill size doubled the total energy released, although in the larger spill case the release rate is slowed and greater energy transfer occurs from the cell gas, thus preventing much higher cell gas temperatures. Nearly all of the oxygen in the containment is used up by the 11.1% Li spill and the fire shows signs of oxygen depletion near its end. Still larger spills would be limited by this lack of oxygen. The larger energy release does, however, manifest itself by markedly increasing the

Fig. 3.7 Temperature History for a lithium Fire in the UWMAK-III Containment

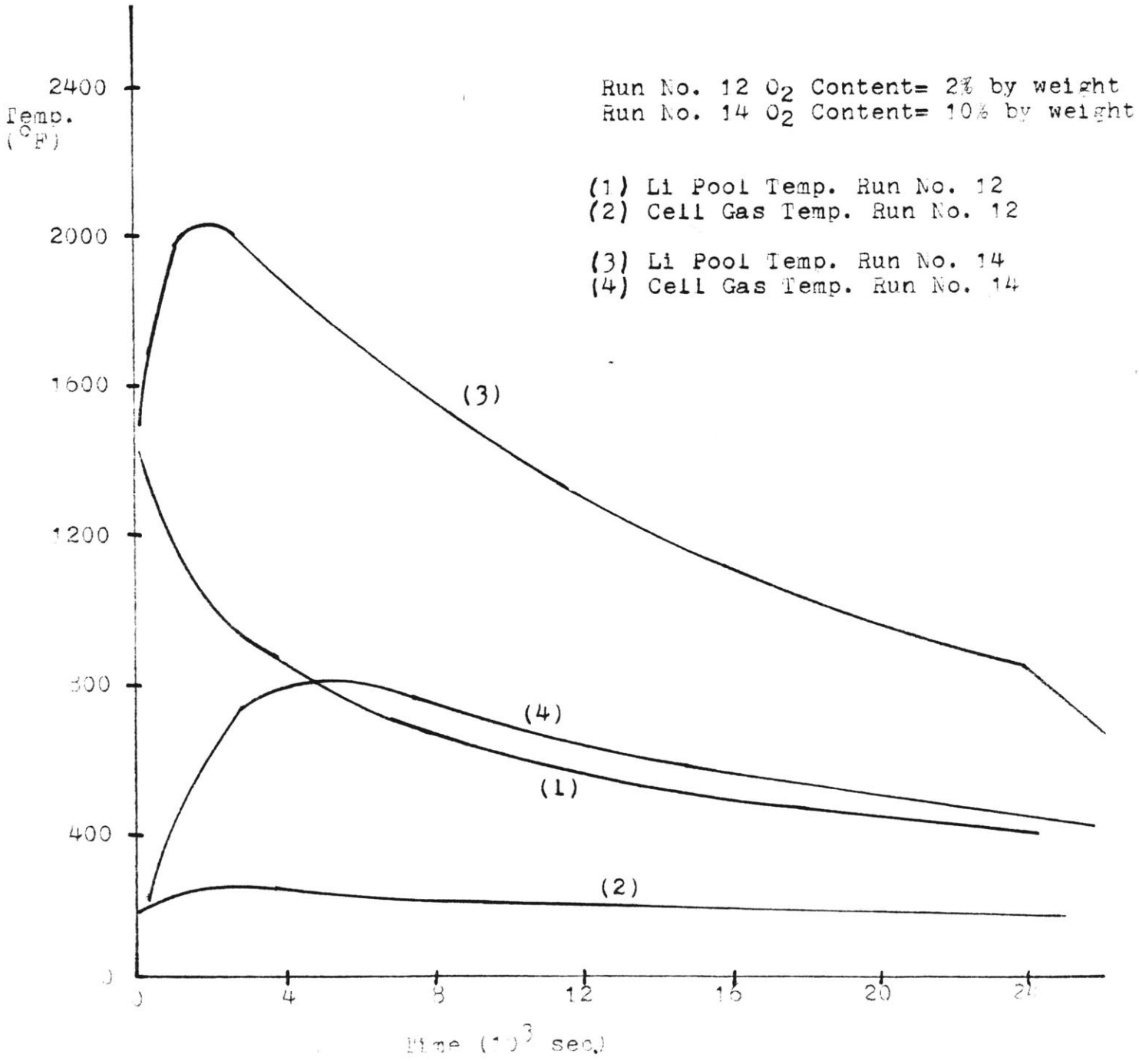

maximum concrete temperatures. The temperature history within the containment as a function of lithium spill volume is shown in Figure 3.8.

3.4.3.c Increasing the Pool Surface Area:

Although the reaction rate per unit area decreases slightly with increasing pool surface area, the total reaction rate increases greatly. For example, a surface area increase by a factor of 4 results in a reaction rate increase by a factor of 3.5. For very hot lithium spills, it appears that dispersing the lithium is not a feasible method of extinguishing the fire, although indications are that lithium dispersal may be feasible for lithium spills at lower temperatures. As can be seen from Figure 3.9, the value of FCMB (the fraction of heat transferred to the lithium pool from combustion) is of major importance in determining whether the lithium fire will be self-sustaining or not. FCMB is of course a function of pool surface area.

3.4.3.d Increasing the Radiative Exchange Factors Between the Pool and the Containment Walls and Gas (EMNAC and EMNAG):

Increasing these radiative exchange factors have the same (although more pronounced) effect as decreasing FCMB. The increased radiation from the pool lowers the pool temperature, hence lowering the reaction rate. The slower reaction rate in turn lowers the maximum gas temperature and pressure. Better estimates of FCMB, EMNAC, and EMNAG must be made before

Fig. 3.8 Temperature History for a Lithium Fire in the UWMAK-III Containment

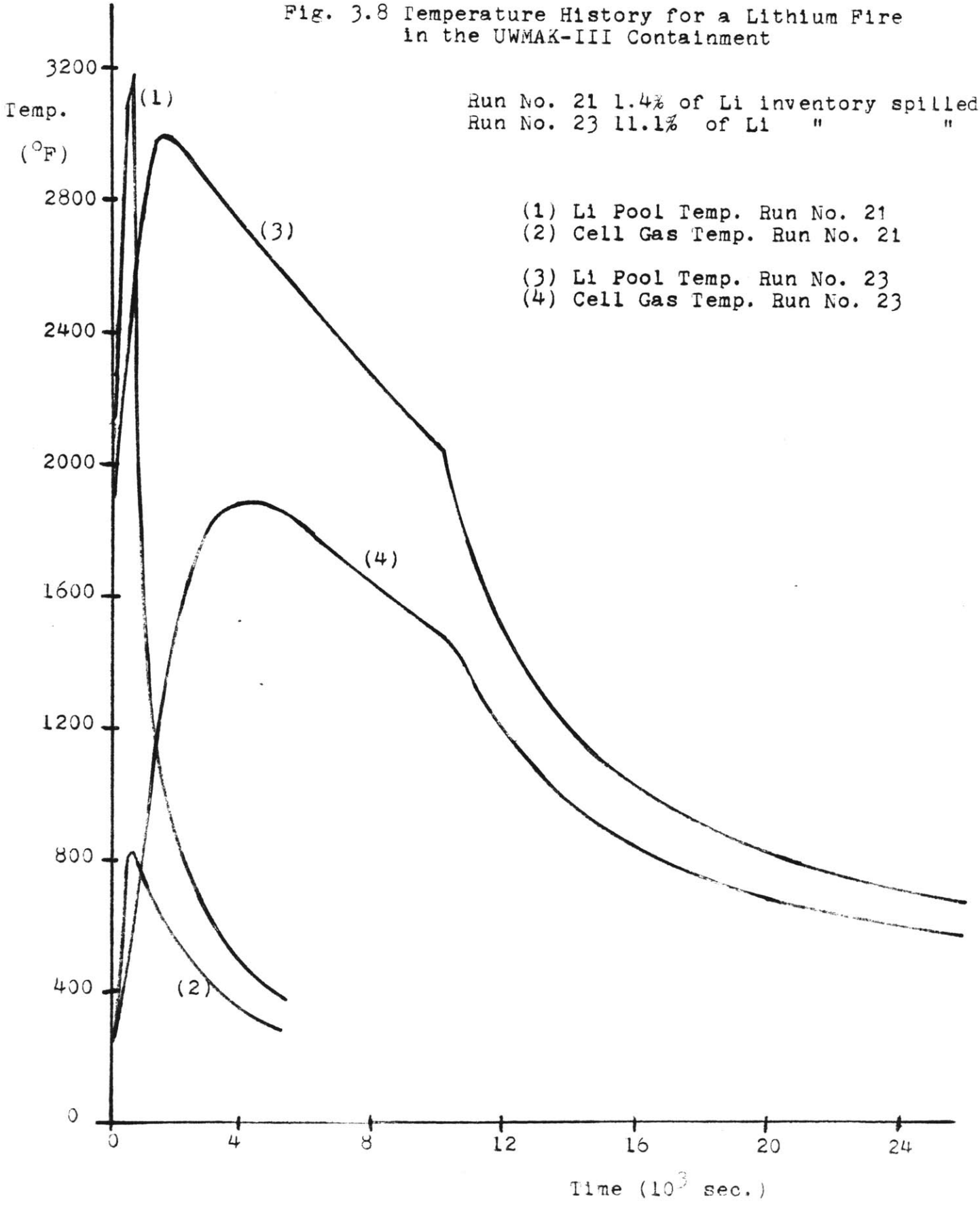

Fig. 3.9 Temperature History for a Lithium Fire in the UWMAK-III Containment

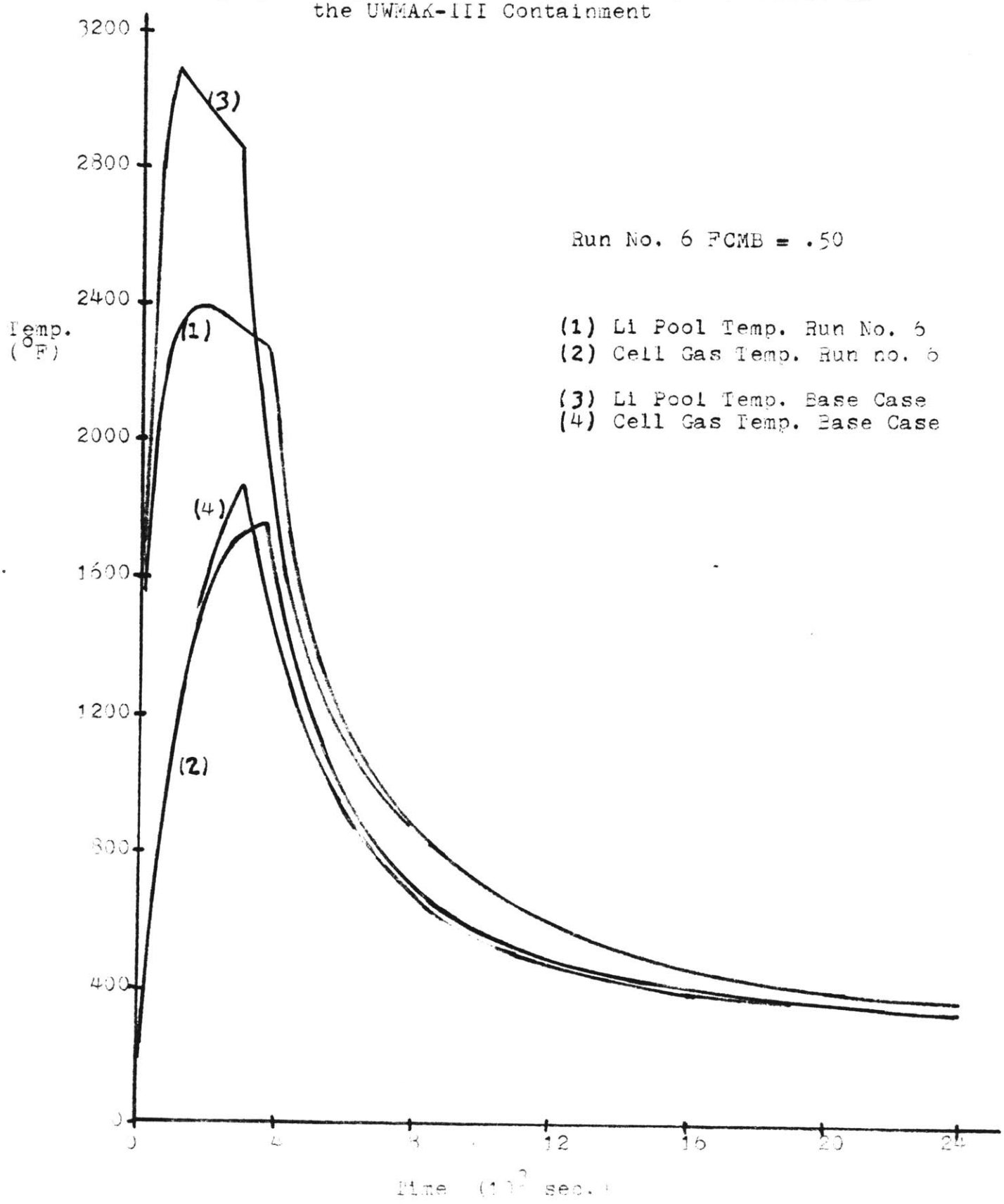

reliable predictions of lithium fire consequences can be made using this model. A combustion zone model would be very helpful in this regard. Also, better values for the emissivities of liquid lithium and its combustion products are needed. Figure 3.10 shows the effects of changing EMNAC and EMNAG on the lithium pool and cell gas temperatures.

3.4.3.e Increasing the Radiative Exchange Factors Between the Steel Liner and the Concrete Surface (EMNAB and EMNAW):

Increasing these exchange factors results in a decrease of the maximum cell pressure obtained in lithium fires, as shown in Figure 3.11. These two parameters obviously constitute a major means of transferring heat out of the containment and should be included in any further studies. Increasing EMNAG and EMNAW also results in a very high concrete floor temperature. Hence, further studies should also consider the release of water from concrete structures as a result of such high temperatures.

3.4.3.f Use of Smaller Convective Coefficient for Mass Transfer Equation:

The use of 0.07 rather than 0.14 for the coefficient in equation (3.7) more than halves the combustion rate. Pool temperature and cell pressure are markedly decreased because more time is available for heat transfer out of the cell. The results are shown in Figure 3.12. There is an urgent need to

Fig. 3.10 Temperature History for a Lithium Fire in the UWMAK-III Containment

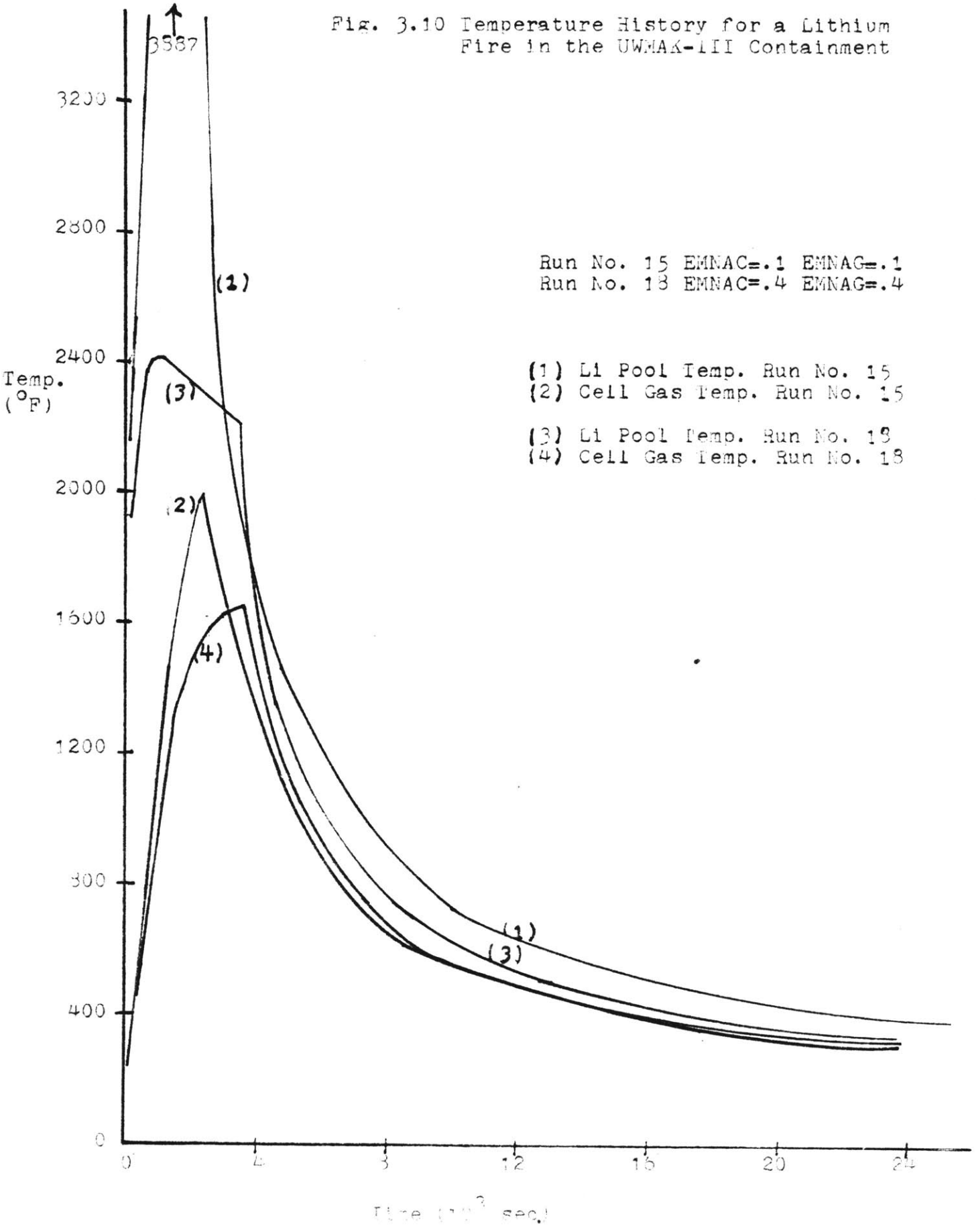

Run No. 15 EMNAC=.1 EMNAG=.1
Run No. 18 EMNAC=.4 EMNAG=.4

(1) Li Pool Temp. Run No. 15
(2) Cell Gas Temp. Run No. 15

(3) Li Pool Temp. Run No. 18
(4) Cell Gas Temp. Run No. 18

Fig. 3.11 Temperature History for a Lithium Fire in the UWMAK-III Containment

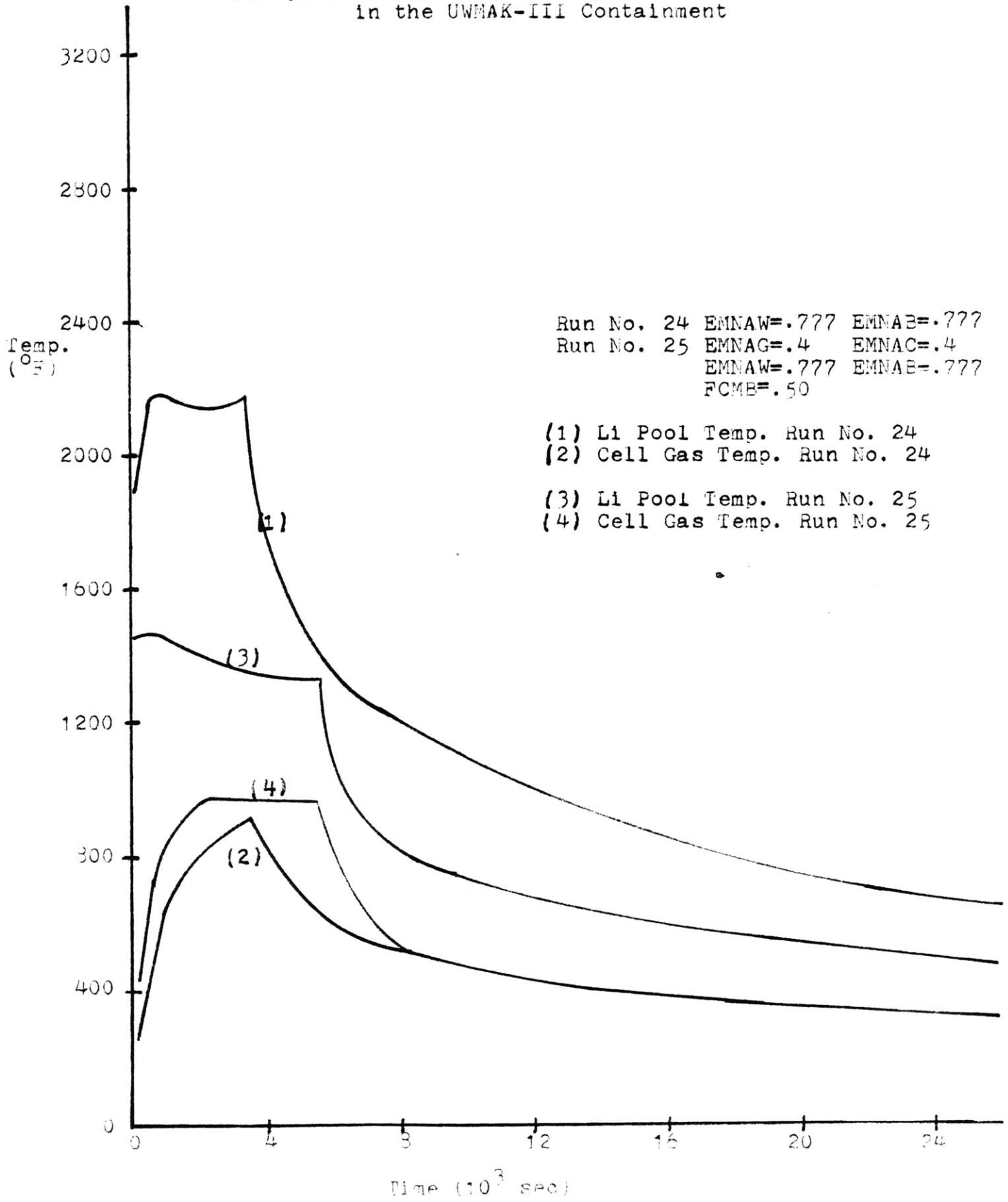

Fig. 3.12 Temperature History for a Lithium Fire in the UWMAK-III Containment

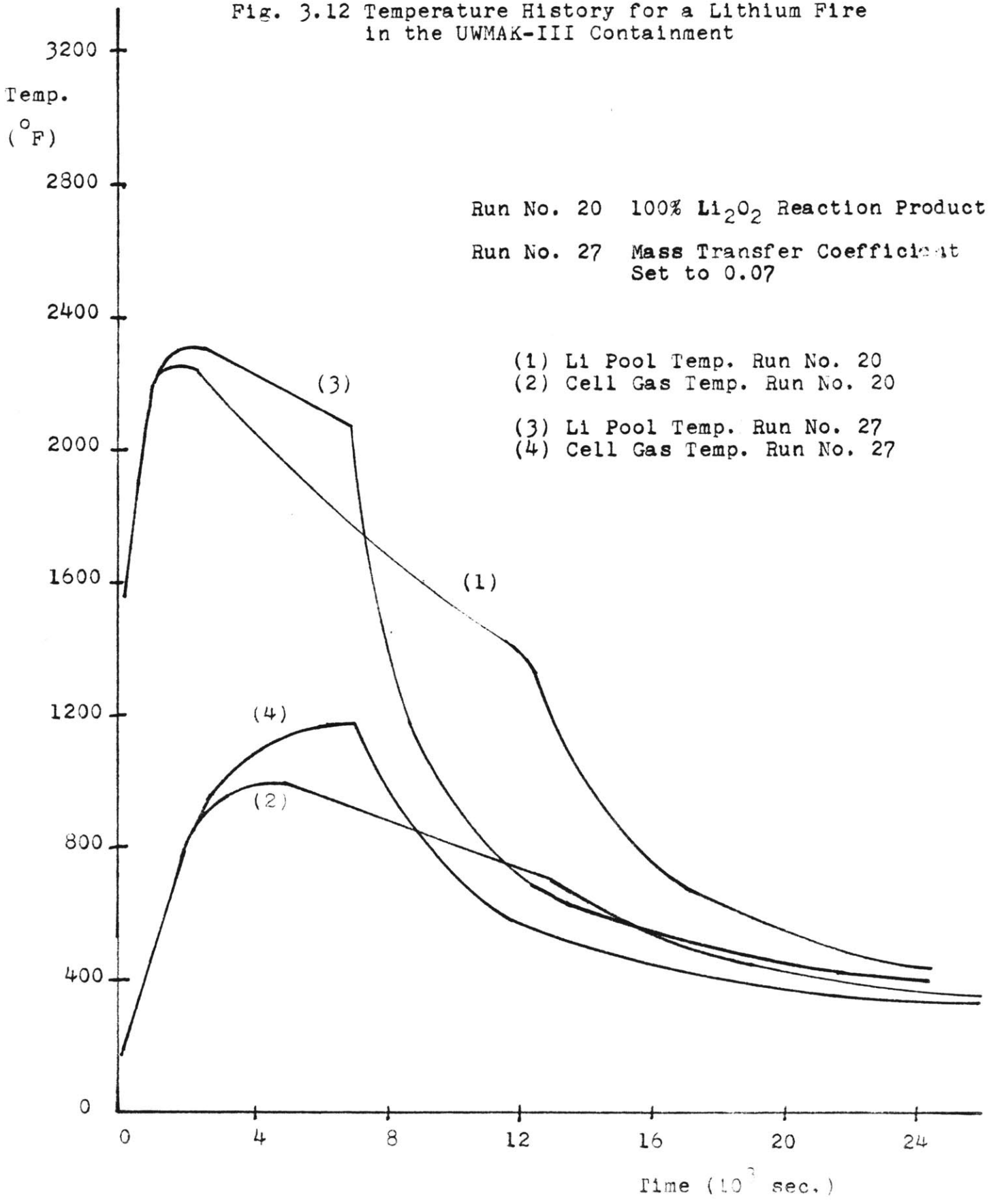

remodel the oxygen transfer mechanism to the lithium pool.

3.4.3.g Decreasing the Fraction of the Heat of Combustion Going to the Pool (FCMB):

FCMB has a very significant effect on the maximum lithium pool temperature as indicated earlier and as shown in Figure 3.9. The lithium pool temperature decreases strongly as FCMB decreases. The decreased pool temperature also decreases the reaction rate, although only slight decreases in the maximum gas temperature and pressure result. The value of FCMB would have greater effect in smaller spills, or in oxygen depleted atmospheres. Again, a better combustion zone model is needed.

3.4.3.h Decreasing the Lithium Spill Temperature:

The initial lithium spill temperature has a negligible effect on the maximum lithium temperature reached. Decreasing the spill temperature does, however, decrease the reaction rate and slightly decrease the maximum gas temperature and pressure. For large spills with ample oxygen present, the initial spill temperature is of little consequence to the final course of the accident. For smaller spills, or for oxygen depleted atmospheres, the initial spill temperature might determine whether or not the fire is self-sustaining.

3.4.3.i. Increasing the Percentage of Lithium Burned as Spray:

Although increasing the percentage of lithium burned as spray directly affects the initial gas temperature and pressure, it has a negligible effect on the overall course of the resulting pool fire.

3.4.3.j Use of 100% Li_2O_2 as Reaction Product:

Using Li_2O_2 as the reaction product from lithium combustion, rather than Li_2O, results in greater energy release. However, the reaction rate resulting is slower because the reaction requires twice as much oxygen as does the production of Li_2O. This effect in turn results in lower peak pool and cell gas temperatures. At high temperatures the Li_2O reaction would normally dominate.

3.4.3.k Use of a Finite Spill Time

Use of an exponentially decaying spill rate had almost no effect on the peak gas temperatures and pressures reached. Because of the combustion model used, the combustion rate in the lithium pool was independent of spill rate. Therefore, the resultant temperature-pressure histories showed very little change from the Base Case.

The results of the sensitivity study as outlined above is summarized in Figure 3.13.

3.5 Conclusions and Recommendations for Future Studies

Lithium-oxygen reactions are capable of releasing large amounts of energy into the containments of fusion reactors as

Figure 3.13 Change of the Maximum Lithium Pool Temperature Due to Variation of SPOOL-FIRE Parameters

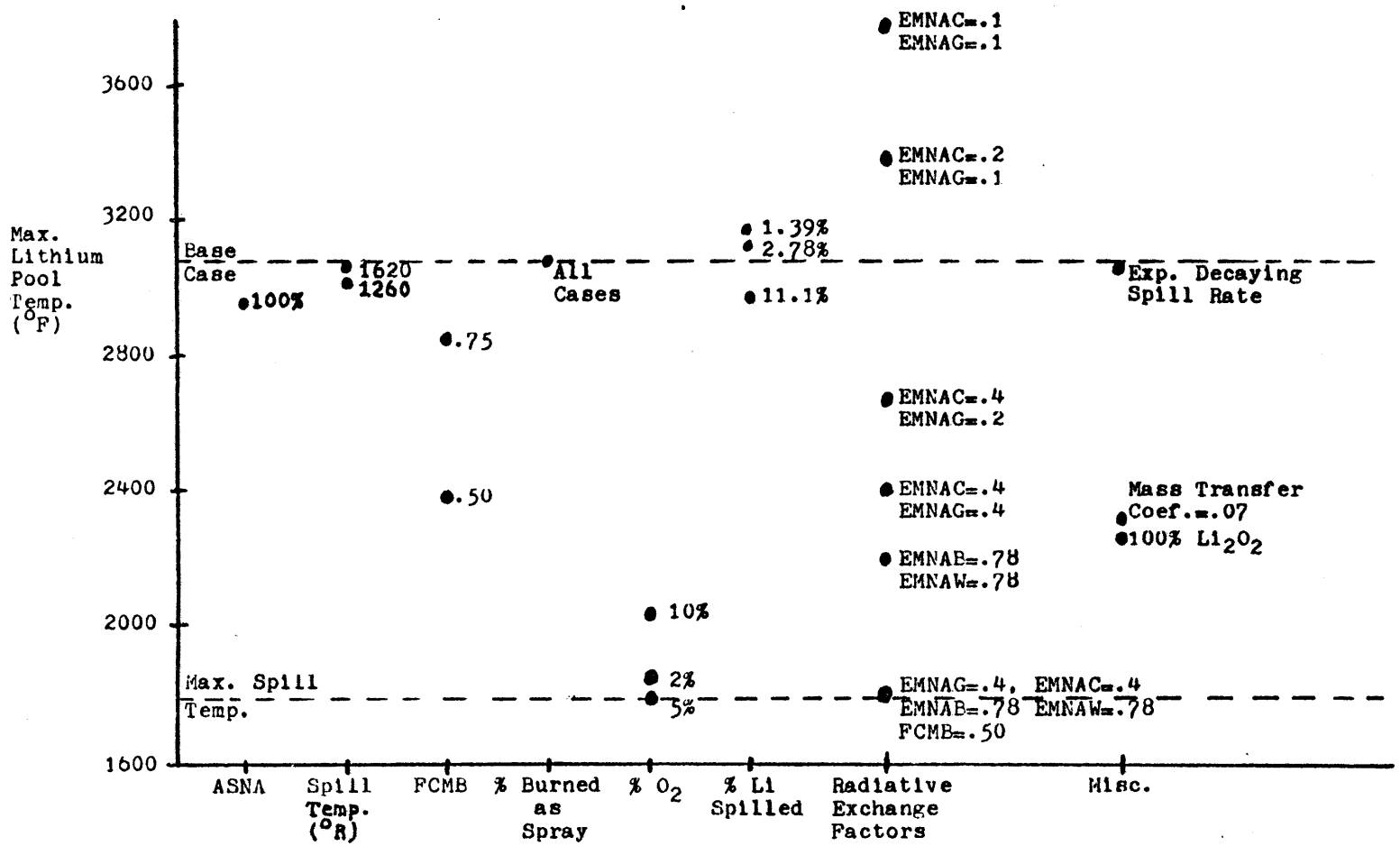

currently designed. Containment overpressures as high as 40 psig may be expected from a lithium-air fire involving 5% of the coolant in normal atmospheres. Removal of oxygen would limit this overpressurization significantly, although the current version of SPOOL-FIRE, used in this study, does not take into account lithium-nitrogen reactions.

SPOOL-FIRE provides a simple model of liquid metal fires, although a number of important modifications should be made:

1) the inclusion of a model for lithium-nitrogen reaction;
2) the effects of humidity;
3) the release of water from heated concrete;
4) the release of energy and gases from lithium-concrete reactions;
5) the inclusion of a "combustion zone" in pool fires;
6) diffusion as well as convection of oxygen (and nitrogen) to the combustion zone;
7) radiant and convective heat transfer from the combustion zone to the environs;
8) the inclusion of models for LiOH and Li_2O_2 formation, using second law thermodynamics and chemical equilibrium effects.

Design strategies which could be studied for mitigating the consequences of a lithium pool fire include:

1) emergency space cooling;
2) inert gas flooding of the containment;

3) containment ventilation;

4) the addition of chemicals for the extinguishment of fires;

5) surface cooling of the lithium pool.

Chapter III References

1. J. O. Cowles and A. D. Pasternak, "Lithium Properties Related to Use as a Nuclear Reactor Coolant," Lawrence Radiation Laboratory, Rept. UCRL-50647 (1968).

2. The University of Wisconsin Fusion Feasibility Study Group, "UWMAK-III, A Non-circular Tokamak Power Reactor Design," UWFDM-150, July, 1976.

3. G. H. Bulmer, "The Thermonuclear Fusion Reactor: Some Aspects of Lithium Fire Safety," FTSG(M&C) (71) p.26, FRESG (71) p.3.

4. The University of Wisconsin Fusion Feasibility Study Group, "UWMAK-I, A Wisconsin Toroidal Fusion Reactor Design," UWFDM-68, March 15, 1974.

5. S. Gordon and B. J. McBride, "Computer Program for Calculations of Complex Chemical Equilibrium Compositions, Rocket Performance, Incident and Reflected Shocks, and Chapman-Jouguet Detonation," NASA SP-273 (1971).

6. I. Charak and L. W. Person, "SPOOL-FIRE: Analysis of Spray and Pool Na Fire," ANL, presented at the ANS International Meeting on Fast Reactor Safety and Related Physics, Oct., 1976, Chicago.

7. JANAF Thermochemical Tables, (Midland, Mich.: Dow Chemical Co., 1970)

8. I. M. Klotz, Chemical Thermodynamics, rev. ed., (New York: Benjamin, Inc., 1964).

9. F. U. Zeggeren and S. H. Storrey, The Computation of Chemical Equilibrium, (London: Cambridge University Press, 1970).

10. D. Okrent, et. al., "On the Safety of Tokamak-Type, Central Station Fusion Power Reactors," Nucl. Eng. Design, (1976).

11. P.R. Shire, "Reactor Sodium Coolant Hypothetical Spray Release for Containment Accident Analysis: Comparison of Theory with Experiment," HEDL, April, 1974.

12. P. Beireger, et. al. "SOFIRE II User Report," AI-AEC-13055, April, 1973.

13. R. D. Peak and D. D. Stepnewski, "Computational Features of the CACECO Containment Analysis Code," HEDL SA-922, May 29, 1975.

14. P. R. Shire, "A Combustion Model for Hypothetical Sodium Spray Fire Within Containment of an LMFBR," M.S. Thesis, Univ. of Wash., 1972.

15. Letter, D. E. Simpson to K. Hikido, "Transmittal of SPRAY Computer Code," w/FFTFC-750140, Jan. 6, 1975.

16. P. R. Shire, et. al. "A Sodium Droplet Combustion Model for Reactor Accident Analysis," Trans. Am. Nucl. Soc. (15), p.812, (1972).

17. R. D. Peak, "CACECO Code," private transmittal, April 1974.

18. L. W. Person, "The Application of SPOOL-FIRE in Theoretical Analysis and Experimental Comparison," Nuclear Technology, Volume 32, March 1977.

19. B. U. Sarma, et. al, "Review of Sodium Fire Analytical Models," GEAP-14053, June 1975.

20. B. U. Sarma, et. al., "Review of Current Sodium Fire Analytical Methods," GEAP-14148, Sept. 1976.

21. J. R. Humphreys, Jr., "Sodium-Air Reactions as They Pertain to Reactor Safety and Containment," Proceedings of the Second International Conference on the Peaceful Uses of Atomic Energy, Geneva, Paper 1893 (1958).

22. International Business Machines Corporation, "Continuous System Modeling Program II (CSMP II) - Program Reference Manual, Publication No. GH20-0367-4, 3rd. ed. (Sept. 1972)

23. Theresa S. Krolikowski, "Violently Sprayed Sodium-Air Reaction in an Enclosed Volume," ANL-7472 (Sept. 1968).

24. P. R. Shire, "Reactor Sodium Coolant Hypothetical Spray Release for Containment Accident Analysis: Comparison of Theory with Experiment," Proc. of the Fast Reactor Safety Meeting, Beverly Hills, Calif., April 2-4, 1974, CONF-740401-P1.

25. W. E. Kastenberg, "Loss-of-Coolant Accidents in Lithium Cooled Fusion Blankets," Trans. Am. Nucl. Soc., (26) pp. 32-33, (1977).

26. Liquid Metals Handbook, 2nd. ed., NAVEXOS-P-733, rev. (June 1952).

27. H. C. Hottel, Review of "Certain Laws Governing the Diffusion Burning of Liquids," by V. I. Blinov and Khudiakov of USSR, Fire Research Abstracts and Reviews, Volume 1, pp. 41-44, (1958).

28. M. Michaud, et. al., "Oxygen and Combustion - Theoretical and Experimental Fundaments," Revue Générale de Thermique, Volume 4, pp. 527-551, (1965).

29. C. S. Kelly, "The Transfer of Radiation from a Flame to its Fuel," Journal of Fire and Flammability, Volume 4, p.56, (1973).

30. F. Huber, et. al., "Behavior of Na Area Conflagrations and Suitable Protecting Systems," presented at the ANS International Meeting on Fast Reactor Safety and Related Physics, Oct. 1976, Chicago.

31. Frank Kreith, Principles of Heat Transfer, 3rd Ed., (New York: Intext Educational Publishers, 1973).

32. W. H. McAdams, Heat Transmission, McGraw-Hill Book Company, Inc., New York, N.Y., p.181, 1954.

33. S. Globe, D. Dropkin, "Natural Convection Heat Transfer in Liquids Confined by Two Horizontal Plates and Heated from Below," Trans. of the ASME, J. of Heat Transfer, February 1959.

34. M. Jakob, Heat Transfer, John Wiley & Sons, Inc., New York, N.Y., Volume 1, p.534, 1949.

35. W. V. R. Malkus, "Discrete Transitions in Turbulent Convection," Proceedings of the Royal Society (London), series A, Volume 225, 1954, p.185.

APPENDIX I

Tritium Release Fault Trees

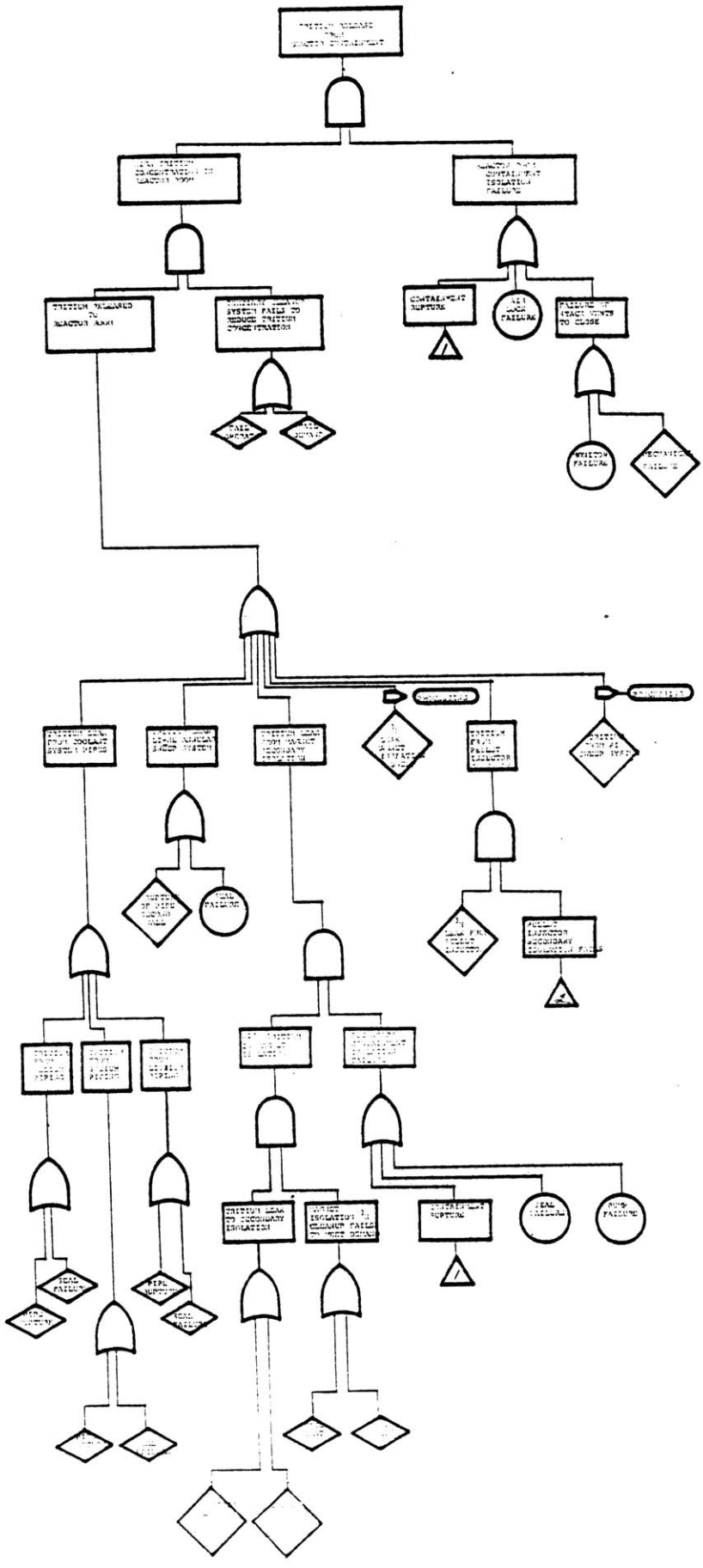

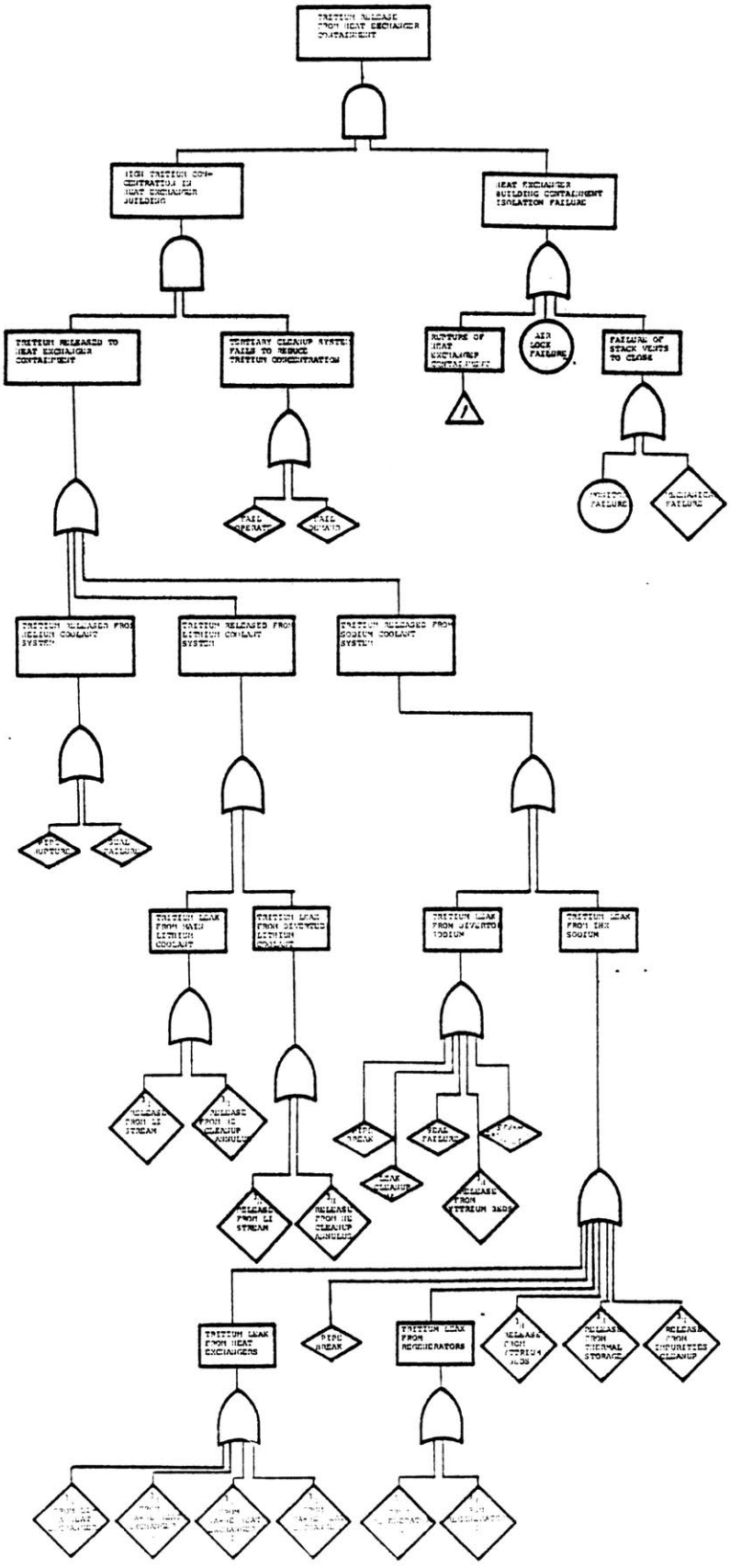

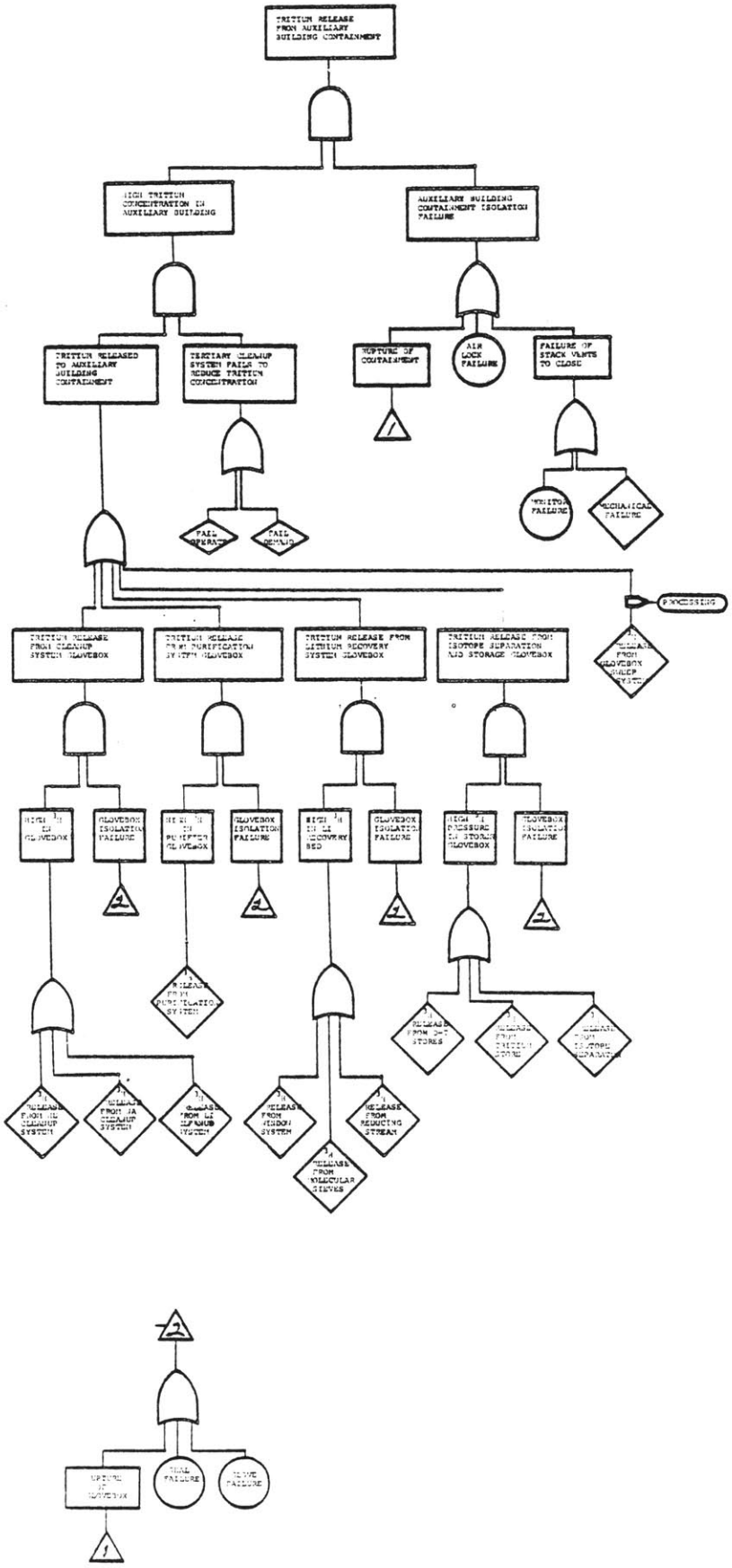
TRITIUM RELEASE FROM AUXILIARY BUILDING CONTAINMENT
HIGH TRITIUM CONCENTRATION IN AUXILIARY BUILDING
AUXILIARY BUILDING CONTAINMENT ISOLATION FAILURE
TRITIUM RELEASED TO AUXILIARY BUILDING CONTAINMENT
TERTIARY CLEANUP SYSTEM FAILS TO REDUCE TRITIUM CONCENTRATION
RUPTURE OF CONTAINMENT
AIR LOCK FAILURE
FAILURE OF STACK VENTS TO CLOSE
FAIL OPERATE
FAIL REMAIN
MECHANICAL FAILURE
PROCESSING
TRITIUM RELEASE FROM CLEANUP SYSTEM GLOVEBOX
TRITIUM RELEASE FROM PURIFICATION SYSTEM GLOVEBOX
TRITIUM RELEASE FROM LITHIUM RECOVERY SYSTEM GLOVEBOX
TRITIUM RELEASE FROM ISOTOPE SEPARATION AND STORAGE GLOVEBOX
GLOVEBOX ISOLATION FAILURE
GLOVEBOX ISOLATION FAILURE
GLOVEBOX ISOLATION FAILURE
GLOVEBOX ISOLATION FAILURE
RELEASE FROM PURIFICATION SYSTEM
RELEASE FROM LI CLEANUP SYSTEM
RELEASE FROM LI CLEANUP SYSTEM
RELEASE FROM LI CLEANUP SYSTEM
RELEASE FROM HYDRO SYSTEM
RELEASE FROM REDUCING STREAM
RELEASE FROM MOLECULAR SIEVES
RELEASE FROM GET STORES
RELEASE FROM CRYOGEN STORE
RELEASE FROM CRYOGEN SEPARATION
RUPTURE OF GLOVEBOX
SEAL FAILURE
GLOVE FAILURE